

1-1-1991

## Stereochemical aspects of Ziegler-Natta catalysts/

James Charles Vizzini  
*University of Massachusetts Amherst*

Follow this and additional works at: [https://scholarworks.umass.edu/dissertations\\_1](https://scholarworks.umass.edu/dissertations_1)

---

### Recommended Citation

Vizzini, James Charles, "Stereochemical aspects of Ziegler-Natta catalysts/" (1991). *Doctoral Dissertations 1896 - February 2014*. 782.  
<https://doi.org/10.7275/jf9e-bp39> [https://scholarworks.umass.edu/dissertations\\_1/782](https://scholarworks.umass.edu/dissertations_1/782)

This Open Access Dissertation is brought to you for free and open access by ScholarWorks@UMass Amherst. It has been accepted for inclusion in Doctoral Dissertations 1896 - February 2014 by an authorized administrator of ScholarWorks@UMass Amherst. For more information, please contact [scholarworks@library.umass.edu](mailto:scholarworks@library.umass.edu).





312066008161115



STEREOCHEMICAL ASPECTS OF ZIEGLER-NATTA CATALYSTS

A Dissertation Presented

by

JAMES CHARLES VIZZINI

Submitted to the Graduate School of the  
University of Massachusetts in partial fulfillment  
of the requirements for the degree of

DOCTOR OF PHILOSOPHY

September 1991

Polymer Science and Engineering

© Copyright by James Charles Vizzini 1991

All Rights Reserved



STEREOCHEMICAL ASPECTS OF ZIEGLER-NATTA CATALYSTS

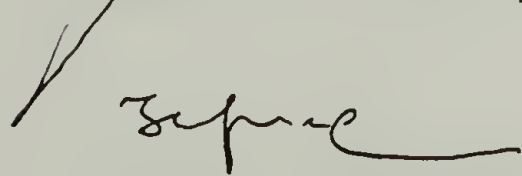
A Dissertation Presented

by

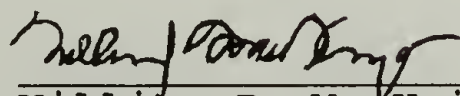
JAMES CHARLES VIZZINI

Approved as to style and content by:

  
James C.W. Chien, Chair

  
Thomas J. McCarthy, Member

  
Ronald D. Archer, Member

  
William J. MacKnight, Department Head  
Polymer Science and Engineering

**DEDICATION**

To Kayo

## ACKNOWLEDGMENT

First and foremost, I would like to express my gratitude to my adviser, Professor James C.W. Chien. He introduced me to the exciting field of Ziegler-Natta catalysis and has been an enthusiastic adviser who was always present to give advice but provided me with enough leeway to be able to introduce my own thoughts and follow my own intuition. My self-motivation has increased tremendously since joining this group and I credit it to the atmosphere created by the adviser. I always felt that I worked with him not only for him.

I give special thanks also to Professors Ronald D. Archer and Thomas J. McCarthy who served on my committee. Their criticism during the formulation of this dissertation was most valuable. Through their comments and questions, I received better insight into what I wanted to say and explain.

It has been a long five years and I had much help along the way. Jack Hirsch, S. Ramakrishnan, Jairo Martinez, and Val Tromantano all gave me a lot of support when I was starting my research. Charlie Dickinson gave me a perspective of the "big picture" when I became bogged down in my research. He along with Jie-Feng Shi produced the MAS  $^{13}\text{C}$  NMR data of my catalysts that is presented in the fifth chapter.



The interactions with Professor Francesco Ciardelli were most valuable and essential in the stereoelective work in chapter IV. The methods and experience I gained from him and his research group at the University of Pisa were also employed in the studies of the homogeneous system in chapter VI.

The constant love and support of my parents throughout my life are deeply appreciated. I hope when I have children, passing through the same rigors, I will be as understanding and patient.

A very heartfelt thanks to Bert Reekmans whose companionship in the last two years has helped me keep my sanity. Our discussions over beer at the Ale House will always be remembered and treasured.

Finally, behind every man there is a woman. I truly believe that I could not have kept up my enthusiasm and succeeded here had it not been for my fiancée, Kayo Umezawa. She is my partner both in science and life. I am always indebted to her for her understanding and encouragement.

## ABSTRACT

### STEREOCHEMICAL ASPECTS OF ZIEGLER-NATTA CATALYSTS

SEPTEMBER 1991

JAMES CHARLES VIZZINI, B.S., INDIANA UNIVERSITY OF PA  
Ph.D., UNIVERSITY OF MASSACHUSETTS

Directed by: Professor James C.W. Chien

The advent of  $\text{MgCl}_2$  supported Ti catalysts and more recently the chiral ansa-bridged metallocene homogeneous systems has sparked interest concerning the stereochemical nature of these two classes of Ziegler-Natta catalysts. A classical method of separating chiral sites in heterogeneous systems is by the introduction of an optically active third component and studying the physical properties of the fractionated polymer obtained from the polymerization of racemic monomer. In the homogeneous case an optically pure catalyst may be obtained and as described above, information may be gleaned from racemic monomer polymerization.

The system  $\text{MgCl}_2 \cdot 3\text{ROH}$ /phthalic anhydride/ $\text{TiCl}_4$ /dialkylphthalate//triethylaluminum/phenyltriethoxysilane was studied. The effect of changing the alkyl group of the ester was that the bulkier alkyl resulted in poorer stereospecific yields of the system. Magic angle spinning cross-polarization  $^{13}\text{C}$  NMR revealed that the ester was rigidly bound to the support and that the above system had

clearly more than one type of complexation of the ester unlike an earlier supported system indicating more diverse defect structures on the surface.

The system was modified with (R,S)- and (S)-2-methyl-1-butanol accompanied by the respective phthalate esters. Activities of 3- and 4- branched  $\alpha$ -olefins were more depressed than that of earlier supported systems. Active site counting in the polymerization of 4-methyl-1-pentene with a supported system revealed that fewer active sites are available for this monomer than for propylene. Polymerizations of racemic monomer were stereoelective but for the 3- branched monomer the polymer produced was more stereoirregular than those from earlier supported systems.

Polymerization of racemic 4-methyl-1-hexene with the homogeneous (S)-ethylenebis( $\eta^5$ -tetrahydroindenyl)zirconiumbis(O-acetyl-(R)-mandalate)/methylaluminumoxane system produced more optically pure and stereoregular polymer than the heterogeneous systems. The existence of fractions in the polymer of opposite optical rotation suggests that at least two stereochemical environments exist during the course of the polymerization, disputing earlier beliefs that this system is stereochemically rigid. Also, it was found that the type of solvent used in the polymerization could affect the stereochemical distribution of the system.



# TABLE OF CONTENTS

	Page
ACKNOWLEDGMENT .....	v
ABSTRACT .....	vii
LIST OF TABLES .....	xii
LIST OF FIGURES .....	xiv
Chapter	
I. INTRODUCTION .....	1
Early Systems .....	1
Active Site Models .....	2
Termination Reactions .....	6
The $MgCl_2$ Supported Systems .....	7
Stereoelective Polymerizations .....	12
Homogeneous Systems .....	16
Statement of the Problem .....	19
References .....	23
II. EXPERIMENTAL METHODS .....	27
Handling and Purification of Chemicals .....	27
Catalyst Synthesis .....	27
$MgCl_2$ .....	27
Catalyst Synthesis Reactor .....	27
CW System .....	29
CH System .....	29
Modified CH Catalysts .....	30
Polymerizations .....	31
Propylene Polymerizations .....	31
Heterogeneous Systems .....	31
Homogeneous Systems .....	31
Higher $\alpha$ -Olefin polymerization .....	33
Polymerization Quench and Work Up .....	33
Kinetics .....	34
Rate Profiles .....	34
Radiolabeling .....	34
Polymer Fractionation .....	37
Molecular Weight Measurement .....	38

	Intrinsic Viscosity .....	40
	GPC .....	40
	IR Analysis .....	40
	Thermal Analysis .....	41
	Stereoelective Polymerizations and Analysis .....	41
	References .....	44
III.	MODIFICATION OF THE CH HETEROGENEOUS SYSTEM .....	45
	Introduction .....	45
	Experimental .....	47
	Materials .....	47
	Preparation of Catalysts .....	47
	Polymerizations .....	48
	Kinetic Isotope Effect (KIE) .....	48
	Active Site Determination .....	48
	Results .....	51
	Discussion of Results .....	61
	Conclusions .....	66
	References .....	68
IV.	STEREOSELECTIVE POLYMERIZATION OF $\alpha$ - OLEFINS BY HETEROGENEOUS CHIRAL ZIEGLER-NATTA CATALYSTS .....	69
	Introduction .....	69
	Experimental .....	71
	CH((R,S)-2MBP) and CH*((S)-2MBP) .....	71
	CW*((-)-MBz) .....	73
	Polymerizations .....	73
	Results .....	74
	Polymerization Activities of Linear and Branched $\alpha$ -Olefins .....	74
	Kinetics of 4MP Polymerization .....	79
	Stereoelective Polymerizations .....	90
	Effect of Optically Active and Racemic Lewis Bases .....	95
	Discussion of Results .....	100
	Conclusions .....	115
	References .....	116
V.	MgCl <sub>2</sub> SUPPORTED HIGH MILEAGE CATALYSTS FOR OLEFIN POLYMERIZATION, AN NMR STUDY ...	117

Introduction .....	117
Experimental .....	119
Results .....	121
CW System .....	121
Magnesium Chloride/Ethylbenzoate .....	121
MgCl <sub>2</sub> /EB/p-Cresol .....	121
MgCl <sub>2</sub> /EB/PC/Triethylaluminum .....	128
MgCl <sub>2</sub> /EB/PC/TEA/TiCl <sub>4</sub> .....	132
CH System .....	135
MgCl <sub>2</sub> ·EH/PA .....	135
TiCl <sub>4</sub> ·BP .....	138
MgCl <sub>2</sub> ·BP .....	138
MgCl <sub>2</sub> ·TiCl <sub>4</sub> ·BP .....	143
MgCl <sub>2</sub> ·EH/PA/TiCl <sub>4</sub> .....	143
MgCl <sub>2</sub> ·EH/PA/TiCl <sub>4</sub> /BP .....	148
MgCl <sub>2</sub> ·EH/PA/TiCl <sub>4</sub> /BP + TiCl <sub>4</sub> Wash .....	148
Discussion .....	153
Conclusions .....	164
References .....	165
VI. STEREOSPECIFICITY AND STEREOELECTIVITY OF HOMOGENEOUS OLEFIN POLYMERIZATION CATALYSTS .....	166
Introduction .....	166
Experimental .....	168
Catalyst .....	168
MAO .....	169
Polymerization of Propylene .....	169
Polymerization of 4MH .....	169
Polymer Characterization .....	170
Results .....	171
Effect of Polarity of the Solvent .....	171
Stereo selective Polymerization of 4MH .....	175
Discussion .....	179
Conclusions .....	189
References .....	191
VII. CONCLUSIONS AND FUTURE WORK .....	194
BIBLIOGRAPHY .....	201



## LIST OF TABLES

Table	Page
3.1 Titanium Content of CH Catalysts.....	52
3.2 Polymerization of Propylene with CH Catalysts.....	57
3.3 Comparison of Various $MgCl_2$ Supported Catalysts.....	60
3.4 Comparison of Active Site Concentrations.....	65
4.1 Polymerization of $\alpha$ -Olefins by Various Ziegler-Natta Catalysts.....	76
4.2 GPC Molecular Weights for P4MH and PDMO.....	78
4.3 Thermal Transition Data of P4MH Obtained by Different Catalysts.....	80
4.4 Kinetic Parameters for 4MP and Propylene Polymerization with CW Catalyst.....	89
4.5 Stereoelective Polymerizations of Racemic $\alpha$ -Olefins.....	91
4.6 Microstructure of Stereoelectively Polymerized P4MH and PDMO Catalyzed with $CH^*((S)2MBP)$ .....	93
4.7 Kinetic Parameters of Propylene Polymerized with Various CH Type Catalysts.....	99
5.1 $^{13}C$ NMR Parameters for $MgCl_2/EB$ .....	123
5.2 $^{13}C$ NMR Parameters for $MgCl_2/EB/p$ -Cresol.....	126
5.3 $^{13}C$ NMR Parameters for $MgCl_2/EB/p$ -Cresol/TEA.....	130
5.4 $^{13}C$ NMR Parameters for $MgCl_2/EB/PC/TEA/TiCl_4$ .....	134
5.5 $^{13}C$ NMR Parameters for $MgCl_2 \cdot EH/PA$ .....	137
5.6 $^{13}C$ NMR Parameters for $TiCl_4 \cdot BP$ .....	140
5.7 $^{13}C$ NMR Parameters for $MgCl_2 \cdot BP$ .....	142

5.8	$^{13}\text{C}$ NMR Parameters for $\text{MgCl}_2 \cdot \text{TiCl}_4 \cdot \text{BP}$ .....	145
5.9	$^{13}\text{C}$ NMR Parameters for $\text{MgCl}_2 \cdot \text{EH/PA/TiCl}_4$ .....	147
5.10	$^{13}\text{C}$ NMR Parameters for $\text{MgCl}_2 \cdot \text{EH/PA/TiCl}_4 /$ BP.....	150
5.11	$^{13}\text{C}$ NMR Parameters for $\text{MgCl}_2 \cdot \text{EH/PA/TiCl}_4 /$ BP + $\text{TiCl}_4$ Wash.....	152
6.1	Fractional Distribution of Polypropylene Polymerized with ETIZC/MAO.....	173
6.2	DSC Melt Endotherms and Molecular Weights for Polypropylene Fractions..	174
6.3	Stereoelective Polymerizations of 4MH with (S)-ETHIZ/MAO.....	176
6.4	Microstructure of Stereoelectively Polymerized 4MH Catalyzed by (S)- ETHIZ/MAO.....	177
6.5	Molecular Weights of Poly(4MH) from Polymerization with (S)-ETHIZ/MAO.....	178
6.6	Comparison of P4MH Melt Transitions.....	180

## LIST OF FIGURES

Figure		Page
1.1	Depiction of $\text{TiCl}_3$ Active Site Described by Cossee and Arlman.....	3
1.2	Lowest Energy Configuration for $\text{TiCl}_3$ Active Site.....	4
1.3	Enantiomeric $\text{TiCl}_3$ Active Sites.....	13
1.4	Model of ETHIZC Active Site Proposed by Corradini.....	18
2.1	Supported Catalyst Synthesis Reactor.....	28
2.2	Gas Polymerization Apparatus.....	32
2.3	Typical DPM/mg Versus MeOH Equivalents Curve for the Calculation of the KIE.....	36
2.4	Apparatus for Sequential Solvent Extraction of Polymer.....	39
3.1	Variation of Tritium Specific Activity Versus Equivalents of MeOH* for Total Polymer.....	49
3.2	Variation of Tritium Specific Activity Versus Equivalents of MeOH* for Isotactic Fraction.....	50
3.3	Propylene Polymerization Profiles for CH(EH) Catalysts.....	55
3.4	Propylene Polymerization Profiles for CH(2-O) Catalysts.....	56
3.5	Variation of Metal-Polymer Bond Concentration Versus Yield for the Total Polymer.....	58
3.6	Variation of Metal-Polymer Bond Concentration Versus Yield for the Isotactic Fraction.....	59
4.1	Polymerizations of 4MP by CW Catalyst at 50°C.....	81



4.2	Variation of [MPB] Versus Yield for P4MP Obtained with CW(-B <sub>e</sub> ) Catalyst.....	83
4.3	Variation of [MPB] Versus Yield for P4MP Obtained with CW(+B <sub>e</sub> ) Catalyst.....	85
4.4	Variation of [MPB] Versus Yield for Stereoirregular P4MP.....	87
4.5	Variation of R <sub>p</sub> Versus Time of Propylene Polymerization Catalyzed by CH((R,S)2MBP).....	97
4.6	Variation of R <sub>p</sub> Versus Time of Propylene Polymerization Catalyzed by CH* ((S)2MBP).....	98
4.7	Variation of [MPB] Versus Yield of Propylene Polymerization Catalyzed by CH* ((S)2MBP).....	101
4.8	Variation of [MPB] Versus Yield of Propylene Polymerization Catalyzed by CH((R,S)2MBP).....	103
4.9	Possible Mechanism for Removal of B <sub>i</sub> by Aluminum Alkyl.....	106
4.10	Minimum Energy Conformations for (R)DMO and (S)4MH.....	111
5.1	MAS-CP <sup>13</sup> C NMR Spectrum of MgCl <sub>2</sub> /EB.....	122
5.2	MAS-CP <sup>13</sup> C NMR Spectrum of MgCl <sub>2</sub> /EB/ p-Cresol.....	124
5.3	MAS-CP <sup>13</sup> C NMR Spectrum of MgCl <sub>2</sub> /EB/ p-Cresol/TEA.....	129
5.4	Comparison of MAS-CP <sup>13</sup> C NMR Spectra for Differently Aged MgCl <sub>2</sub> /EB/PC/TEA Catalyst.....	131
5.5	MAS-CP <sup>13</sup> C NMR Spectrum of MgCl <sub>2</sub> /EB/PC/ TEA/TiCl <sub>4</sub> .....	133
5.6	Liquid <sup>13</sup> C NMR Spectrum of MgCl <sub>2</sub> ·EH/PA in CDCl <sub>3</sub> .....	136
5.7	MAS-CP <sup>13</sup> C NMR Spectrum of TiCl <sub>4</sub> ·BP.....	139
5.8	MAS-CP <sup>13</sup> C NMR Spectrum of MgCl <sub>2</sub> ·BP.....	141

5.9	MAS-CP $^{13}\text{C}$ NMR Spectrum of $\text{MgCl}_2 \cdot \text{TiCl}_4 \cdot \text{BP}$ .....	144
5.10	MAS-CP $^{13}\text{C}$ NMR Spectrum of $\text{MgCl}_2 \cdot \text{EH}/$ $\text{PA}/\text{TiCl}_4$ .....	146
5.11	MAS-CP $^{13}\text{C}$ NMR Spectrum of $\text{MgCl}_2 \cdot \text{EH}/$ $\text{PA}/\text{TiCl}_4/\text{BP}$ ... ..	149
5.12	MAS-CP $^{13}\text{C}$ NMR Spectrum of $\text{MgCl}_2 \cdot \text{EH}/\text{PA}/$ $\text{TiCl}_4/\text{BP} + \text{TiCl}_4$ Wash.....	151
5.13	Possible Structures of Monoester/Metal Complex.....	155
5.14	Possible Structures of Diester/Metal Complex.....	161
6.1	Profiles of Propylene Polymerization Catalyzed with ETIZC/MAO in Various Solvents.....	172
6.2	Considered Bond Rotations in Insertion Models.....	185
6.3	Possible Path for Continuous Si Insertion.....	187
6.4	Possible Path for Continuous Re Insertion.....	188

## CHAPTER I

### INTRODUCTION

#### Early Systems

Since the discovery by Natta in 1954 of isotactic polypropylene, there has been much research aimed at the creation of such stereoregular materials.<sup>1</sup> Key to this research is the understanding of the mechanism for the stereoselection.

The first work in polypropylene polymerization was with the  $\text{TiCl}_4/\text{AlR}_3$  system.<sup>2</sup> Yields of isotactic polypropylene were low and this stereoregular fraction had to be isolated by solvent extractions. The yield of the isotactic polymer could be increased by the use of  $\alpha\text{-TiCl}_3$ , that is  $\text{TiCl}_4$  that has been reduced with hydrogen.<sup>3</sup> The activity was further increased by grinding either the  $\alpha\text{-}$  or the  $\gamma\text{-}$  modifications mechanically, thereby producing the disordered crystalline  $\delta\text{-}$  modification.<sup>4</sup>

Electron donors have been used in these systems to increase activity and/or stereospecificity depending upon the catalyst and the polymerization conditions. The effects of the donor are not well understood and there are conflicting results concerning these. They may be due to

the complexes formed between the metal alkyl and the donor, selective poisoning or conversion of aspecific sites to isospecific sites.<sup>5,6</sup>

The significant advance made in the discovery of the so called Solvay catalyst must be noted.<sup>7</sup> In this system,  $\beta$ - $\text{TiCl}_3$  is produced at low temperature by the interaction of  $\text{TiCl}_4$  with  $\text{Et}_2\text{AlCl}$ . The resultant precipitate is treated with diisoamylether. After washing, the solid is treated with fresh  $\text{TiCl}_4$ .

It is believed that the diisoamylether extracts out the  $\text{AlCl}_3$  contained in the initial solid and, thus, produces a large surface area. Also, a large number of unsaturated potential active centers are believed to be produced. Upon subsequent treatment with  $\text{TiCl}_4$ , it is believed that the site structure of the epitaxially placed  $\text{TiCl}_4$  is conducive for active site creation. The resultant activity is about  $715 \text{ g polymer}(\text{mmol Ti} \cdot \text{h})^{-1}$  and the isotactic index (II, the amount of heptane insoluble polymer) is 95%.

### Active Site Models

In the cases of the heterogeneous catalysts, several authors have given explanations of the stereospecific nature of these systems.<sup>8-10</sup> The most accepted model is that proposed by Arlman and Cossee.<sup>11</sup> The stereospecific



active site is seen as a Ti ion on the 100 edge of an  $\alpha$ - $\text{TiCl}_3$  crystallite. The resultant Ti species is surrounded by one alkyl ligand and four Cl ions. Three of the chlorides are below the crystallite plain while the remaining one is exposed or lies above the crystallite plain (figure 1.1).

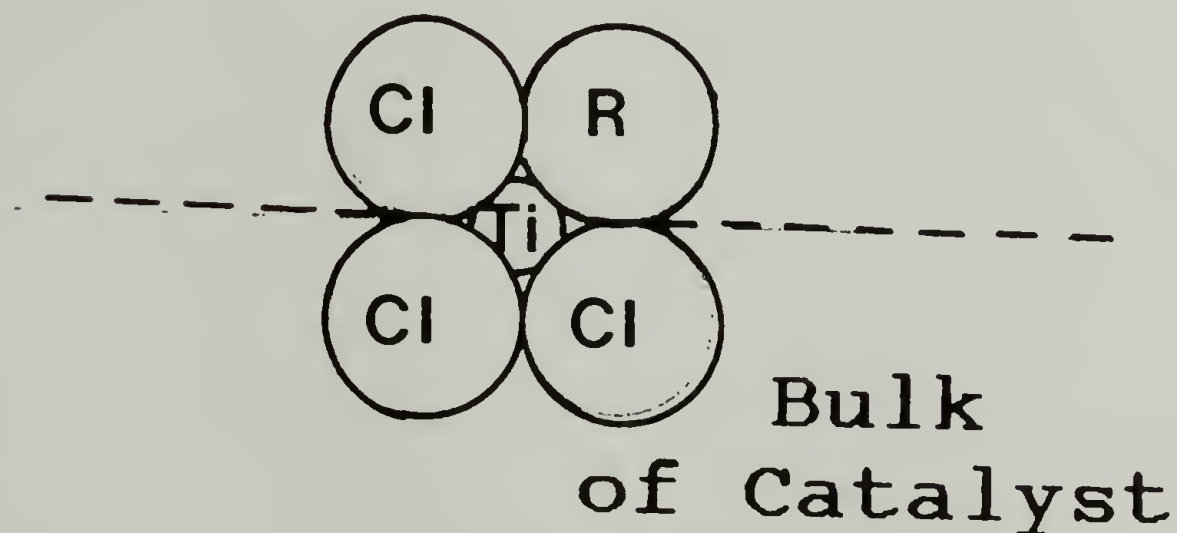
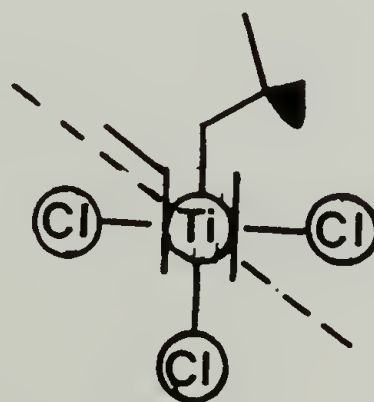


Figure 1.1 Depiction of  $\text{TiCl}_3$  Active Site Described by Cossee and Arlman.

The Cossee model is one of least movement during the insertion step. The olefin to be inserted is coordinated parallel to the alkyl (or polymer) ligand so when insertion occurs, only a perpendicular movement of the

alkyl ligand occurs; there is no rotation. In this proposed mechanism four possible coordinations are possible prior to the insertion. But for steric reasons only two are energetically feasible and one much more so than the other. As shown in figure 1.2, this is the coordination where the methyl of the propylene monomer has the least interaction with the crystalline bulk and the polymer chain.



Bulk  
of Catalyst

Figure 1.2 Lowest Energy Configuration for  $\text{TiCl}_3$  Active Site.

One problem in the mechanism of the Cossee model is the proposed shift of the polymer position when the insertion occurs. When the insertion is completed, the polymer chain occupies the site previously coordinated to the olefin. The resultant active site is a mirror image of the initial. For isotactic polymerization of propylene to occur, coordination must always occur at one coordination vacant position and after insertion the polymer chain must migrate back to that position. An aspecific site would be one where two vacant coordination positions are present. And if the migration to the original position does not occur after insertion, syndiotactic polymerization should result.

Another phenomenon which cannot be explained is the influence of the main group metal alkyl on the polymerization stereospecificity. The effect of the main group metal ligands was shown in some elegant NMR investigations by Zambelli and co-workers.<sup>12</sup> When metal alkyl halides are used as opposed to the metal alkyls, a 10% increase in the stereoregulation of the system occurs. This may be indicative of interaction between Ti-Cl and the metal alkyl.

More recent steric calculations by Corradini et al also support the suppositions of Cossee for stereochemical control.<sup>13</sup> Stereoregulation can be explained by considering near neighbor steric interactions.

### Termination Reactions

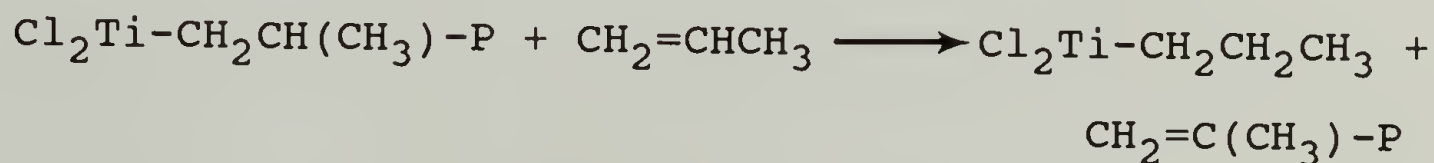
Three modes of chain termination reactions have been proposed by Natta.<sup>14</sup> Transfer to the metal alkyl co-catalyst and transfer to the monomer are both dependent upon the monomer concentration. The spontaneous termination or  $\beta$ -hydride elimination is independent of the monomer concentration.

The proposed mechanisms are as follows:

transfer to metal alkyl:



transfer to monomer:



$\beta$ -hydride elimination:



The  $\beta$ -hydride elimination process is not prominent in the heterogeneous systems at temperatures below 60° C.  $\beta$ -hydride eliminations play a larger role in the homogeneous catalyst polymerizations where the polymers formed have relatively low molecular weight.



### The $\text{MgCl}_2$ Supported Systems

The problem of stereochemical control became evident when improved activities were obtained by supporting  $\text{TiCl}_3$  or  $\text{TiCl}_4$  on  $\text{MgCl}_2$ .<sup>15</sup>  $\text{MgCl}_2$  is probably the best support because of the similarity of the unit cell dimensions of that and  $\text{TiCl}_3$ .<sup>16</sup> The activities were increased by some three orders of magnitude because of more efficient use of the metal in the active site formation. But the stereoregularity was decreased to below 50% ( about the same as that obtained from the  $\text{TiCl}_4$ /triethylaluminum (TEA) system).

The supposed problem was the creation of exposed  $\text{TiCl}_3$  species which had a plane of symmetry. To counteract this development, electron donors were used in an attempt to block these potential aspecific sites.<sup>17</sup> The formulation of the  $\text{MgCl}_2$  supported systems are often complex as evidenced by the plethora of patents and literature concerning them.

Crystalline  $\text{MgCl}_2$  will not support  $\text{TiCl}_4$  efficiently without modification. The low surface area and lack of unsaturated surfaced defects leave little opportunity for epitaxial placement of the Ti. There are several ways to increase the surface area; ball-milling is the classical method.<sup>18</sup> The large energy/surface area expended in the

ball-milling process breaks up the  $\text{MgCl}_2$  crystallites and converts them from cubic close packing to a rotational disordered material. New faces are revealed as lateral fractures of the crystallite are created.

An aromatic ester is usually employed in the ball-milling process. The ester is believed to coordinate with the new surface, stabilizing it.<sup>19</sup>  $\text{TiCl}_4$  may be co-ground for the epitaxial placement to occur or the resultant support may be immersed in  $\text{TiCl}_4$  at elevated temperatures for the affixation.<sup>17,20</sup>

Several other methods may be used in the creation of the support. These include the chlorination of Grignards or magnesium alkyls<sup>21,22</sup> and precipitation of the support from  $\text{MgCl}_2$  adduct solutions in the presence of  $\text{TiCl}_4$ .<sup>23</sup> These methods, however, usually require precomplexing agents, again organic esters, to control the precipitation in the formation of the support.

As stated before, the as formed  $\text{MgCl}_2$  supported Ti catalyst exhibits high activity albeit low stereoselectivity when activated with the aluminum alkyl. To raise the stereoselectivity of the system, electron donors such as esters, amines, or siloxanes are introduced with the aluminum alkyl.<sup>24-26</sup> The resultant isotactic index may be increased to >92% The particular donor which is effective is peculiar to the particular system. But generally, aromatic esters are the most widely used.

Now, the elucidation of the possible mechanism in the polymerization is complicated by the number of components of the system. The specific roles of the donors added in the procatalyst formation (internal base) and those added with the aluminum alkyl co-catalyst (external base) are under dispute.

The role of the internal base may be either one of complexation with both  $\text{MgCl}_2$  and Ti forming the active species or by controlling the fixation of the Ti (as described before) and, thus, playing an indirect role for the active site. In support of the former, Chien<sup>27</sup> and Spitz<sup>28</sup> have seen in the IR a broadening of the carbonyl stretch of ethylbenzoate (EB) when  $\text{MgCl}_2 \cdot \text{EB}$  is treated with  $\text{TiCl}_4$ , whereas, Sevini<sup>16</sup> actually saw a band intermediate between that of  $\text{MgCl}_2 \cdot \text{EB}$  and  $\text{TiCl}_4 \cdot \text{EB}$ . From experimental data Kezler and Simon<sup>29</sup> also concluded that a ternary complex forms for  $\text{TiCl}_4/\text{EB}$  ratios were constant despite the duration of the ball-milling process.

Terano et al through a combination of thermal analysis and FTIR have shown the contrary.<sup>30</sup> Peaks in differential thermal analysis were identified for specific decompositions of complexes  $\text{MgCl}_2 \cdot \text{EB}$  and  $\text{TiCl}_4 \cdot \text{EB}$ . At long periods of grinding  $\text{MgCl}_2$  with  $\text{EB}/\text{TiCl}_4$  the endotherm unique to the  $\text{TiCl}_4$  complex disappears. In addition, the FTIR band ( $1568 \text{ cm}^{-1}$ ) for the carbonyl in the  $\text{TiCl}_4 \cdot \text{EB}$



complex disappears. Conversely, catalyst activity and isospecificity increases with grinding time.

Regardless of the form of the active species, the internal base has been found to increase the number of active sites and even to increase the propagation constant of the sites.<sup>31</sup> The isospecificity has also been seen to increase with  $\text{MgCl}_2/\text{EB}$  ratio reaching a constant value.<sup>29</sup>

Without an external base, the isotacticity of the polypropylene produced is only about 50%. Upon use of the donor in a molar ratio empirically optimized, the stereospecificity of the system can be improved to better than 90%. Again the role of this donor is disputed. Two roles have been proposed. One is the preferential poisoning of the aspecific sites with little or no poisoning of the isospecific sites.<sup>32</sup> The other is the conversion of the aspecific sites to isospecific sites.<sup>33</sup> Also, it has been said that both modes may be operative.<sup>34</sup>

One must keep in mind that the species of interest in the alkylaluminum external base co-mixture is not merely the electron donor but the reaction product of the donor and the alkylaluminum. The alkylaluminum donor complexes and the reaction products have been identified in FTIR.<sup>27</sup> Indeed, set stoichiometric ratios of alkylaluminum to donor give optimal performance. For example, for the aromatic esters, the ratio is usually 2.0 to 2.5<sup>35</sup> and for organosilanes, it is about 20.<sup>36</sup>



On addition of the external donor to the catalyst system, a drop in the overall activity is seen.<sup>37</sup> Also, there is an increase in the activity decay rate. The molecular weight distribution broadens as the molecular weight of the heptane insoluble fraction increases.

Some authors have seen little or no decrease in the propagation rate of the isospecific sites.<sup>38-40</sup> On the contrary in some cases, an increase in the isospecific propagation rate has been seen. Kashiwa, using stop flow polymerization techniques, has measured the doubling of the isotactic propagation rate when the external donor is introduced.<sup>41</sup>

In an experiment to show the external donor's ability to convert the aspecific sites to isospecific sites, Soga prepared a catalyst that was  $\text{TiCl}_3$  supported on  $\text{MgCl}_2$ .<sup>44</sup> This catalyst when activated with TEA produces atactic polypropylenes. When EB is introduced, activity drops significantly but accompanying this is the production of isotactic polymer. At a ratio of 2.5 for Al/EB, 94% isotactic polymer is produced after a 50 fold rate drop. Also of evidence is the increase in molecular weight with EB addition and an appearance of a melt endotherm at  $160^\circ\text{C}$  which is not present in the polymer produced in the absence of EB. This seems to unequivocally show that the external donor can convert an aspecific site to an isospecific one.

In the course of discussions concerning the polymerization of propylene, one receives the impression that only two types of active sites exist: those that produce heptane insoluble or isotactic polymer and those that produce soluble or atactic polymer. But in practice, the soluble fraction may be separated further by employing the appropriate solvents in soxhlet extractions.<sup>43</sup> By this method the polymer is separated not only by molecular weight but by microtacticity as evidenced by NMR and FTIR.<sup>44</sup> Because of this evidence a variety of active sites may be postulated.

### Stereoelective Polymerizations

Two factors characterize an active center. One is the stereospecificity imposed by the steric nature of the ligand field and the other is the chirality which is determined by the spatial arrangement of the ligands. Octahedral sites are chiral when they possess at least two bidentate ligands as defined by the IUPAC nomenclature.<sup>45</sup> Thus, there may be two chiralities of the active site with lambda or delta configuration. These are depicted in figure 1.3 for an  $\alpha$ -TiCl<sub>3</sub> isospecific site model.

The first evidence of the two chiral sites was given in the polymerization of (R),(S)-4-methyl-1-hexene (4MH) with the TiCl<sub>3</sub>/Al(i-bu)<sub>3</sub>(TIBA) system.<sup>46</sup> The polymer

produced gave no rotation to plain polarized light (in the case of prevalent chirality of one enantiomer, optical rotation would be evident) But when a solution of the polymer was passed through a column containing poly((S)-3-methyl-1-pentene), the fractions that were eluted were of opposite chirality as evidenced by the optical rotation that they exhibited.

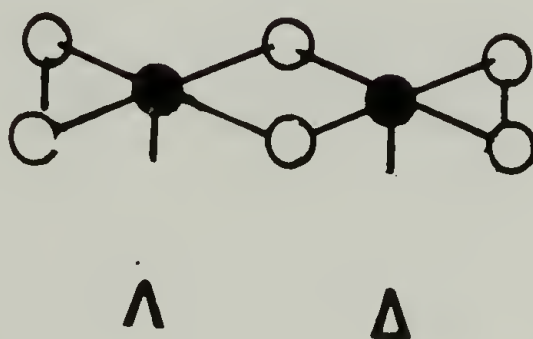


Figure 1.3 Enantiomeric  $\text{TiCl}_3$  Active Sites.

This prompted investigators to modify the chiral character of the active sites by the use of an optically active third component. Bulky olefins such as (-)- $\alpha$ -

pinene were used to modify the  $\text{TiCl}_4/\text{AlR}_3$  for the polymerization of (R),(S)-3,7-dimethyl-1-octene (DMO).<sup>47</sup> It must be remembered that the active species in these experiments is  $\text{TiCl}_3$  <ARA>. Therefore, chiral sites are present. Small stereoelective (that is the preference of one enantiomer to polymerize) inductions were present (<1.5%). A surprising result was the large stereoelectivity induced when poly((R)-4-phenyl-1-hexene) was present. Optical purity of the polymerized monomer was 11.5%.<sup>48</sup> This showed that a chiral matrix could increase the selection at the site.

In the studies of the polymerization of (R),(S)-4MH with the system  $\text{MgCl}_2/(-)\text{-menthylanisate/TiCl}_4//\text{TIBA}$ , Pino first showed that supported catalysts contained various steric structures.<sup>49</sup> The poly(4MH) was fractionated with acetone, ethylacetate, ethylether, diisopropylether, and methylcyclohexane. The prevailing chirality of the total polymer was R. But the amorphous ethylacetate soluble fraction had S chirality, the same as the unpolymerized monomer. But the optical purity of the amorphous polymer was higher than the unpolymerized monomer indicating that the polymerization in the stereoirregular polymer was stereoelective.

It was proposed that at least two types of sites existed, the chiral  $C_1$  and  $C_d$  sites (of the chiral configurations described previously) and the achiral C



sites. The former stereospecific sites were said to be modified by the complexation of the electron donor in the following manner. The relative stabilities of the  $C_1 \cdot B$  versus the  $C_d \cdot B$  complexes determine the chiral preference of the system. If, for example,  $C_1 \cdot B$  is less stable, it will dissociate more than the other complex and prevail in the polymerization. Complexed sites should not be active. C sites may be converted to isospecific sites by complexation. If the complexation is stable, isospecific polymerization will result. If the base dissociates and reassociates in another coordination vacancy producing a mirror site, stereoblock polymers should result.

One experiment of interest performed by Pino was the variation of the internal base/Ti ratio and comparison of the resultant rate drops in the polymerizations of propylene, 4MH, and DMO.<sup>50</sup> At (-)-menthylanisate/Ti of 0.05, propylene had a decrease in rate of 35%, 4MH - 55%, and DMO - 70%. For propylene and 4MH the decrease in the productivity of the stereoirregular fraction was much greater than that of the stereoregular fraction. For DMO the decrease in both of the fractions was the same. This suggests that DMO is polymerized by more exposed sites than propylene and 4MH. Thus, the structure of the monomer determines what sites polymerize it.

This does not seem to be the case for linear olefins. Chien showed in active site counting in the polymerization

of propylene and 1-decene with the  $\text{MgCl}_2/\text{EB}/p\text{-cresol}/\text{TEA}/\text{TiCl}_4//\text{TEA}/\text{methyl-}p\text{-toluate}$  system that the same number of sites polymerize both monomers.<sup>51</sup> The only difference in the polymerizations were the propagation constants.

### Homogeneous Systems

The first homogeneous system was  $\text{Cp}_2\text{TiCl}_2/\text{AlR}_2\text{Cl}$  ( $\text{Cp} = \eta^5\text{-cyclopentadienyl}$ ).<sup>52</sup> The activity in the polymerization of ethylene was low ( $1.2 \times 10^4$  g P/mol Ti·atm·hr) and the polymers had relatively low MW. This catalyst was unable to polymerize  $\alpha$ -olefins. The breakthrough in homogeneous systems was the discovery by Kaminsky and co-workers that oligomeric aluminoxanes increase the activities of these systems to  $10^6$  g P/mol Ti·atm·hr and for the first time the polymerization of propylene was possible.<sup>53</sup>

These catalysts were still poor in the polymerization of propylene having low activity and producing atactic polymer. Ewen had reported that at low temperatures  $\text{Cp}_2\text{TiPh}_2/\text{methylaluminumoxane}$  (MAO) polymerized propylene with some degree of chain end stereochemical control.<sup>54</sup>

The first bridged metallocene chiral systems were synthesized by Brintzinger and co-workers.<sup>55</sup> These were ethylenebis(tetrahydroindenyl)zirconiumdichloride (ETHIZC)

and ethylenebis(indenyl)zirconiumdichloride (ETIZC). Other systems with chiral ligands have been synthesized since then.

Kaminsky has claimed that the previously mentioned bridged ligand systems are able to polymerize propylene to highly isotactic polymer.<sup>56</sup> These results were disputed by Chien et al who showed that the polymers had low isotacticity as demonstrated by  $^{13}\text{C}$  NMR (mmmm < 90%) and low DSC melt endotherms ( $\leq 154^\circ\text{C}$ ).<sup>57</sup> Chien coined the term anisotactic to describe the polymer which was stereoblock in nature as a result of a large number of non-correcting misinsertions.

Also observed in the study was the dependence of the isotacticity on the MAO concentration indicating that MAO plays some role in the stereochemical environment. The activity decreased and the rate of deactivation increased with decrease in MAO concentration.<sup>58</sup>

In his calculations Corradini has shown that the stereoselectivity of the active species may be explained by the near neighbor interactions.<sup>59</sup> Figure 1.4 shows a model of the active site described by Corradini. The bulk of the polymer chain is forced to the quadrant of least steric interference. The coordination of the olefin is then on the enantiomeric face which provides the least steric interaction with the polymer chain during the insertion. This model does not consider the type of

misinsertions discussed by Chien.<sup>57</sup> But the model was supported by the elegant hydro-oligomerization studies performed by Pino using the pure (R)-ETHIZC/MAO system with propylene.<sup>60</sup> The results showed that 80% of the (S)-oligomer was produced as would be predicted.

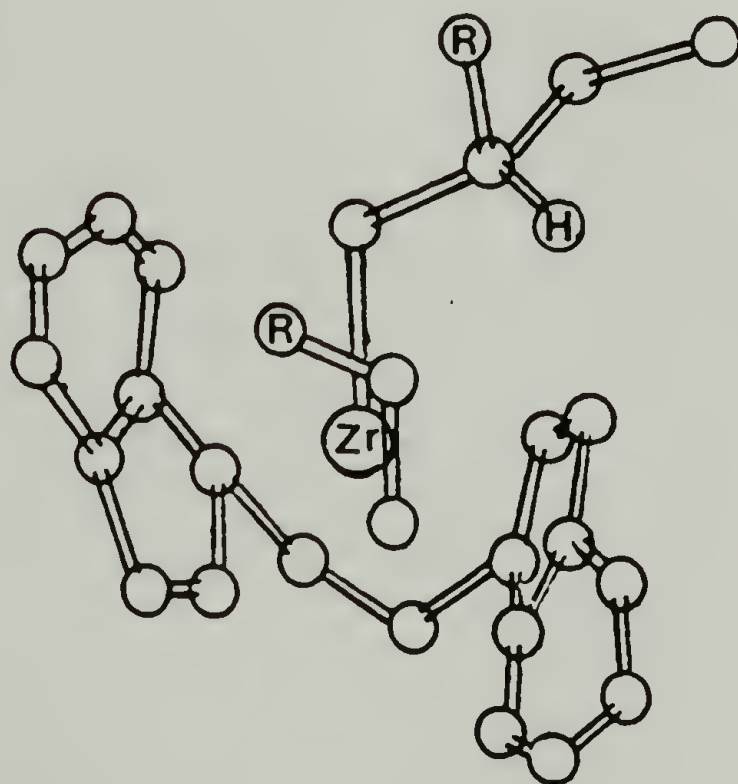


**Figure 1.4** Model of ETHIZC Active Site Proposed by Corradini.

The synthesis of MAO is dangerous and of low yield making the study of these systems costly in both time and money.<sup>55</sup> A major advance was the synthesis by Jordon of a



stable cationic alkyl species,  $\text{Cp}_2\text{ZrMe}(\text{THF})^+ \cdot \text{B}\phi_4^-$ , supporting the belief of many that the active species is cationic in nature.<sup>61</sup>

This species polymerized ethylene slowly because of the presence of a Lewis base. Hlatky et al isolated a base free complex containing a stable peralkylated ( $\text{B}\phi'_4$ ) anion,  $\text{Cp}^*_2\text{Zr}^{(+)}-\phi'\text{B}\phi'_3(-)$   $\text{Cp}^*=\text{C}_5\text{Me}_5$ , possessing high activity.<sup>62</sup> As can be seen, the active species was actually a zwitterion.

Zambelli also was able to form a base free system by using dimethylaluminumfluoride (DMAF) with ETHIZC.<sup>63</sup> The activity was two orders of magnitude lower than when MAO was used but the stereoregulating ability of the system was comparable. He postulated that the DMAF was able to form a stable anion.

Now, a major thrust of various laboratories is to make such cationic catalysts. New ligands for various types of stereoregular polymerizations are being synthesized. And an effort is being made to eliminate the  $\beta$ -hydride terminations to raise the molecular weight.

### Statement of the Problem

The main interest of this research is the characterization of the  $\text{MgCl}_2 \cdot 3\text{-ethyl-1-hexanol}$  (EH)/Phthalic Anhydride(PA)/ $\text{TiCl}_4$ /di-isobutylphthalate(BP)

procatalyst.<sup>64</sup> This procatalyst when activated with (TEA) and the electron donor Phenyltriethoxysilane(PES) becomes a system which can polymerize propylene with an activity of 16 Kg/g Ti·atm·hr having an isotactic index (that part which is insoluble to boiling heptane) of 98%. This is four fold more active than its progenitor MgCl<sub>2</sub>/Ethylbenzoate(EB)/p-cresol(PC)/TEA/ TiCl<sub>4</sub>//TEA/Methyl-p-toluate(MPT)<sup>34</sup> and the isospecificity is 2% higher.

The former catalyst presented above was termed the CH system in previous studies in our group and was seen that the sites classified to be isotactic and atactic had the same propagation constant ( $k_p$ ) as the latter system above termed the CW catalyst. The main difference was a greater number of isospecific sites, 25% as compared to 6.7%, and aspecific sites, 15% as compared to 6.3%.<sup>38</sup> This was found to arise from greater structural disorder of the support as seen by X-ray which created more potentially active sites.<sup>64</sup>

The question arises as to what other differences between the CW and the CH catalysts exist. Subtleties concerning the stereochemical nature have been observed in the studies of such systems that contain optically active components. Supported systems modified in this way have modest enhancements in the stereoelective polymerization of racemic monomers, that is, there is a slight enantiomeric preference. Pino and Ciardelli have performed such

work and more recently, Ciardelli and co-workers have investigated a modified CW system.<sup>65</sup> The type of information which can be gleaned from such studies concerns the elucidation of separate types of stereochemical sites.

Another useful method in the analysis of supported catalyst systems is the use of solid state NMR spectroscopy.<sup>66</sup> Shifts in peak positions can reveal useful information as to the chemical environment of each component in the system. Relaxation and cross-polarization times reflect the degree of molecular motion within the system.

In this project the previous types of analysis have been used to compare and contrast the two systems, CH and CW. The behavior of the catalysts in the polymerization of racemic branched  $\alpha$ -olefins was observed. Also, the catalyst syntheses were dissected and the changes were observed using solid NMR techniques.

The last group of catalysts of interest are the unsupported or homogeneous systems. Those of particular interest are the bridged ansa-metallocenes ETIZC and ETHIZC. Two problems present themselves. What is the role of MAO if any in the stereochemistry of the system? And how efficient is the chiral metal center in stereoelective polymerization?

If the catalyst is really a cation-anion pair, possibly increase in the solvent polarity will cause some separation of the ion pair and affect the stereochemistry. This has been investigated in this project.

Since the ETHIZC may be isolated in an enantiomerically pure form, studies of the stereoelective polymerization of  $\alpha$ -olefins as described previously may be performed. Of interest is how efficient is the stereoelective process and the presence of more than one type of active site.



## References

1. G. Natta, P. Pino, P. Corradini, F. Danusso, E. Mantica, G. Mazzanti, and G. Moragio, *J. Am. Chem Soc.*, **77**, 1708 (1955).
2. J. Boor, **"Ziegler-Natta Catalysts and Polymerizations"**, Academic Press, New York, 109-111 (1979).
3. J. Boor, **"Ziegler-Natta Catalyst and Polymerizations"**, 95.
4. Z.W. Wilchinsky, R.W. Looney. and E.G.M. Tornquist, *J. Catal.*, **28**, 399 (1961).
5. A.D. Caunt, *J. Polym. Sci., Part C.*, **4**, 49 (1963).
6. T. Keii, **"Kinetics of Ziegler-Natta Polymerization"**, Kodansha Ltd., Tokyo, 164-170 (1972).
7. R.P. Nielson in **"Transition Metal Catalyzed Polymerizations"**, R.P., Quirk, Ed., Harwood Acad. Press, New York, 47-82 (1983).
8. L.A.M. Rodriguez and H.M. Looy, *J. Polym. Sci.*, (A-1), **4**, 1951 (1966).
9. K.J. Ivin, J.J. Rooney, and C.D. Stewert, *J. Chem. Soc. Comm.*, 603 (1978).
10. J.D. Fellman, G. A. Rupprecht, and R.R. Schrock, *J. Am. Chem. Soc.*, **101**, 5099 (1979).
11. E.J. Arlman and P. Cossee, *J. Catal.*, **3**, 80 (1964).
12. A. Zambelli, M. Sacchi, P. Locatelli, and G. Zannoni, *Macromol.*, **15**, 211 (1982).
13. P. Corradini, V. Baroni, and G. Guerra, *Macromol.*, **15**, 1242 (1982).
14. G. Natta and I. Pasquon, **Advances in Catalysis**, **11**, 1 (1959).
15. Montedison S.p.A., British Patent 1,286,867 (1972).
16. P.C. Barbe, G. Cecchin, L. Noristi, *Adv. in Polym. Sci.*, **81**, 3 (1987).
17. Montedison S.p.A., British Patent 1,387,890 (1975).

18. R. Gerbasi, A. Marigo, A. Martorana, R. Zannetti, G. Guidetti, and G. Baruzzi, **Eur. Polym. J.**, **20**, 967 (1984).
19. B. Kezler, G. Bodor, and A. Simon, **Polymer**, **21**, 1037 (1984).
20. Montedison S.p.A. and Mitsui Petrochemical Ltd., German Offen. 2,643,143 (1977).
21. L.L. Bohm, **Polymer**, **19**, 545 (1978).
22. D.R. Burfield, **Polymer**, **25**, 1645 (1984).
23. Montedison S.p.A., U.S. Patent 4,107,413 (1978).
24. P. Pino and R. Mulhaupt, **Angew. Chem. Int. Ed. Engl.**, **19**, 857 (1980).
25. P. Pino, R. Ratzinger, and E. von Achenbach, **Makromol. Chem. Suppl.**, **13**, 105 (1985).
26. J. Seppala, M. Harkonen, and L. Luciani, **Makromol. Chem.**, **190**, 2535 (1989).
27. J.C.W. Chien, J.C. Wu, and C.I. Kuo, **J. Polym. Sci., Polym. Chem. Ed.**, **21**, 725 (1983).
28. R. Spitz, J.L. Lacombe, and A. Guyot, **J. Polym. Sci., Polym. Chem. Ed.**, **22**, 2641 (1984).
29. B. Kezler and A. Simon, **Polymer**, **23**, 916 (1982).
30. M. Terano, T. Kataoka, and T. Keii, **J. Polym. Sci., Polym. Chem. Ed.**, **28**, 2035 (1990).
31. J.C.W. Chien and Y. Hu, **J. Polym. Sci., Polym. Chem. Ed.**, **25**, 2847 (1987).
32. V. Busico, P. Corradini, L. DeMartino, A. Proto, V. Savino, and E. Albizzati, **Makromol. Chem.**, **186**, 1279 (1985).
33. K. Soga, T. Sano, K. Yamamoto, and T. Shiono, **Chem. Lett.**, 425 (1982).
34. K. Soga, T. Shiono, and Y. Doi, **Makromol. Chem.**, **189**, 1531 (1988).
35. J.C.W. Chien, J.C. Wu, and C.I. Kuo, **J. Polym. Sci., Polym. Chem. Ed.**, **20**, 2019 (1982).

36. Montedison S.p.A., U.S. Patent 4,107,413 (1978).
37. N. Kashiwa, M. Kawasaki, and J. Yoshitake in **"Catalytic Polymerizations of Olefins"**, T. Keii and K. Soga, Eds., Kodanashi Ltd., Tokyo, 43 (1986).
38. J.C.W. Chien and Y. Hu, **J. Polym. Sci., Polym. Chem. Ed.**, **26**, 2973 (1988).
39. V.A. Zakharov, G.D. Bukatov, and Y.I. Yerkamov, **Polymer Sci. and Tech.**, **19** (1983).
40. G.D. Bukatov, S.H. Shepelev, V.A. Zakharov, S.A. Sergeev, and Y.I. Yermakov, **Makromol. Chem.**, **182**, 2657 (1982).
41. N. Kashiwa and Y. Yoshitake, **Polym. Bull.**, **11**, 479 (1984).
42. K. Soga, J.R. Park, T. Shiono, and N. Kashiwa, **Makromol. Chem., Rapid Commun.**, **11**, 117 (1990).
43. G. Natta, **J. Polym. Sci.**, **34**, 531 (1959).
44. D.R. Burfield and P.S.T. Doi in **"Catalytic Polymerization of Olefins"**, 387.
45. **"Nomenclature of Inorganic Chemistry"**, **Pure Appl. Chem.**, **28**, 1 (1971).
46. P. Pino, F. Ciardelli, G.P. Lorenzi, and G. Natta, **J. Am. Chem. Soc.**, **84**, 1487 (1962).
47. C. Carlini and F. Ciardelli, **Chim. Ind.**, **63**, 486 (1981).
48. C. Carlini, R. Noristi, and F. Ciardelli, **J. Polym. Soc., Polym. Chem. Ed.**, **15**, 767 (1977).
49. P. Pino, G. Fochi, O. Piccolo, and U. Giannini, **J. Am. Chem. Soc.**, **104**, 7381 (1982).
50. P. Pino, G. Guastalla, B. Rotzinger, and R. Mulhaupt, in **"Transition Metal Catalyzed Polymerizations"**, p. 435.
51. J.C.W. Chien and T. Ang, **J. Polym. Sci., Polym. Chem. Ed.**, **25**, 1011 (1987).
52. D.S. Breslow and N.R. Newburgh, **J. Am. Chem. Soc.**, **79**, 5072 (1957).



53. H. Sinn and W. Kaminsky, **Adv. Organomet. Chem.**, **18**, 99 (1980).
54. J.A. Ewen, **J. Am. Chem. Soc.**, **106**, 6355 (1984).
55. F.R.W.P. Wild, L. Zsolnai, G. Huttner, and H.H. Brintzinger, **J. Organomet. Chem.**, **232**, 233 (1982).
56. W. Kaminsky, K. Kulper, H.H. Brintzinger, and F.R.W.P. Wild, **Ang. Chem.**, **97**, 507 (1985).
57. B. Rieger, X. Mu, D.T. Mallin, M.D. Rausch, and J.C.W. Chien, **Macromol.**, **23**, 3559 (1990).
58. J.C.W. Chien and R. Sugimoto, **J. Polym. Sci., Polym. Chem. Ed.**, **29**, 459 (1991).
59. P. Corradini, G. Guerra, M. Vacatello, and V. Villani, **Gazz. Chim. Ital.**, **118**, 173 (1988).
60. P. Pino, M. Cioni, J. Wei, and N. Piccolrovazzi in **"Transition Metals and Organometallics for Olefin Polymerization"**, W. Kaminsky and H. Sinn, Eds., Springer-Verlag, Berlin, 269 (1988).
61. R.F. Jordon, C.S. Bajgur, R. Willet, and B. Scott, **J. Am. Chem. Soc.**, **108**, 7410 (1986).
62. G.G. Hlatky, H.W. Turner, and R.R. Eckman, **J. Am. Chem. Soc.**, **111**, 2728 (1989).
63. A. Zambelli, L. Pasquale, and A. Grassi, **Macromol.**, **22**, 2186 (1989).
64. Y. Hu and J.C.W. Chien, **J. Polym. Sci., Polym. Chem. Ed.**, **26**, 2003 (1988).
65. F. Ciardelli, C. Carlini, A. Altomare, F. Menconi, and J.C.W. Chien in **"Transition Metal Catalyzed Polymerizations"**, R.P. Quirk, Ed., Cambridge Univ. Press, Cambridge, 25 (1988).
66. L. Abis, E. Albizzati, U. Giannini, E. Santoro, and L. Noristi, **Makromol. Chem.**, **189**, 1595 (1988).



## CHAPTER II

### EXPERIMENTAL METHODS

#### Handling and Purification of Chemicals

All chemicals were handled by Schlenk techniques under dry argon. The argon was purified by passing through Cu/CuO catalyst and 13X molecular sieves. Solvents were distilled from Na under argon prior to use. Propylene monomer was purified in the same manner as the argon. The other liquid monomers were distilled from Na.

#### Catalyst Synthesis

##### MgCl<sub>2</sub>

MgCl<sub>2</sub> was purified and dried by passing HCl gas over it at 380°C for 30 minutes. Argon was then passed through at the same temperature for 5 minutes and then the material was vacuum dried for 5 hours.

#### Catalyst Synthesis Reactor

The reactor developed by Hu and Chien and used in the synthesis of the supported catalysts is depicted in figure

2.1.1 The joints were all greased with Apiezon T grease except for the stirring post which was lubricated with the Apiezon M grease. The reactor was vacuumed and flame dried prior to use. All additions, reactions, and filtrations were performed within this reactor.

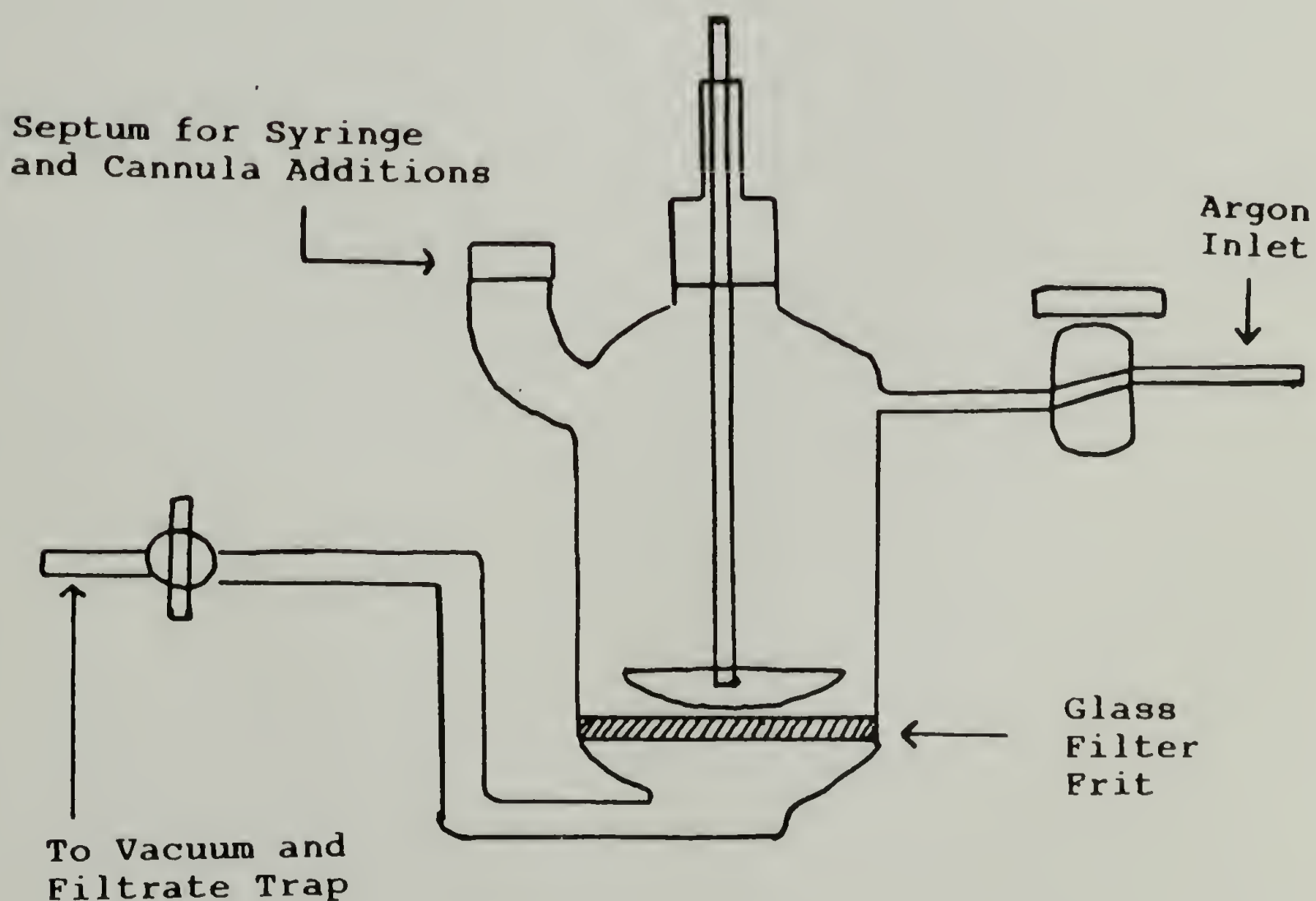


Figure 2.1 Supported Catalyst Synthesis Reactor.

### CW System<sup>2</sup>

Anhydrous  $\text{MgCl}_2$  and ethylbenzoate ( $\text{MgCl}_2/\text{EB} = 6.5$  mol/mol) were ball-milled under argon for 72 hours. Freshly distilled p-cresol was added slowly to the support which was suspended in n-heptane ( $\text{MgCl}_2/\text{PC} = 2.0$ ). The mixture was stirred for 1 hour at  $50^\circ\text{C}$ . Triethylaluminum ( $\text{MgCl}_2/\text{TEA}$ ) was then added at room temperature. The support was stirred for one hour. It was filtered, washed with heptane and resuspended in heptane.  $\text{TiCl}_4$  was then added ( $\text{TiCl}_4/\text{MgCl}_2 = 5.7$ ). The mixture was stirred for one hour at  $100^\circ\text{C}$ . The final catalyst was then filtered and washed with heptane. A catalyst slurry of known concentration was made in heptane. Typical Ti content of the catalyst was 3.5% by weight.

### CH System<sup>1</sup>

A  $\text{MgCl}_2$  alcohol adduct was synthesized by reacting anhydrous  $\text{MgCl}_2$  with 2-ethyl-1-hexanol ( $\text{EH}/\text{MgCl}_2 = 3.0$ ) in decane for two hours at  $110^\circ\text{C}$ . Phthalic anhydride ( $\text{MgCl}_2/\text{PA} = 6.5$ ) was added and the clear adduct solution was stirred at that temperature for another hour.

The adduct solution was dropped into neat  $\text{TiCl}_4$  ( $\text{TiCl}_4/\text{MgCl}_2 = 40$ ) at  $-20^\circ\text{C}$  over a one hour period. The temperature was then increased steadily to  $110^\circ\text{C}$  over a four hour period. At that time diisobutylphthalate was added ( $\text{MgCl}_2/\text{BP} = 5.0$ ). The mixture was stirred for two

hours at the same temperature. The catalyst was filtered. It was then resuspended in  $\text{TiCl}_4$  (the same amount as initially used). It was then stirred for two hours after which it was hot filtered and washed with decane. When the mixture was cooled sufficiently, heptane washes were performed. Typical Ti content was 2.0% by weight.

### Modified CH Catalysts

Modifications were made by changing the alcohol of the  $\text{MgCl}_2$  adduct and the diester used. Changes of the alcohol required changes in the synthesis procedure. Those adducts with 2-octanol and 2-methyl-1-butanol were not soluble in decane at room temperature. The adducts were more soluble in toluene at  $40^\circ\text{C}$  so this solvent and temperature were used in the manipulation of the adducts. Because of the poor solubility, the Ti content of those catalysts were higher than the original progenitor.

Optically active esters were synthesized from the respective optically active alcohols and phthaloyl-dichloride. In a typical synthesis 200 mmol of the alcohol was placed in a dry Schlenk tube with 198 mmol of pyridine and ether solvent. 83.2 mmol of phthaloyldichloride was then dropped in slowly. The solution was stirred for twelve hours at room temperature. It was washed with 1%  $\text{HCl}$  followed by 1%  $\text{NaHCO}_3$  and finally with



distilled water. The ester was isolated by vacuum distillation.

## Polymerizations

### Propylene Polymerizations

Heterogeneous Systems. The polymerization apparatus shown in figure 2.2 was used in the polymerization of propylene. The reactor was a 250 ml glass bottle sealed with a rubber septum and a crown cap. The reactor was dried overnight at 200°C. After being capped, it was attached to the polymerization line and vacuumed and subsequently filled with argon for six cycles. 50 ml of heptane solvent was introduced via cannula. 2.0 mmol of TEA was then introduced via syringe. The argon was removed and replaced with 22 psig of propylene. The reactor was then heated to polymerization temperature (typically 50°C). The external base was introduced (for the CW system, 0.66 mmol of methyl-p-toluate and for the CH system, 0.10 mmol of phenyltriethoxysilane). The catalyst was then introduced as a slurry in heptane (0.012 mmol of Ti) to initiate the polymerization.

Homogeneous Systems. The preparation for homogeneous polymerizations was similar to that of the heterogeneous

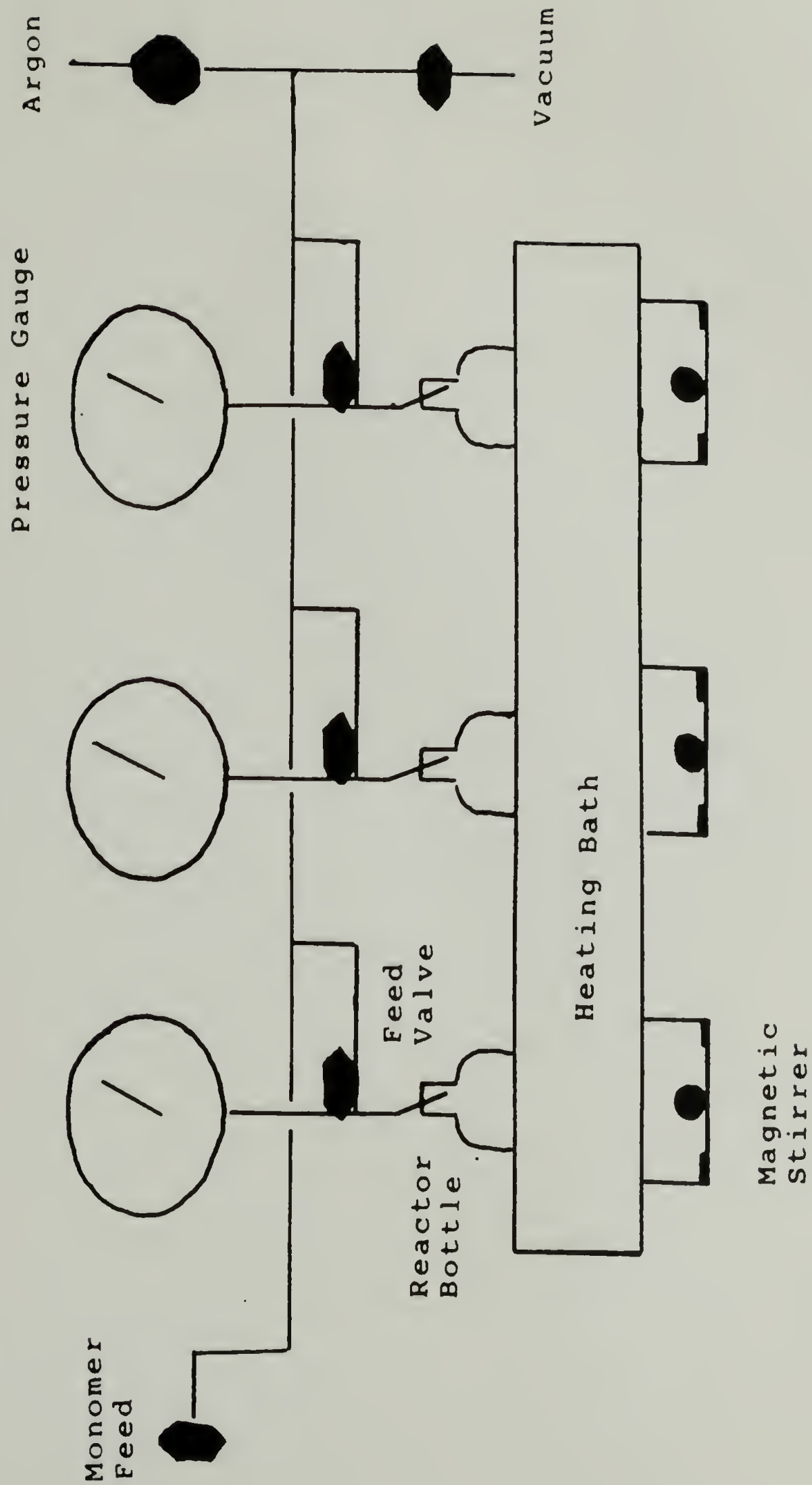


Figure 2.2 Gas Polymerization Apparatus.

with the following exceptions. 50 ml of toluene was used as the solvent. Methylaluminumoxane (7.7 mmol of Al) in toluene was introduced via syringe followed by replacement of the argon atmosphere with propylene. 0.29  $\mu$ mol of the catalyst was then introduced to begin the polymerization.

### Higher $\alpha$ -Olefin Polymerizations

Because these monomers are liquids, the polymerization apparatus previously described is not necessary. Instead, polymerizations were simply carried out in Schlenk tubes. The same addition protocol was followed as for the propylene polymerizations. Because of low activities of some of the monomers, low monomer to Ti ratios of 1200 and 300 were used (for propylene polymerizations, the ratio was 3600). This was achieved by using neat monomer and raising the concentration of the catalyst.

### Polymerization Quench and Work Up

Polymerizations were quenched with a 2% HCl/MeOH solution. In the case of propylene polymerizations, the reactor was first evacuated and filled with argon. The polymer was stirred in the acidic medium for 12 hours to insure catalyst removal. (Because these are high activity catalysts, this de-ashing step is not really necessary for yield measurement. But for subsequent intrinsic viscosity

and GPC analysis, this is necessary to insure the removal of insoluble particulates.) The polymer is filtered, washed with copious amounts of MeOH and vacuum dried.

## Kinetics

### Rate Profiles

Polymerization rates were obtained at various points in time. For propylene polymerizations, the measurement was made by stopping the monomer feed flow into the reactor and observing the monomer uptake within the reactor. Typically, the flow was not halted for more than one minute. After the restoration of the flow, there was a one minute interval until the next measurement was made. This was to insure that the monomer solubilization reached a steady state.

For the liquid monomers, polymerizations had to be halted at various times and the yield measured. The rate was then calculated from the tangents to the yield time curves.

### Radiolabeling

To obtain active site concentrations, the polymerizations were quenched with tritiated methanol (MeOH\*, 24 mCi/mol) and analyzed using a Beckman 1800 scintillation counter. To obtain meaningful data, the kinetic isotope



effect (KIE) needed to be measured. This was made by running six 30 minute polymerizations and quenching each with 0.5, 1.0, 2.0, 3.0, 6.0 and 12.0 equivalents of MeOH\* (an equivalent is equal to the number of metal alkyl bonds. For the heterogeneous Ti systems, 1 equivalent =  $4[\text{Ti}] + 3[\text{Al}]$ ). Figure 2.3 shows a typical DPM/mg versus equivalent curve. At around 1.0 equivalent all of the tritium will react. At higher amounts, hydrogen will preferentially react by a factor which is the KIE. So KIE would be equal to the peak DPM value divided by the value at the high equivalent plateau.

For active site counting, six polymerizations were run for various time periods. A typical experiment consisted of polymerization times of 5, 10, 15, 20, 25, and 30 minutes. Each polymerization was quenched with 4.0 equivalents of MeOH\* with a contact time of 4.5 hours. 2% HCl/MeOH was then introduced to remove the catalyst. After 12 hours of stirring, the polymers were filtered, washed with methanol, and vacuum dried.

Scintillation counting was then performed and the metal-polymer bond concentration ([MPB]) was calculated as follows:

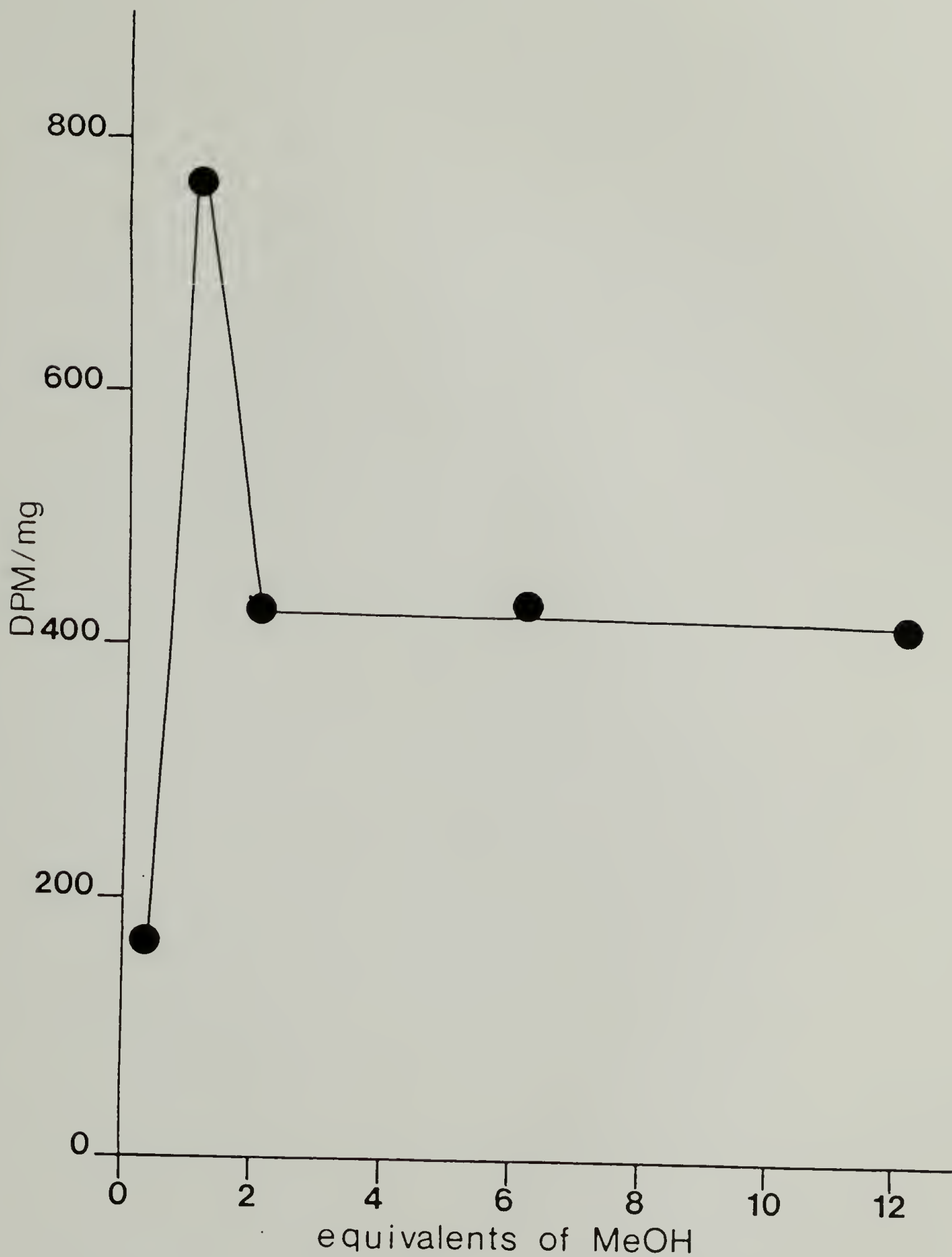


Figure 2.3 Typical DPM/mg Versus MeOH Equivalents Curve for the Calculation of the KIE.

$$\begin{aligned}
[\text{MPB}] = & \text{count(DPM)} \cdot (\text{KIE}/2.2 \times 10^9 (\text{DPM/mCi})) \cdot \\
& (1/[\text{MeOH}^*] (\text{mCi/mol})) \cdot \\
& (\text{Yield mass}/\text{Sample mass}) \cdot \\
& (1/\text{reaction volume(l)})
\end{aligned} \tag{1}$$

A plot was then made of [MPB] versus the yield. The plot fits the following equation:<sup>3</sup>

$$[\text{MPB}] = [\text{C}^*]^\circ + (k_{\text{tr}}^{\text{Al}} Y / k_p [\text{M}]) \tag{2}$$

where  $[\text{C}^*]^\circ$  = the initial active site concentration,  $k_{\text{tr}}^{\text{Al}}$  = the transfer constant to aluminum,  $k_p$  = the propagation constant,  $Y$  = the yield, and  $[\text{M}]$  = the monomer concentration.  $k_p$  is determined from the relationship,  $R_{\text{pmax}} = k_p [\text{C}^*] [\text{M}]$ .

Error in the scintillation counting and the massing of the sample is less than 2.0%. But because of the polymerization activity reproducibility of  $\pm 20\%$ , the extrapolation to zero yield results in errors in the active site concentration in excess of  $\pm 50\%$ .

### Polymer Fractionation

Solvent extraction was used to separate the polymers according to both stereoregularity and molecular weight. Classically, extraction of polypropylene with n-heptane allowed for the separation of the isotactic fraction as the insoluble portion.<sup>4</sup>

The isotactic fraction of the polypropylene was isolated using a soxhlet extractor with a cellulose extraction thimble. Heptane was refluxed into the extractor for 6 hours. After that time, the isolated isotactic fraction was vacuum dried.

For the higher  $\alpha$ -olefins, a different extraction system was used (see figure 2.4). The solvent is refluxed up around the cellulose extraction thimble and drips down into it from the condenser. This modification insures that the solvent in the thimble is always close to the boiling point of the solvent.

For the separation into several fractions, a regiment of solvents was used in the order: acetone, ethylacetate, ethylether, and cyclohexane. The order for polypropylene separation was: acetone, ethylacetate, ethylether, hexane, heptane. Each extraction was performed for 24 hours. After each extraction, solvent was flash evaporated from the pot and the extract was collected and massed.

### Molecular Weight Measurement

Two methods have been utilized in the measurement of molecular weight, gel permeation chromatography and intrinsic viscosity.



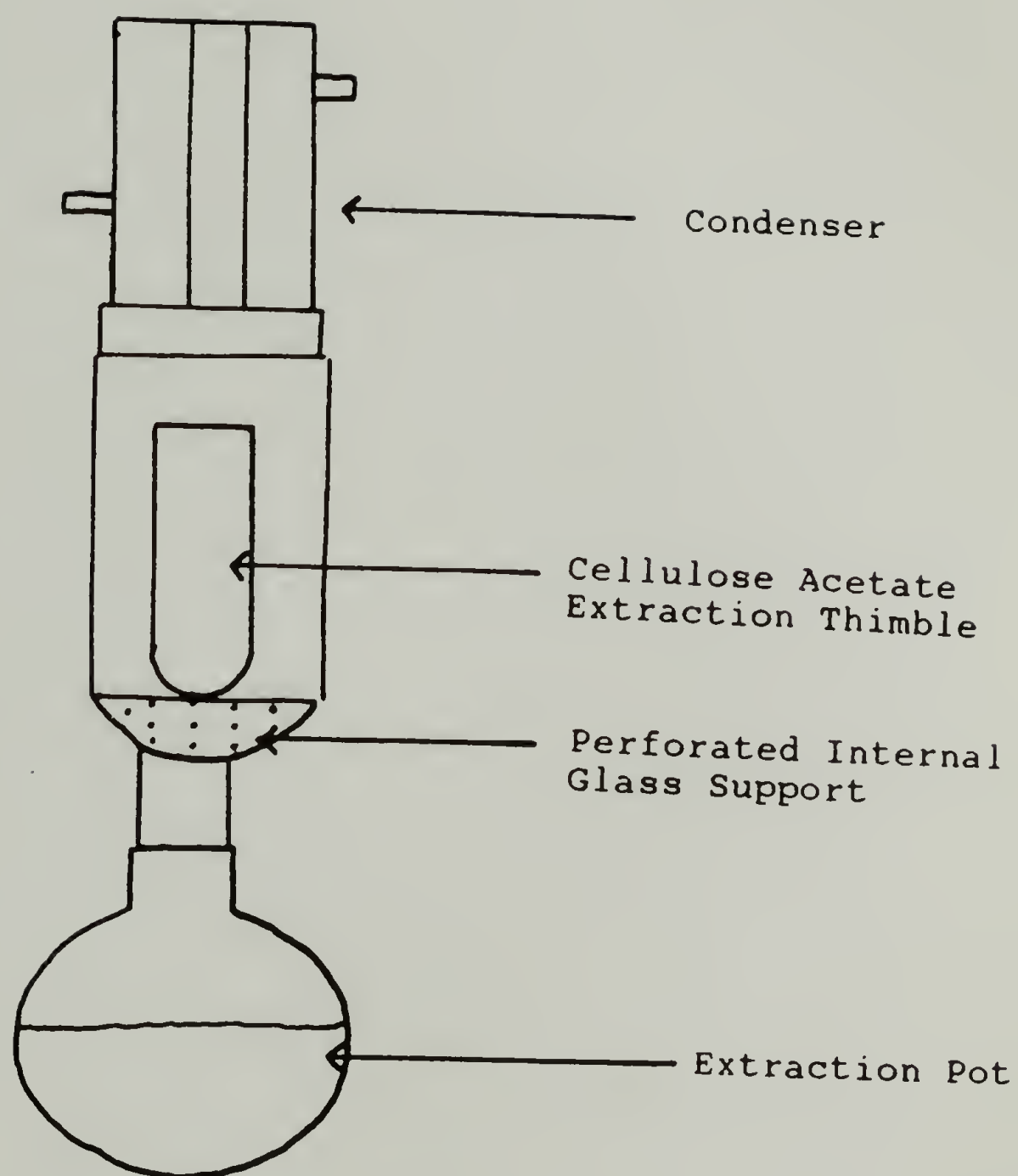


Figure 2.4 Apparatus for Sequential Solvent Extraction of Polymer.

### Intrinsic Viscosity

Intrinsic viscosity measurements were performed on polypropylene samples at 135°C in decalin. 10 ml samples of about 0.5 g/dl were run and diluted with 5 ml of solvent twice to obtain measurements at different concentrations. Extrapolation of  $[\eta_{sp}/c]$  to zero yield gave the intrinsic viscosity. The same method was used for the measurement of poly(4-methyl-1-hexene) (P4MH) except cyclohexane was used as the solvent at 30°C.

The following equations were used to obtain  $M_w$ :  
for polypropylene in decalin at 135°,

$$[\eta] = 1.0 \times 10^{-4} M_w^{0.805}$$

for P4MH in cyclohexane at 30°C,

$$[\eta] = 5.75 \times 10^{-5} M_w^{0.786}$$

### GPC

Chromatographic measurements were made using a Waters 150C ALC/GPC with styrogel columns. The solvent used was trichlorobenzene at a temperature of 135°C. Styrene standards were used for the calibration.

### IR Analysis

The infrared isotactic indices ( $I_s$ ) were obtained for P4MH and poly(3,7-dimethyl-1-octene) (PDMO) on a Perkin Elmer 1600 FTIR spectrometer. The  $I_s$  was found as the

ratio of the absorptions of the band corresponding to vibrations in a helical sequence to an internal reference band.

The ratio for P4MH as given by Pino<sup>7</sup> was  $D_{997}/D_{964}$  with the baseline drawn between 1060 and 935  $\text{cm}^{-1}$ . For PDMO, the ratio was  $D_{1217}/D_{1168}$  with the baseline drawn between 1186 and 954  $\text{cm}^{-1}$ . No distinguishing peaks could be seen for poly(3-methyl-1-hexene) and none have been recorded in the literature.

### Thermal Analysis

The thermal transitions were measured on a Perkin-Elmer DSC 4 instrument. The scan rate was 20°C/min. Three scans were made to approximately 50° above the melt transition. The temperature was held there for 5 minutes and then the sample was cooled at 20°C/min. The data of the third scan was used.

### Stereoelective Polymerizations and Analysis

Polymerizations of racemic monomer with optically active catalyst were performed at low conversion (<40%) so as not to influence the results by any resulting monomer enantiomeric excess. Polymerizations were quenched with methanol and the polymers were filtered under normal

pressure. The polymer was then washed with 2% HCl/MeOH to remove any catalyst residue. The polymers were filtered and vacuum dried.

The filtrate from the first filtration was distilled to remove the olefin/heptane/MeOH azeotrope. The MeOH was removed from the azeotrope by washing with ice water. The remaining mixture was then treated with Br<sub>2</sub> in CCl<sub>4</sub> at 0°C and in the dark. The brominated olefin was isolated by vacuum distillation and regenerated by treatment with Zn in refluxing MeOH. The olefin was isolated by the distilling the olefin/MeOH azeotrope and washing with ice water.

Optical purity of the polymer was determined by the measurement of the optical purity of the monomer using a Perkin Elmer 141 spectrometer having a sensitivity of  $\pm 0.003^\circ$  using 589 nm light at 25°C. Specific optical rotation measurements,  $[\alpha]$ , were obtained at these conditions by the following relationship:

$[\alpha] = \alpha_{\text{obs.}}/c$ , where  $\alpha_{\text{obs.}}$  is the observed optical rotation. In the case of a solution,  $c$  is the concentration in g/ml. In the case of a neat liquid,  $c$  is the density at the measurement temperature.

The  $[\alpha]$  of the neat monomer was obtained and the optical purity of the recovered monomer was obtained as:  
 $P_m = [\alpha]/[\alpha]^\circ$ , where  $[\alpha]^\circ$  is the specific optical rotation of the optical pure monomer. For the monomers used in



this study,  $[\alpha]^\circ$  used were  $+3.03^\circ$ ,  $+28.9^\circ$ , and  $+16.3^\circ$  for (R)-4MH, (S)-3-methyl-1-hexene((S)-3MH) and (S)-DMO, respectively.<sup>8,9</sup>

The purity of the polymerized monomer was determined with the knowledge of  $P_m$  and the % conversion (Y) of the polymerization:  $P_p = ((100-Y)/Y)P_m$

The stereoelective efficiency (E)<sup>10</sup> which is a measure of the effectiveness of the internal base to influence the stereoelectivity of the system was determined by:

$$E = \frac{P_p}{[B^*]/[Ti]} \%$$

where  $[B^*]$  is the concentration of optically active Lewis base.

## References

1. Y. Hu and J.C.W. Chien, *J. Polym. Sci., Polym. Chem. Ed.*, **26**, 2003 (1988).
2. J.C.W. Chien, J.C. Wu, and C.I. Kuo, *J. Polym. Sci., Polym. Chem. Ed.*, **20**, 2019 (1982).
3. J.C.W. Chien and Y. Hu, *J. Polym. Sci., Polym. Chem. Ed.*, **25**, 2847 (1987).
4. G. Natta and I. Pasqual, *Adv. in Catalysis*, **11**, 1 (1959).
5. J.B. Kinsinger and R.E. Hughes, *J. Phys. Chem.*, **63**, 2002 (1959).
6. J.B. Kinsinger and L.E. Ballard, *J. Polym. Sci.*, **A3**, 3963 (1965).
7. P. Pino, *Adv. Polym. Sci.*, **4**, 393 (1965).
8. P. Pino, G. Guastalla, B. Rotzinger, and R. Mulhaupt in *"Transition Metal Catalyzed Polymerizations"*, R.P. Quirk, Ed., Harwood Pub., New York, 435 (1983).
9. R. Lezzaroni, P. Salvadori, and P. Pino, *Tetrahedron Lett.*, 2507 (1986).
10. F. Ciardelli, C. Carlini, F. Menconi, A. Altomare, and J.C.W. Chien in *"Transition Metals and Organometallics as Catalysts for Olefin Polymerizations"*, W. Kaminsky and H. Sinn, Eds., Springer-Verlag, Berlin, 109 (1988).

## CHAPTER III

### MODIFICATION OF THE CH HETEROGENEOUS SYSTEM

#### Introduction

As already described in chapter I, Ziegler-Natta catalysts of greatly improved activity and stereospecificity have been developed using  $\text{MgCl}_2$  as the support. There are many ways to prepare the  $\text{MgCl}_2$  having high surface area such as has been described in the first chapter: ball-milling, precipitation of soluble  $\text{MgCl}_2$  complex, reaction of magnesium alkoxides with  $\text{TiCl}_4$ , etc. In our group, we have been investigating the performance of  $\text{MgCl}_2$  supported catalysts prepared by two methods. The one is the CW procatalyst<sup>1</sup> which is obtained by ball-milling crystalline  $\text{MgCl}_2$  in the presence of Lewis base [ $\text{B}_i$  = ethylbenzoate (EB)]; this support is referred to as c- $\text{MgCl}_2$ . The CW catalyst derived from the c- $\text{MgCl}_2$  support is activated with  $\text{AlEt}_3$  (TEA) and an external Lewis base ( $\text{B}_e$  = methyl-p-toluate). In this system, both the internal and the external Lewis bases are mono-functional esters.

The other system prepared is the CH procatalyst.<sup>2</sup> The support is prepared from a soluble  $\text{MgCl}_2$  alcoholate and phthalic anhydride. This support is referred to as s-

$\text{MgCl}_2$ ; it contains a diester as  $\text{B}_i$ . The support is reacted with  $\text{TiCl}_4$  in the presence of another diester, diisobutylphthalate (BP), to give the procatalyst which is activated with TEA and phenyltriethoxysilane (PES).

The optimum CW and CH catalysts contain 3.5 and 1.9% of Ti, respectively, but the latter is about four times more active than the former. The II (isotacticity index = wt% of refluxing heptane insoluble polymer) of the polypropylene obtained with the CW and CH catalysts is about 92 and 99%, respectively. The s- $\text{MgCl}_2$  and c- $\text{MgCl}_2$  have very similar x-ray diffraction patterns and comparable surface areas, but they behave differently towards the Lewis bases. The best CH catalyst is prepared with a difunctional ester whereas the optimum CW catalysts are obtained with monofunctional esters.<sup>2</sup>

Even though the esters play a very important role in the  $\text{MgCl}_2$  supported catalysts, without the esters the catalysts have a very poor stereoselectivity, there is little knowledge about the relationship between the structure of an ester and its effectiveness in contributing toward the stereospecificity of a  $\text{MgCl}_2$  supported catalyst.

The central purpose of the work described in this chapter was the preparation of a series of CH catalysts using the isomeric pairs of esters to compare their propylene polymerization activities and selectivities and



to relate these performance parameters back to the ester structures. The particular esters were chosen because they could be obtained or prepared in enantiomers. Those optically active catalysts which most closely resemble the original CH catalyst as far as stereospecificity and activity were to be used in the subsequent study of stereoelective polymerization to elucidate the stereochemical functions of the chiral  $B_i$ .

## Experimental

### Materials

The purification of the solvents have been described in chapter II. The 2-ethyl-1-hexanol (EH) and (R)- and (S)-2-octanols (R-2-O and S-2-O) being high boiling solvents were purified in a different manner. The alcohols were dried over 3Å molecular sieves for several days and degassed by bubbling argon through it for one hour. The purification of the commercial BP was the same. Other esters such as (-)-menthylterephthalate (MT) were synthesized from the respective alcohol and terephthaloyl-dichloride as described in chapter II.

### Preparation of Catalysts

The preparation of the modified catalysts was the same as described in the last chapter. When using

alcohols other than EH to form the adduct, toluene was used to solubilize that adduct and manipulations of the adduct were performed at 40°C to insure solubility.

### Polymerizations

Polymerizations were performed in the crown capped polymerization reactors on the gas polymerization line as previously described. Polymerizations were run for 1 hour and the work up of the polymers was in the usual manner.

### Kinetic Isotope Effect (KIE)

The KIE was determined as previously described in chapter II for the CH catalyst containing MT as  $B_i$ . The isotactic fraction obtained after extraction with boiling heptane was also radioassayed. The plots of the specific activity versus the amount of tritiated methanol are shown in figures 3.1 and 3.2. The KIE for the total polymer and the isotactic fractions were 1.82 and 1.64, respectively. These values were in good agreement with those determined for the CW catalyst.<sup>3</sup>

### Active Site Determination

Active site counting was performed as described previously. Radioassay of the total polymer and the isotactic fraction gave the concentration of metal-polymer bonds ([MPB]). The difference between the two gave the

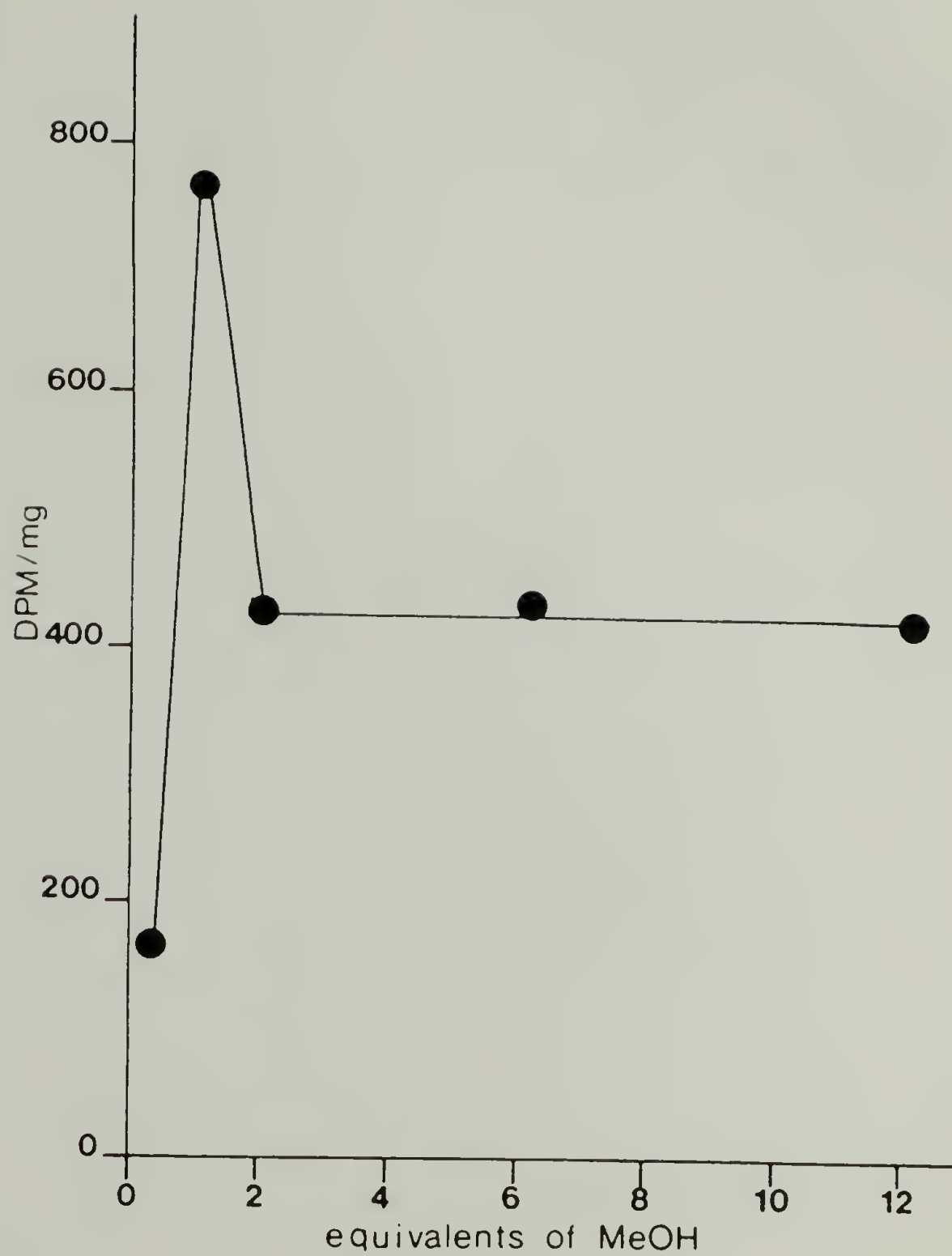


**Figure 3.1** Variation of Tritium Specific Activity Versus Equivalents of MeOH\* for Total Polymer.

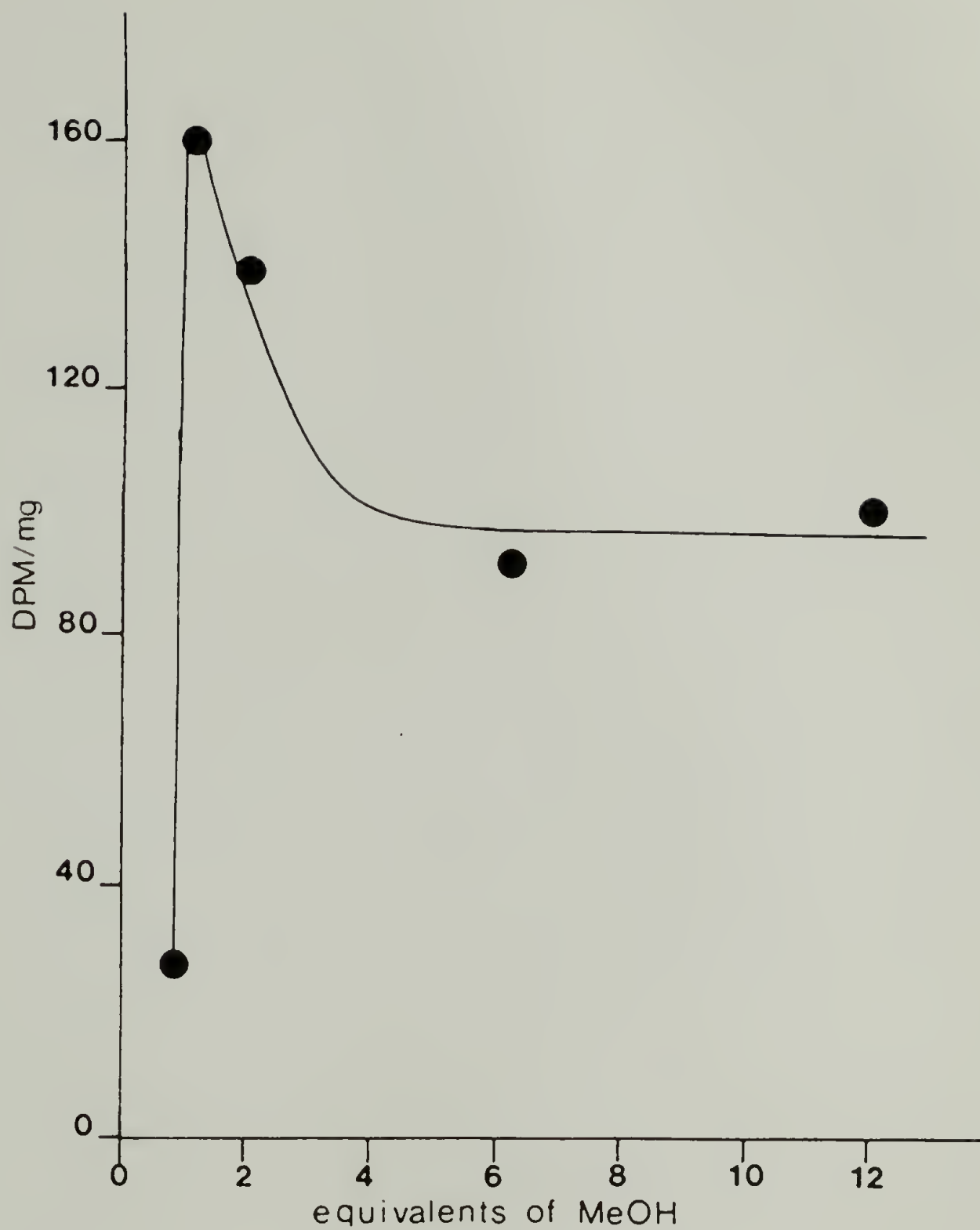


**Figure 3.2** Variation of Tritium Specific Activity Versus Equivalents of MeOH\* for Isotactic Fraction.



[MPB] for the atactic fraction. This procedure is more accurate than one of radioassaying the amorphous fraction directly because of the difficulty of isolating that fraction quantitatively.

### Results

The CH catalysts of this work were prepared with two different alcohols EH and 2-O, and difunctional esters BP, diisobutylterephthalate (BT), di-(-)-menthylphthalate (MP), and di-(-)-menthylterephthalate (MT). The catalysts were designated as CH(EH,BP) etc. according to the constituents of the catalyst as given in table 3.1. The catalysts were also analyzed for titanium; the analyses are given in column 5 of table 3.1.

The amount of Ti in a catalyst depends strongly upon the structure of the diester. The phthalate ester catalysts contain 1.9-2.6% Ti. The amount of Ti is larger for the dimethylphthalate catalysts than that of the diisobutylphthalate catalysts. The terephthalate catalysts contain much greater amounts of Ti, especially for the dimethylterephthalate systems which have 9-13% Ti. The Ti loading in the CH systems is also very sensitive to the alcohol used in the preparation of the  $s\text{-MgCl}_2$  adduct. The catalysts obtained with EH contain much less Ti than the corresponding catalyst obtained with 2-O.

**Table 3.1 Titanium Content of CH Catalysts**

Designation	Alcohol · MgCl <sub>2</sub>	Diester	Color	Ti (wt%)
CH(EH, BP)	2-ethyl hexanol	di- <i>i</i> -butylphthalate	beige	1.89
CH(EH, MP)	2-ethyl hexanol	(-)-dimenthyl phthalate	black	2.10
CH(EH, BT)	2-ethyl hexanol	di- <i>i</i> -butyl terephthalate	brown	2.56
CH(EH, MT)	2-ethyl hexanol	(-)-dimenthyl terephthalate	black	8.9
CH(R-2-O, BP)	(R)-2-octanol	di- <i>i</i> -butyl phthalate	red-brown	2.11
CH(R-2-O, MT)	(R)-2-octanol	(-)-dimenthyl terephthalate	yellow-brown	13.2
CH(S-2-O, BP)	(S)-2-octanol	di- <i>i</i> -butyl phthalate	red-brown	2.63
CH(S-2-O, MT)	(S)-2-octanol	(-)-dimenthyl terephthalate	yellow-brown	12.4

For the EH series the menthyl esters give black catalysts, the butyl esters are lighter in color by comparison, and the CH(EH,BT) is darker than the CH(EH,BP) catalysts. The visible absorption may be due to charge transfer interactions. If this is the case, it may explain the higher Ti contents in the darker catalysts.

The differences in the polymerization activities of the EH and 2-O series prompted a study of the reactions between the alcohols and phthalic anhydride (that is added in the creation of the adduct). 1.11 g (7.5 mmol) of phthalic anhydride and 15 mmol were massed into a Schlenk tube in a dry-box and 30 ml of decane added. The solution was heated to 130°C and reacted with stirring for 1 hour. The EH reaction mixture was homogeneous; proton NMR peak areas of the  $\text{OCH}_2$  of the alcohol and of the ester were in a 1:10 ratio. Thus, the reaction between EH and phthalic anhydride was over 90% complete. In contrast, the reaction mixture of 2-O produced white needles that melted at the same temperature as that for phthalic anhydride. Proton NMR of the supernatant was comprised only of protons of 2-O and decane; there was no absorption between 4.90 and 5.25 ppm expected for the  $\text{OCH}_2$  protons of 2-octylphthalate. The differences between the reactivities of the primary alcohol (EH) and the secondary alcohol (2-O) with phthalic anhydride are large even at 130°C.

Propylene polymerizations were carried out at about 0.24 mM Ti, and Al/Ti ratio of 167 at 50°C activated with 20:1 TEA/PES mixture. The polymerization profiles are shown in figures 3.3 and 3.4. The maximum polymerization rates ( $R_{p,m}$ ) range from 4.7 to  $55 \times 10^{-4} \text{ Ms}^{-1}$ . The performances of the various catalysts are compared in table 3.2. All of the polymerizations show a large decay of the activity to one-fifth to one-fourth of the  $R_{p,m}$  within 0.5 hours. This behavior is generally observed for  $\text{MgCl}_2$  supported high activity catalysts.<sup>1,2</sup>

For a given  $\text{MgCl}_2 \cdot 3\text{ROH}$ , the catalysts prepared with BP have 3-5 fold greater  $R_{p,m}$ 's than the corresponding ones obtained with MT. To compare the CH(EH,MT) with the CH(EH,BP) catalysts, the active site concentration,  $[C^*]$ , was determined by the method outlined in chapter III. The intercept of the plots for the total and isotactic products (figures 3.5 and 3.6) gave the initial  $[C^*]$  for the total and the isospecific sites; the number of aspecific sites was determined from the difference. These quantities had been previously determined for the CH(EH,BP) and CW catalysts.<sup>4</sup> A comparison of these parameters are shown in table 3.3.



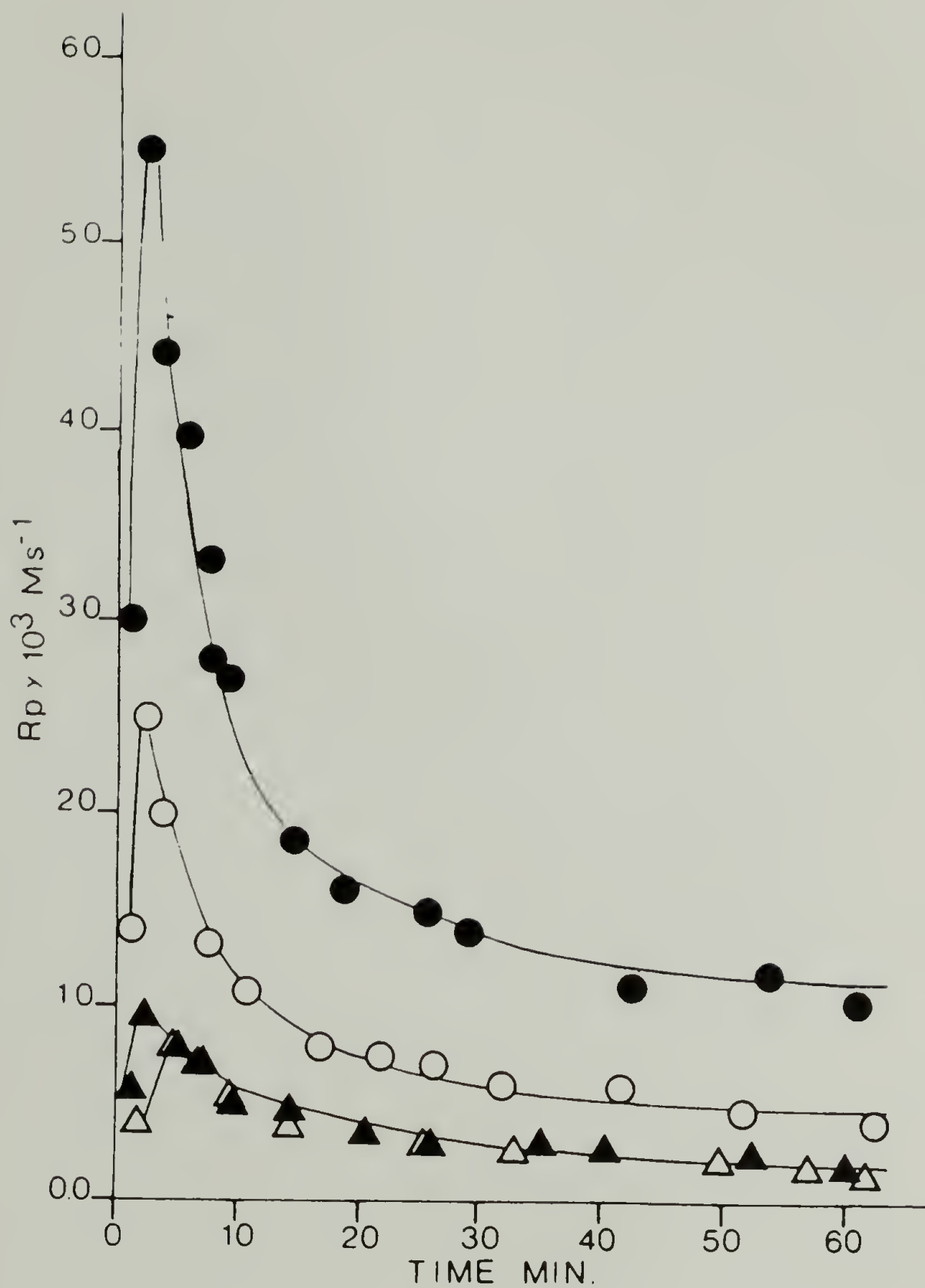


**Figure 3.3** Propylene Polymerization Profiles for CH(EH) Catalysts. ● CH(EH,BP); ○ CH(EH,BT); ▲ CH(EH,MP); △ CH(EH,MT) at  $[\text{Ti}] = 0.24 \text{ mM}$ ,  $[\text{TEA}] = 40 \text{ mM}$ ;  $\text{A/T} = 162$ ;  $[\text{PES}] = 2 \text{ mM}$ ;  $[\text{TEA}]/[\text{PES}] = 20$ ;  $T = 50^\circ$ ,  $\text{PC}_3\text{H}_6 = 20 \text{ psig}$ .

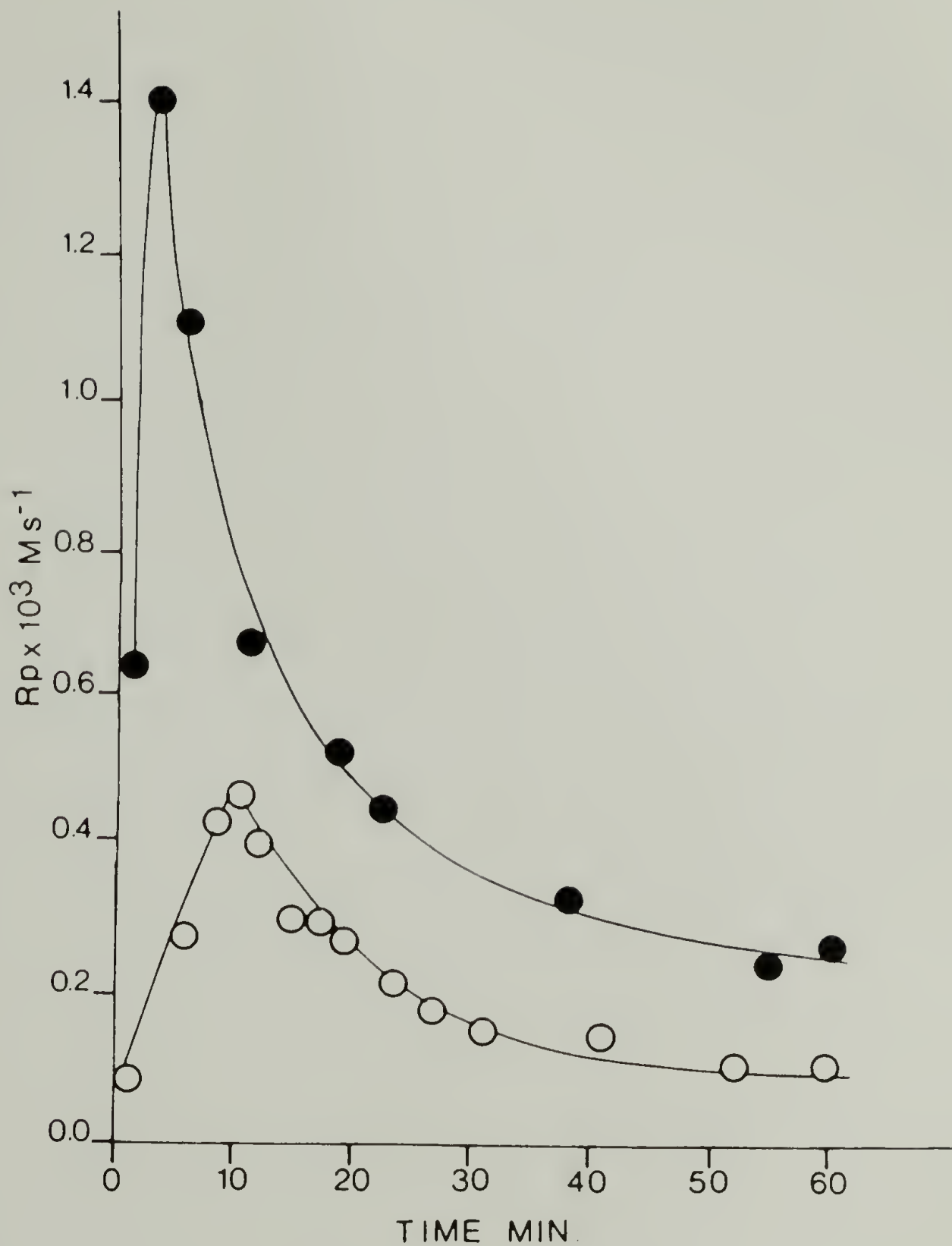


**Figure 3.4** Propylene Polymerization Profiles for CH(2-O) Catalysts. (●) CH(R-2-O, BP) and (○) CH(S-2-O, MT); Conditions are the Same as in Figure 3.3.

**Table 3.2 Polymerization of Propylene with CH Catalysts<sup>a</sup>**

Catalysts	Productivity (kg PP/g Ti-atm h)	$R_{p,m} \times 10^4$ ( $M s^{-1}$ )	$11^b$ (%)	$\bar{M}_n \times 10^{-5}$
CH(EH, BP)	12	55	97.0	3.3
CH(EH, MP)	3.3	9.6	89.1	
CH(EH, BT)	6.2	24	89.9	
CH(EH, MT)	2.4	8.0	84.7	1.2
CH(R-2-O, BP)	5.9	14	91.8	1.3
CH(R-2-O, MT)	1.5	4.7	72.3	1.1

<sup>a</sup> Polymerization conditions [Ti] ~ 0.2 mM, A/T = 167, temperature = 50°C, coactivator 20 TEA/1 PDS, [M] = 0.71-0.73M.

<sup>b</sup> Extraction with boiling *n*-heptane for 6 h.

<sup>c</sup> Measured in decalin at 135°C.

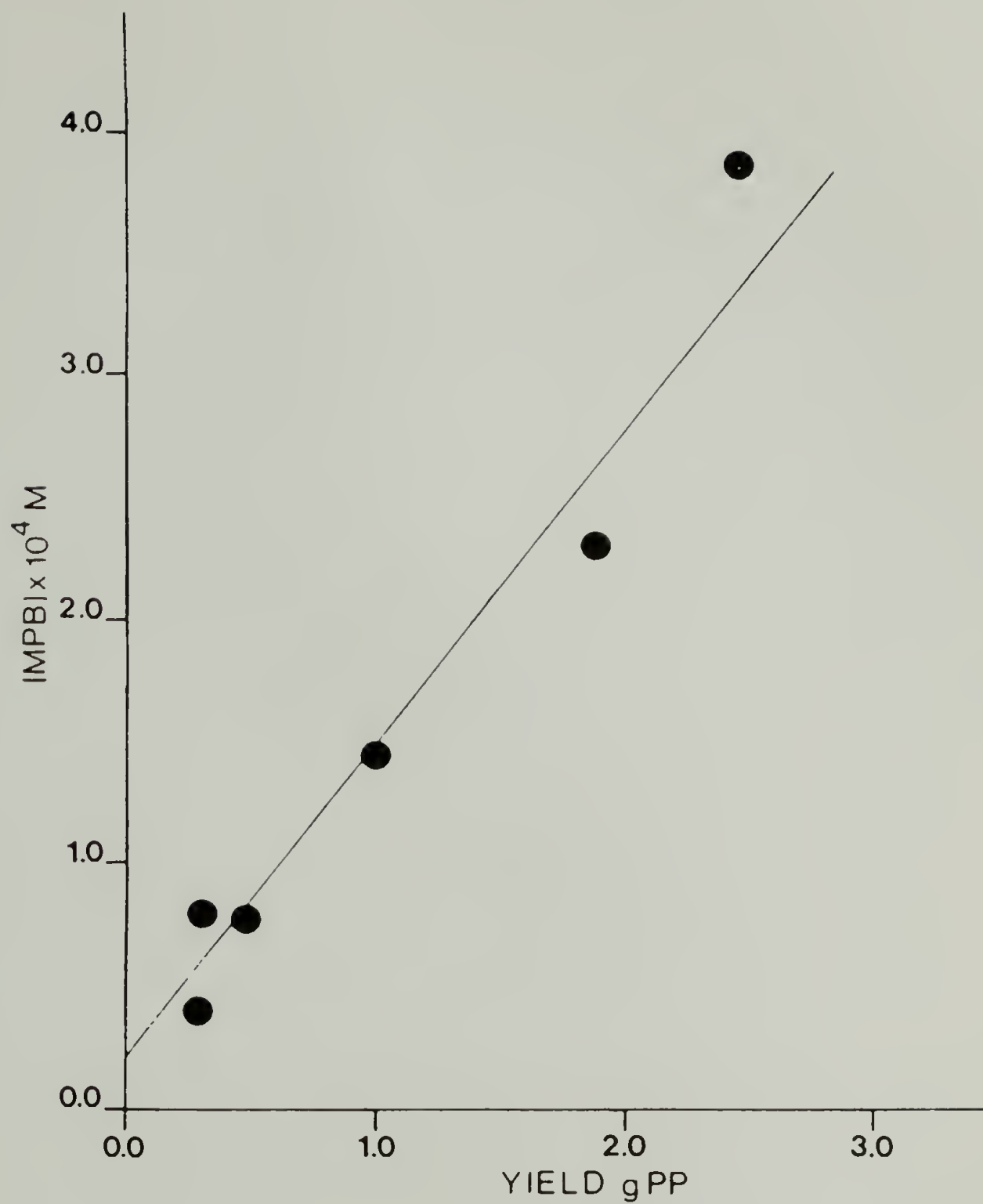


Figure 3.5 Variation of Metal-Polymer Bond Concentration Versus Yield for the Total Polymer.



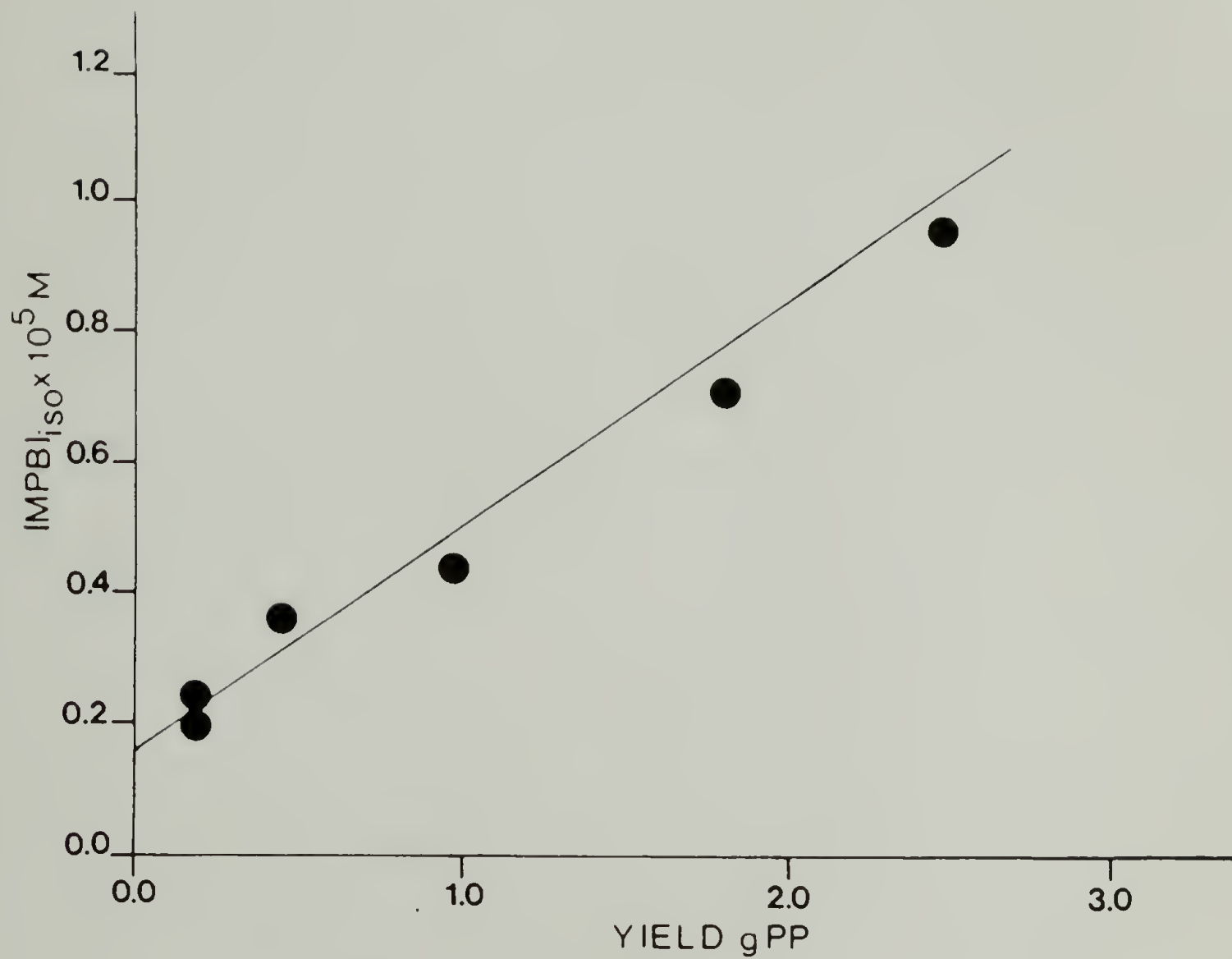


Figure 3.6 Variation of Metal-Polymer Bond Concentration Versus Yield for the Isotactic Fraction.

**Table 3.3 Comparison of Various  $\text{MgCl}_2$  Supported Catalysts**

	CH(EH, MT) <sup>a</sup>	CH(EH, BP) <sup>a</sup>	CW <sup>b</sup>
Active site concentration, mole % of Ti			
Isotactic	6.7	25	6.7
Atactic	6.3	15	6.3
Total	13	40	13
$R_{p,m} \times 10^3, M s^{-1}$			
Isotactic	0.67	8.1	2.1
Atactic	0.12	0.25	0.12
$k_p (M s)^{-1}$			
Isotactic	59	206	200
Atactic	11	11	11
$k_{tr} \times 10^4, s^{-1}$			
Isotactic	3.0	24.8	0.17
Atactic	7.2	22.6	0.26

<sup>a</sup>Activated with 20TEA/1PES.

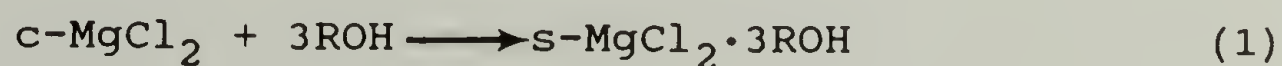
<sup>b</sup>Activated with 3 TEA/1MPT.

## Discussion of Results

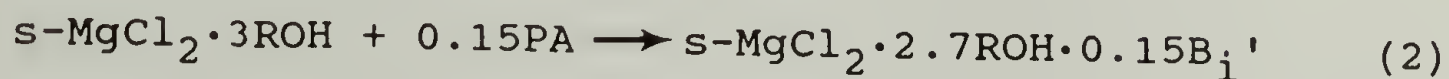
A lot of research has been performed in the industrial laboratory to find the particular Lewis bases for the  $\text{MgCl}_2$  supported catalysts to optimize stereospecificity, productivity, morphology, etc. Virtually all conceivable esters have been claimed in the patent literature without quantitative descriptions of their relative merits.

In the previous study in our group on the superactive and stereospecific catalysts, eight catalysts were prepared from  $\text{s-MgCl}_2 \cdot 3\text{EH}$  and  $\text{B}_i'$ , where  $\text{B}_i$  was either mono- or difunctional esters. These supports were reacted with  $\text{TiCl}_4$  alone or with  $\text{TiCl}_4$  in the presence of a second diester,  $\text{B}_i''$ . The former types of procatalysts were found to have high Ti contents and low activities whereas the latter contained much less Ti and possessed higher polymerization activities. It was recognized in that study that the most active CH catalysts contain at least two diesters; their probable roles had been discussed.

In the preparation of CH catalyst, anhydrous  $\text{c-MgCl}_2$  was reacted with 3 equivalents of alcohol

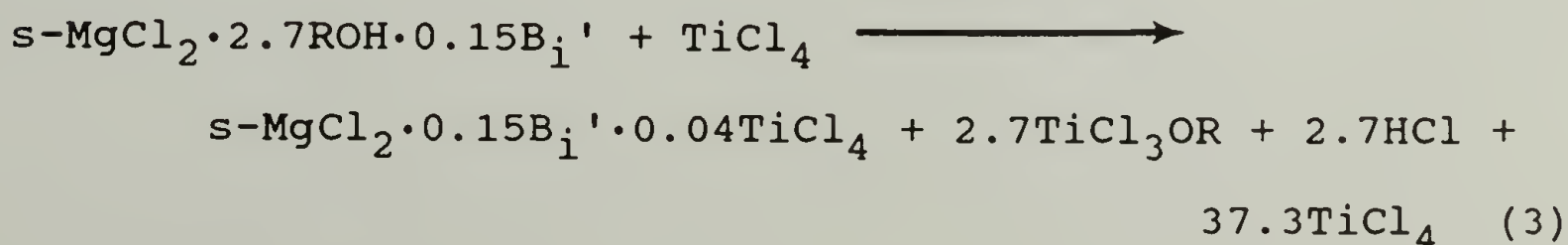


The amount of ROH was exactly that needed to form the soluble alcoholate. The 0.15 mol equivalent of phthalic anhydride, PA, was added which reacts with 0.3 equivalents of ROH to produce the corresponding phthalate ester which is referred to as  $B_i'$ .



It is interesting to note that the amount of  $B_i'$  used here is exactly the same as the amount of EB required to prepare the CW catalyst.<sup>2</sup> 0.15 equivalents of EB was added to the  $c\text{-MgCl}_2$  and the mixture was ball-milled. The EB was complexed to  $\text{MgCl}_2$  as shown by IR,<sup>5</sup> and it could not be removed by repeated extraction with heptane. This ratio was reported to be the optimum one for catalysts of the CW type.<sup>6,7</sup>

The adduct solution of equation 2 was added to  $\text{TiCl}_4$  that was 40 times the amount of  $\text{MgCl}_2$  or 15 times the amount of ROH. There was certainly sufficient  $\text{TiCl}_4$  to convert all the ROH into  $\text{TiCl}_3\text{OR}$  resulting in the precipitation of  $\text{MgCl}_2$





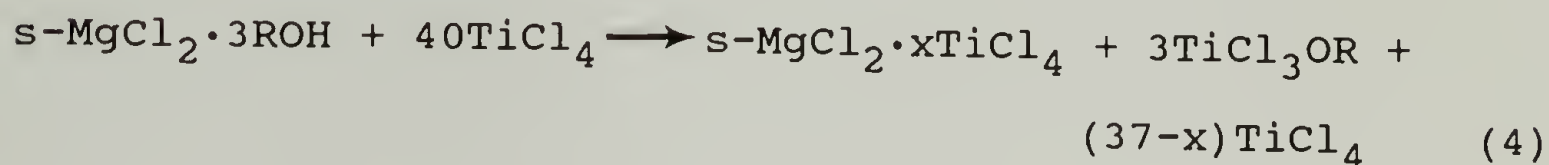
Previously, it had been established that the 0.15 mol of complexed  $B_i'$  was not extracted by reaction with  $TiCl_4$ . Also, it is important to note that without the complexed  $B_i'$  there are many more surface sites of  $MgCl_2$  which are able to complex with  $TiCl_4$  and form potentially aspecific sites (it is believed that the majority of the sites which complex with  $B_i$  are potentially aspecific; the potential isospecific sites are assumed to be relatively less Lewis acidic).<sup>4</sup>

In the reaction with  $TiCl_4$ , there was added 0.2 mol equivalents of BP which may serve two functions. If any of the  $B_i'$  becomes solubilized, BP will occupy that coordination site blocking any potential formation of aspecific sites. Secondly, the reaction between PA and ROH may not be complete and there may be some half esters on the surface of the  $MgCl_2$ . These should be replaced by the BP. Of the two proposed functions, the former is probably more likely due to the results of the PA/EH reaction experiments.

Even though  $TiCl_3OR$  is depicted to be in a dissolved state in equation 3, there is experimental evidence that some  $TiCl_3OR$  is complexed to  $MgCl_2$ : the variations in the CH catalysts<sup>2</sup> observed and the relatively high Ti levels after the first treatment with  $TiCl_4$  (filtration and resuspension of the support in fresh  $TiCl_4$  produces a

catalyst with lower Ti levels and improved productivity and stereospecificity).<sup>4</sup>

The EH catalysts are far superior to the 2-0 catalysts. It was found (as previously mentioned) that the secondary 2-0 is virtually unreactive towards PA. Therefore, in this case equation 3 must be rewritten as



where  $x \gg 0.04$ . This results in catalysts with low productivity and stereospecificity.

The catalysts prepared with terephthalates contain particularly high loading of Ti which range from 9% to 13% for the dimethylterephthalates. There is similarity between the catalysts prepared using the terephthalates and those prepared with monoesters in that both contain high levels of Ti.<sup>2</sup> Both types of catalysts have very low activities and stereospecificities.

A quantitative comparison of the CH(EH,BP) and CH(EH,MT) catalysts is given in table 3.4, which shows that the two catalysts have almost the same number of  $C_i^*$  but fewer  $C_a^*$  sites for the CH(EH,BP) catalyst, where the subscripts i and a denote isospecific and nonspecific sites, respectively.

**Table 3.4 Comparison of Active Site Concentrations**

Catalyst	Total Ti (wt %)	C* (% of Ti)		Total Ti (mmol/g)	C* (mmol/g)	
		Isotactic	Atactic		Isotactic	Atactic
CH(EH, BP) <sup>x</sup>	1.89	25	15	0.39	0.098	0.01
CH(EH, MT)	8.89	6.7	6.3	1.85	0.12	0.11

From the knowledge of  $C_i^*$  and  $C_a^*$ , the  $k_{p,i}$  and the  $k_{p,a}$  values were calculated from the maximum rates of polymerization. The nonspecific sites in the CH(EH,MT) catalyst was found to have the same  $k_{p,a}$  value as was determined previously for the CH(EH,BP) catalyst. However, the MT catalysts have a  $k_{p,i}$  value that is only one-fourth of that for the BP catalyst. Since the isospecific sites polymerize propylene many times faster than the nonspecific sites, the lower rate of polymerization per unit concentration of Ti found for the CH(EH,MT) catalyst is due both to the large content of Ti in the catalyst as well as the low inherent activity of the isospecific sites. Together with the large number of nonspecific sites in the MT catalyst, the lower II of 84.7% for the CH(EH,MT) catalyst and the higher II of 97% for the CH(EH,BP) catalyst can be accounted for.

### Conclusions

The structure of the  $B_i$  strongly affects the activity and the stereospecificity of the CH catalyst. High Ti contents (and subsequently low activities) result when a terephthalate ester or a monoester is used in the preparation. The terephthalate may function in the same way as a monoester. Also, the steric size of the alkyl group of the ester has a smaller albeit definite effect on



the catalyst performance with the bulkier alkyl group giving rise to lower activity and stereospecificity. EH is the alcohol of choice in the synthesis of the  $\text{MgCl}_2 \cdot 3\text{ROH}$  adduct; the secondary 2-O produces catalysts of inferior quality. Any modification of the CH system should use a  $\text{B}_i$  of similar structure as BP and primary alcohols should be used in the synthesis of the adduct.

### References

1. J.C.W. Chien, J.C. Wu, and C.I. Kuo, *J. Polym. Sci., Polym. Chem. Ed.*, **20**, 2019 (1982).
2. Y. Hu and J.C.W. Chien, *J. Polym. Sci., Polym. Chem. Ed.*, **26**, 2003 (1988).
3. J.C.W. Chien and C.I. Kuo, *J. Polym. Sci, Polym. Chem. Ed.*, **23**, 731 (1985).
4. J.C.W. Chien and Y. Hu, *J. Polym. Sci., Polym. Chem. Ed.*, **26**, 2973 (1988)
5. J.C.W. Chien, J.C. Wu, and C.I. Kuo, *J. Polym. Sci., Polym. Chem. Ed.*, **21**, 725 (1983).
6. T. Keii, E. Suzuki, M. Tamura, M. Murata, and Y. Doi, *Makromol. Chem.*, **183**, 2285 (1982).
7. V. Busico, P. Corradini, L. DeMartino, A. Proto, V. Savino, and E. Albizzati, *Makromol. Chem.*, **186**, 1279 (1975).

## CHAPTER IV

# STEREOSELECTIVE POLYMERIZATION OF $\alpha$ -OLEFINS BY HETEROGENEOUS CHIRAL ZIEGLER-NATTA CATALYSTS

### Introduction

As was shown in chapter III, the choice of internal Lewis base (denoted by  $B_i$ ) can greatly affect the productivity and stereoselectivity (as shown by isotactic yield (IY)). This is also true for the external Lewis base (denoted by  $B_e$ ). In spite of intensive researches in this field, the basic knowledge of the catalytic titanium species and the Lewis base is still unsatisfactory.

It is common knowledge that the Lewis base greatly reduces the overall productivity of  $MgCl_2$  supported catalyst but increases the stereospecificity. Pino et al<sup>1</sup> stated that "the Lewis base either selectively poisons the catalytic centers producing polymers with low stereoregularity or it modifies the nonstereospecific centers by increasing their stereospecificity and decreasing their productivity, or it acts in both ways". Previously, our group has quantitatively shown the influence of the Lewis base by radiotagging techniques<sup>2</sup> to count separately the numbers of stereospecific sites ( $C_i$ ) and the nonstereo-

specific sites ( $C_a$ ) in catalysts with or without  $B_i$  and/or  $B_e$ . The results showed that the function of  $B_i$  is to create active centers of both kinds while  $B_e$  acts to preferentially inhibit the nonstereospecific ones. All the catalytic centers for propylene polymerization were found to be Ti(III) ions by redox titrations.<sup>3</sup> The stereospecific sites were observable by EPR, but the nonstereospecific sites were EPR silent.<sup>4</sup>

Polymerizations of racemic and optically active  $\alpha$ -olefins were used to establish that the catalytic sites in Ziegler-Natta catalysts are chiral centers.<sup>5</sup> In the case of the  $MgCl_2$  supported catalysts, the use of optically active Lewis bases in the preparation offers means to investigate the stereoelective process of the chiral catalytic centers.<sup>1,6</sup> The  $MgCl_2/(-)MA/TiCl_4//TBA/(-)MA$  catalyst ((-) $MA$  = (-)-menthylalansate,  $TBA$  = tri-*i*-butylaluminum) was shown to possess centers polymerizing the *S*-antipode of 3,7-dimethyl-1-octene ((*S*)DMO) from the racemic mixture to PDMO (poly(DMO)) with positive optical rotation and others consuming the (*R*)DMO to PDMO with negative optical rotation. The same effect was observed for 4-methyl-1-hexene (4MH).<sup>7</sup> Pino et al<sup>1</sup> proposed six types of catalytic centers of different Lewis acidity. The most Lewis acidic centers are coordinatively highly unsaturated, sterically accessible, nonchiral and nonstereospecific. The least Lewis acidic centers are



less coordinatively unsaturated, sterically restrictive, chiral and stereospecific. But the relationship between these catalytic centers and the Lewis base is uncertain.

In the work described in this chapter,  $\text{MgCl}_2$  supported catalysts were synthesized with optically active base,  $B_i^*$ , or with the corresponding racemic  $B_i$  and also those that contain nonchiral Lewis bases. These were compared with ordinary  $\text{TiCl}_3$  in the stereoselective and stereoelective polymerizations of nonchiral and racemic 3- and 4-methyl substituted olefins regarding the active center types and concentrations, kinetic parameters, and stereoregularity and optical purity of the poly(olefins) produced. The main objective is to elucidate the various classes of active centers involved in the polymerization of different types of  $\alpha$ -olefins and the roles of the Lewis base in the catalysis.

### Experimental

#### $\text{CH}((R,S)-2\text{MBP})$ and $\text{CH}^*((S)-2\text{MBP})$

These are the modified versions of the high activity (fourth generation) Ziegler-Natta catalysts synthesized by the protocol described in chapter II. The alcohols used in the  $\text{MgCl}_2$ -adduct synthesis were 2-methylbutanol and (S)-2-methylbutanol ( $[\alpha]_{25}^D = -5.8^\circ$  (neat)). The esters used as  $B_i$ , di(2-methylbutyl)phthalate (2MBP) and di((S)-

2-methylbutyl)phthalate (S)2MBP) ( $[\alpha]_{25}^D = +4.8^\circ$  (in cyclohexane) were synthesized from the respective alcohols using phthaloyldichloride in pyridine. Elemental analysis (% calculated in parenthesis): di(2-methylbutyl)phthalate: C 70.9% (70.6), H 8.31% (8.57), O 21.0% (20.9) and for di((S)-2-methylbutyl)phthalate: C 70.5%, H 8.39%, O 21.0%.

Because of the insolubility of the  $\text{MgCl}_2$ -adduct in decane, the synthesis of the adduct was performed using toluene as the solvent. The percent Ti in the resulting racemic and the optically active catalysts was 3.76 and 3.60% , respectively.

The  $\text{CH}^*((\text{S})\text{-2MBP})$  catalyst was more extensively characterized. The analysis from Galbraith Laboratories gave the following elemental compositions in wt%: Ti 3.60, Mg 13.1, Cl 55.8, C 16.7, and O 6.90. The organic components were analyzed by hydrolysis-GC. A catalyst sample (0.1 to 0.2 g) was dissolved in 3 ml of 1N HCl and stirred for either 4 or 24 hours then extracted twice with diethylether. The extract was analyzed by GC for 2-methylbutanol (2MB) and 2MBP with n-hexanol added as the internal standard. Extraction efficiencies were determined by extracting known amounts of 2MB and 2MBP from 1N HCl; they were found to be quantitative (99.3% for 2MB and 100.2% for 2MBP). The analysis showed the catalyst to contain 0.811 mmol of 2MBP/g, 0.063 mmol of 2MB/g and 0.752 mmol of Ti/g, the analyses were the same for both

the 4 and 24 hour hydroxylates. The mole ratio of the 2MBP/Ti was 1.08. The original CH(EH,BP) catalyst also contained equimolar amounts of the phthalate ester and Ti. The amount of 2MB was found to be only 8% of 2MBP.

#### CW\* ((-)-MBz)

This is the modified version of the high activity (third generation) Ziegler-Natta catalyst which is less active and less stereospecific than the above fourth generation catalyst. It was synthesized in the same manner as the original version. (-)-menthylbenzoate which was synthesized from (-)-menthol and benzoylchloride was substituted for ethylbenzoate. The percent of Ti in the resulting catalyst was 3.92.

#### Polymerizations

The polymerizations were performed in dry Schlenk tubes under argon with magnetic stirring. The catalytic productivity was affected by the order of mixing of the reactants. The best results were obtained with the mixing order of diluent, monomer, aluminum alkyl, external Lewis base, and finally the catalyst. n-heptane was used to adjust the concentration of the reactants. An exception to this polymerization procedure was that for the  $\alpha$ -TiCl<sub>3</sub>/TBA catalyst system. In that case,  $\alpha$ -TiCl<sub>3</sub> was



introduced first, followed by monomer, and then finally TBA.

The catalyst compositions employed in the polymerizations were as follows. The CH catalysts used  $[TEA]/[PES]$  (PES = phenyltriethoxysilane)/ $[Ti] = 167/8.35/1$  and  $[M]/[Ti]$  ( $[M]$  = monomer concentration) ranged from 3600 to 300 depending upon the monomer. In the case of the CW catalyst, the ratios were  $[TBA]/[MPT]$  (MP = methyl-p-toluate)/ $[Ti] = 167/55.7/1$ . The ratio for the  $[TBA]/[Ti]$  system was simply 3/1.

Polymerization temperatures were 50°C for the  $MgCl_2$  supported systems and 70°C for the  $\alpha-TiCl_3$  system. These were determined empirically to optimize the activities and stereospecificities. The polymerization times were 1 hour, for propylene and 4-methyl-1-pentene (4MP), 5-12 hours for 4MH, and 72 hours for 3-methyl-1-hexene (3MH) and DMO. The polymerization quench and work up was that given in chapter II.

## Results

### Polymerization Activities of Linear and Branched $\alpha$ -Olefins

Both linear and branched  $\alpha$ -olefins were polymerized by the optically active  $CH^*((S)-2MBP)$  and  $CW^*((-)-MBz)$  and compared with the  $\alpha-TiCl_3$  catalyst. The results are



summarized in table 4.1. The CH\* catalyst is slightly more active than the CW\* catalyst for both propylene and 4MP polymerizations. The activity of 4MP polymerizations normalized to the propylene polymerization activities, given in parenthesis, are the same for the two catalysts. Of course, they are orders of magnitude greater than  $\alpha$ -TiCl<sub>3</sub>. The propylene polymerization activities of the CW\*((-)-MBz) catalyst is about the same as similar catalysts using nonchiral Lewis bases CW(EB,MPT). Similar behavior is observed for the chiral and nonchiral CH systems.

Previously, in our laboratories, we have polymerized decene-1 with the CW(EB,MPT) catalyst,<sup>8</sup> the activity was 1 kg polydecene (g Ti·[M]·h)<sup>-1</sup>. The total amount of catalytic centers was 12% of Ti, the overall rate constant of propagation ( $k_p$ ) was 24 (Msec)<sup>-1</sup>. Recently, we have found that hexene-1 was polymerized by this catalyst with an activity of 1.7 kg polyhexene (g Ti·[M]·h)<sup>-1</sup>.<sup>9</sup> Therefore, the CW(EB,MPT) polymerizes decene and hexene with comparable activity, number of active centers, and  $k_p$ .

There are large differences between the catalysts in the polymerizations of other branched olefins. 4MH was polymerized 400 times slower than 4MP by the CH\* catalyst; it was 50 to 70 fold slower by the CW\* and  $\alpha$ -TiCl<sub>3</sub> catalysts. The polymerization activities of the 3-methyl

**Table 4.1 Polymerization of  $\alpha$ -Olefins by Various Ziegler-Natta Catalysts**

Monomer	Activity (g polymer / g Ti [M] h)		
	CH <sup>+</sup> ((S)2MBP)	CW <sup>+</sup> ((-)MBz)	$\alpha$ -TiCl <sub>3</sub> <sup>c</sup>
C <sub>3</sub> H <sub>6</sub>	22,000(1.0) <sup>d</sup>	15,000(1.0) <sup>d</sup>	7.4(1.0) <sup>d</sup>
4MP	3,800(0.17)	2,500(0.17)	5.0(0.61)
4MH	55(0.0025)	230(0.015)	0.1(0.014)
DMD	0.60(2.7x10 <sup>-5</sup> )	38(0.0025)	0.0081(0.0011)
3MH	0.60(2.7x10 <sup>-5</sup> )	-	-

<sup>a</sup>MgCl<sub>2</sub>/(S)2MBP/ TiCl<sub>4</sub>// AlEt<sub>3</sub>/ PTES; [Al]/[Ti] = 167, [Al]/[PTES] = 20; <sup>b</sup>ball milled MgCl<sub>2</sub>/(-)MBz/*p*-cresol// TEA / TiCl<sub>4</sub>// TBA / (-) MBz; [Al]/[Ti] = 167, [Al]/[(-)MBz] = 3; <sup>c</sup> $\alpha$ -TiCl<sub>3</sub>// TBA = 1/3;

<sup>d</sup>Activities normalized to propylene in parenthesis.

substituted olefins are two orders of magnitude smaller than 4MH for the CH\* catalyst, the difference is only a factor of six to thirteen for the CW\* and  $\alpha$ -TiCl<sub>3</sub> catalysts. Therefore, the CH\* catalyst active centers are much more sensitive to the steric structure of the monomer than those in the CW\* catalysts. The large activity differences between the polymerizations of 4MP and 4MH by all three kinds of catalysts are unexpected and difficult to rationalize.

The P4MH was fractionated and the molecular weights of the fractions were determined by GPC (table 4.2). All the fractions of P4MH obtained with the CW\*((-)-MBz) and the  $\alpha$ -TiCl<sub>3</sub> catalysts have comparable  $M_n$ ,  $M_w$ , and polydispersity (P.D. =  $M_w/M_n$ ). These catalysts produced 4-5% of acetone soluble fractions, whereas, there was 11% of acetone soluble polymers in P4MH obtained with the CH\*((S)-2MBP) catalyst. A further difference is that the ethylacetate, diethylether, and cyclohexane fractions of P4MH obtained with the CH\* catalyst have  $M_n$  values which are only 0.14 to 0.2 times as large as the corresponding fractions of P4MH polymerized by the other two catalysts.

The most stereoregular fraction (cyclohexane) of PDMO's produced by the MgCl<sub>2</sub> supported catalysts had lower  $M_n$  than the cyclohexane fraction of P4MH, the converse was true in the case of the  $\alpha$ -TiCl<sub>3</sub> catalysts. All the PDMO's were more polydispersed than the P4MH's (table 4.2).

Table 4.2 GPC Molecular Weights for P4MH and PDMO

Polymer Fraction	Catalyst							
	CH <sup>+</sup> ((S)2MBP)				CW <sup>+</sup> ((-)MBZ)			
	$\alpha$ -TiC <sub>3</sub>							
	$M_n$ $\times 10^{-4}$	$M_w$ $\times 10^{-4}$	P.D.	$M_n$ $\times 10^{-4}$	$M_w$ $\times 10^{-4}$	P.D.	$M_n$ $\times 10^{-4}$	$M_w$ $\times 10^{-4}$
P4MH Acetone	0.18	0.75	4.1	-	-	-	-	-
P4MH Ethylacetate	0.52	1.7	3.3	2.5	9.2	3.6	2.3	14
P4MH Diethylether	0.99	2.7	3.0	7.1	29	4.2	6.3	31
P4MH Cyclohexane	1.1	5.2	4.9	7.2	82	11	7.8	72
PDMO Cyclohexane	0.72	5.7	8.0	6.6	150	22	12	17
								14



The catalytic centers in the  $\text{CH}^*((\text{S})\text{-2MBP})$  catalyst are more stereospecific than they are in the other two catalysts. This is evidenced by the DSC data on the P4MH fractions (table 4.3). The fractions of polymers produced by the  $\text{CH}^*$  catalyst have either the same or higher  $T_m$  (melting transition temperature) and appreciably greater  $\Delta H_m$  (enthalpy of fusion) in spite of their lower molecular weights (compare tables 4.2 and 4.3).

### Kinetics of 4MP Polymerization

The branched  $\alpha$ -olefins with asymmetric carbons are quite expensive chemicals and the polymerization yields are low. For practical reasons, polymerizations of the inexpensive 4MP were conducted, to count the number of catalytic centers for comparison with propylene polymerization. CW catalysts containing EB for  $B_i$ , with or without MPT as  $B_e$ , were used for the polymerizations.

Polymerizations were performed for various time periods to obtain yield/time curves (figure 4.1). The  $R_p$  was calculated from the tangent of these curves. The  $R_p$  was greatly reduced by the presence of  $B_e$ , and it decayed during the first 30 minutes of polymerization. Both of these phenomena are similar to the corresponding propylene polymerizations. The average productivity of P4MP was 1.3 kg and 9.7 kg  $(\text{g Ti} \cdot [\text{4MP}] \cdot \text{h})^{-1}$  with and without  $B_e$ , respectively.

**Table 4.3 Thermal Transition Data of P4MH Obtained by Different Catalysts**

fractions	CH <sup>+</sup> ((S)2MBP)		CW <sup>+</sup> ((-)MBZ)		$\alpha$ -TiCl <sub>3</sub>	
	T <sub>m</sub> (°C)	$\Delta H_m$ (cal g <sup>-1</sup> )	T <sub>m</sub> (°C)	$\Delta H_m$ (cal g <sup>-1</sup> )	T <sub>m</sub> (°C)	$\Delta H_m$ (cal g <sup>-1</sup> )
Ethylacetate	97-121	1.02	-	-	-	-
Diethylether	186-191	2.37	186-194	0.54	191-196	0.25
Cyclohexane	209-214	7.29	194-208	2.72	205-213	3.25

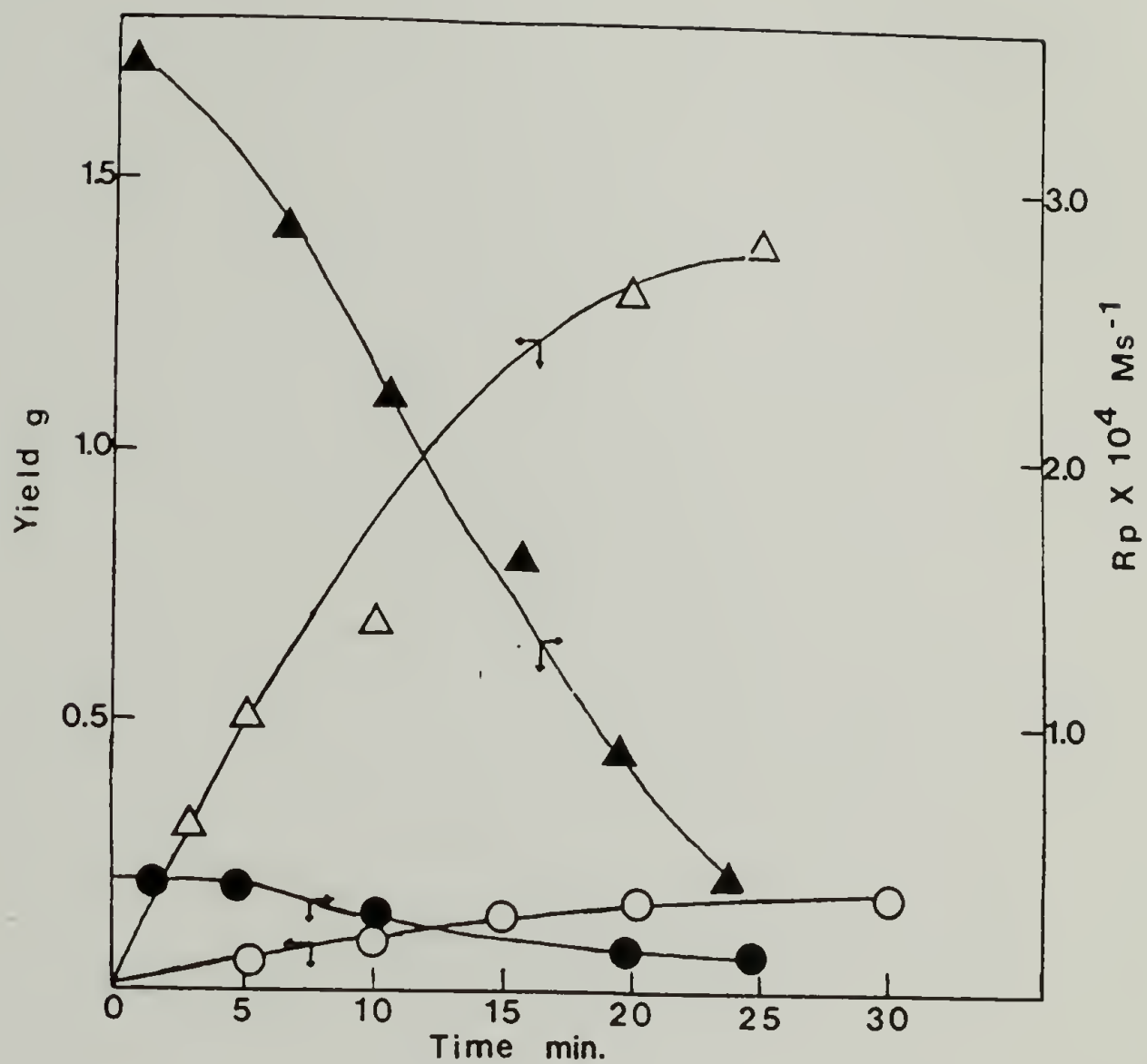


Figure 4.1 Polymerizations of 4MP by CW Catalyst at 50°C.  
 [Ti] = 0.22 mM, and [4MP] = 0.65 M: with MPT  
 (○) Yield and (●)  $R_p$  Versus Time; without MPT  
 (△) Yield and (▲)  $R_p$  Versus Time.

The concentration of metal-polymer bonds was determined as previously described. Figures 4.2a and 4.3a present the [MPB] versus yield of the total P4MP by the CW(-B<sub>e</sub>) and CW(+B<sub>e</sub>) catalysts, respectively. The radio-labeled P4MP was subjected to extraction with refluxing n-pentane for 6 hours. Radioassay of the insoluble stereoregular P4MP afforded the [MPB] for the isotactic fraction versus the yield of that fraction data as shown in figures 4.2b and 4.3b. Figure 4.4 contains the [MPB] versus yield data for the stereoirregular fraction.

Table 4.4 summarizes the kinetic parameters for 4MP polymerization by the CW catalysts (columns 2 and 5). Also given are the results of propylene polymerizations<sup>10</sup> (columns 3 and 6); and the ratios of the kinetic parameters for C<sub>3</sub>H<sub>6</sub>/4MP (columns 4 and 7). CW(-B<sub>e</sub>) catalyst has the same low stereospecificity for both the monomers, IY = 57 ± 2%. CW(+B<sub>e</sub>) catalyst polymerized the two monomers with comparable stereospecificity, IY = 92.5 ± 1.5%. MPT reduces the [C<sub>a</sub>] by a factor of 7-8 for both monomers, it reduces [C<sub>i</sub>] by two fold for propylene polymerization but four fold for 4MP polymerization. The number of either [C<sub>i</sub>] or [C<sub>a</sub>] is greater for propylene than 4MP polymerization, with or without MPT, by 10.6 ± 2.7 fold. B<sub>e</sub> has no effect on the stereospecific propagation of propylene but lowers slightly the k<sub>p</sub> of that process for



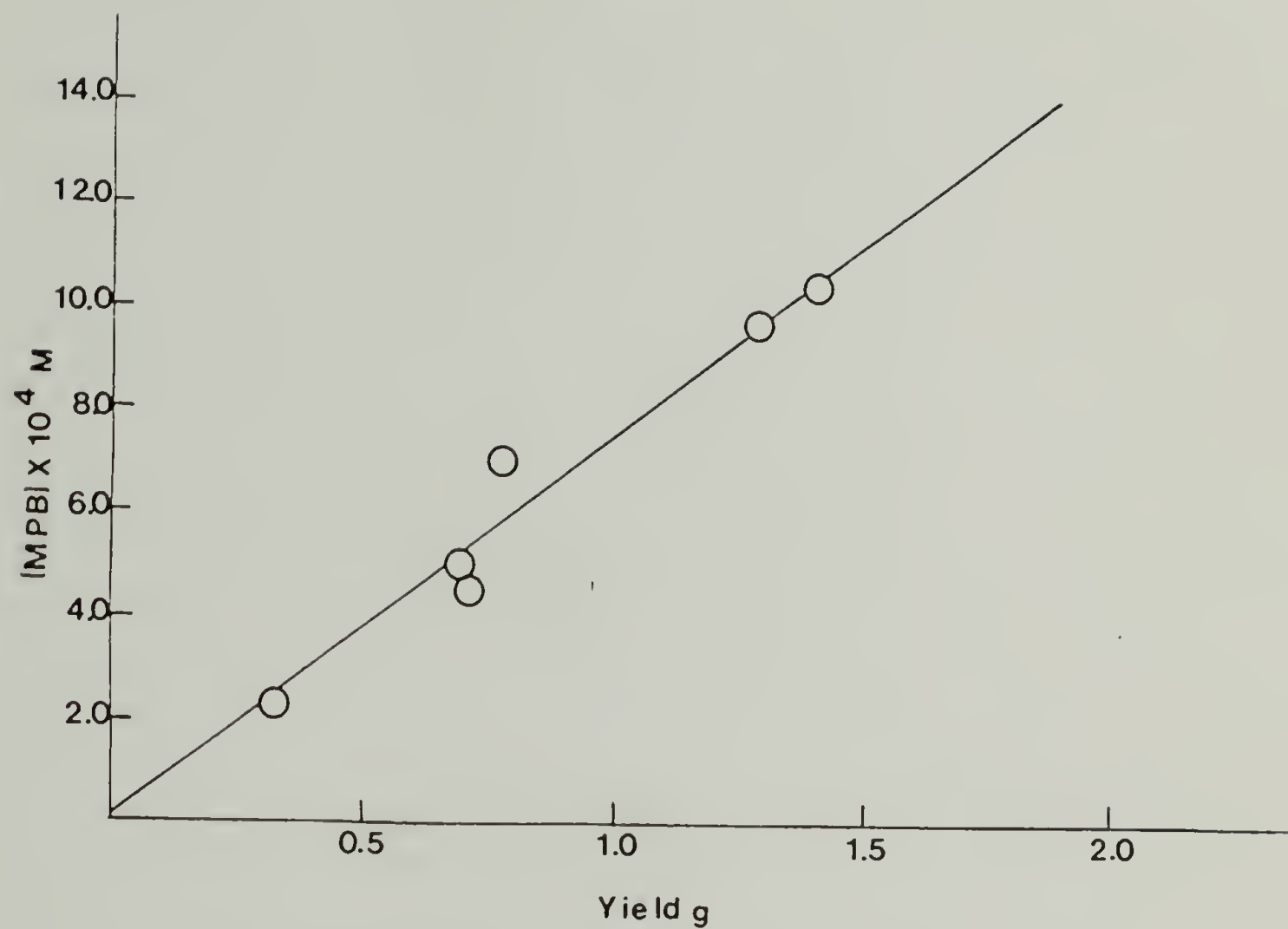


Figure 4.2 Variation of [MPB] Versus Yield for P4MP Obtained with CW(-B<sub>e</sub>) Catalyst. (a) Total Polymer.

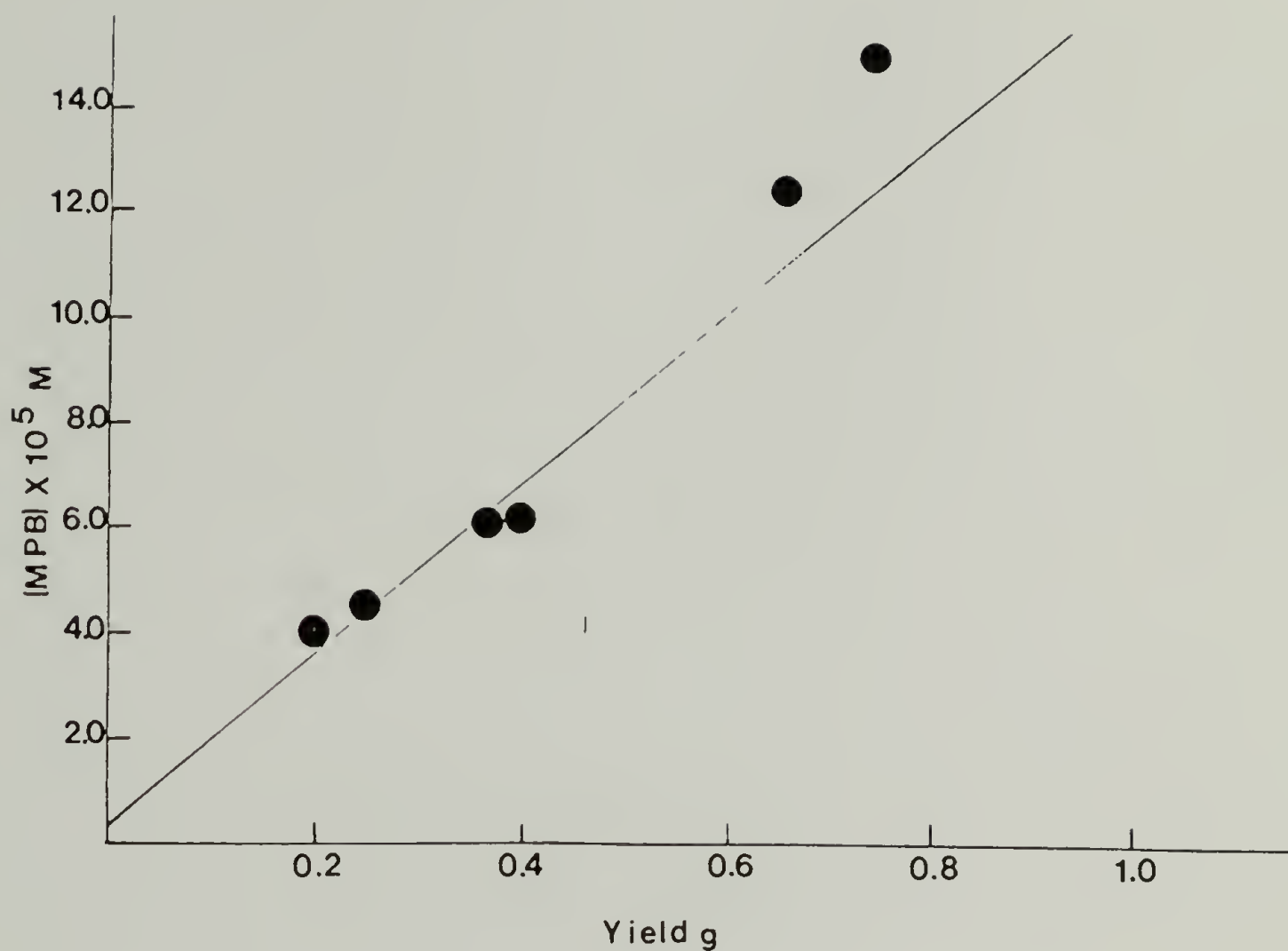


Figure 4.2 Variation of [MPB] Versus Yield for P4MP Obtained with CW(-B<sub>e</sub>) Catalyst. (b) Stereoregular Fraction.

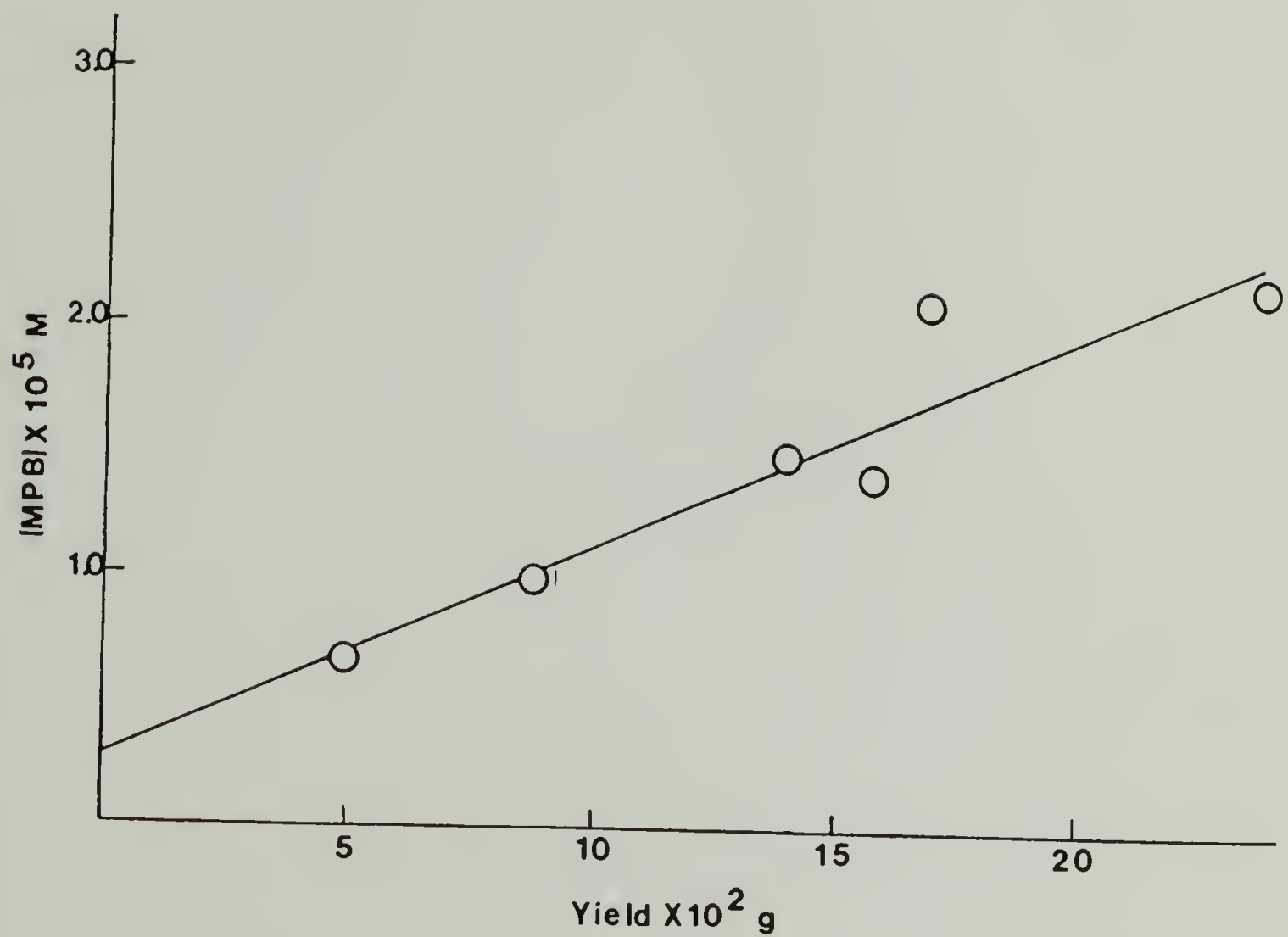


Figure 4.3 Variation of [MPB] Versus Yield for P4MP Obtained with  $\text{CW}(+\text{B}_e)$  Catalyst. (a) Total Polymer.

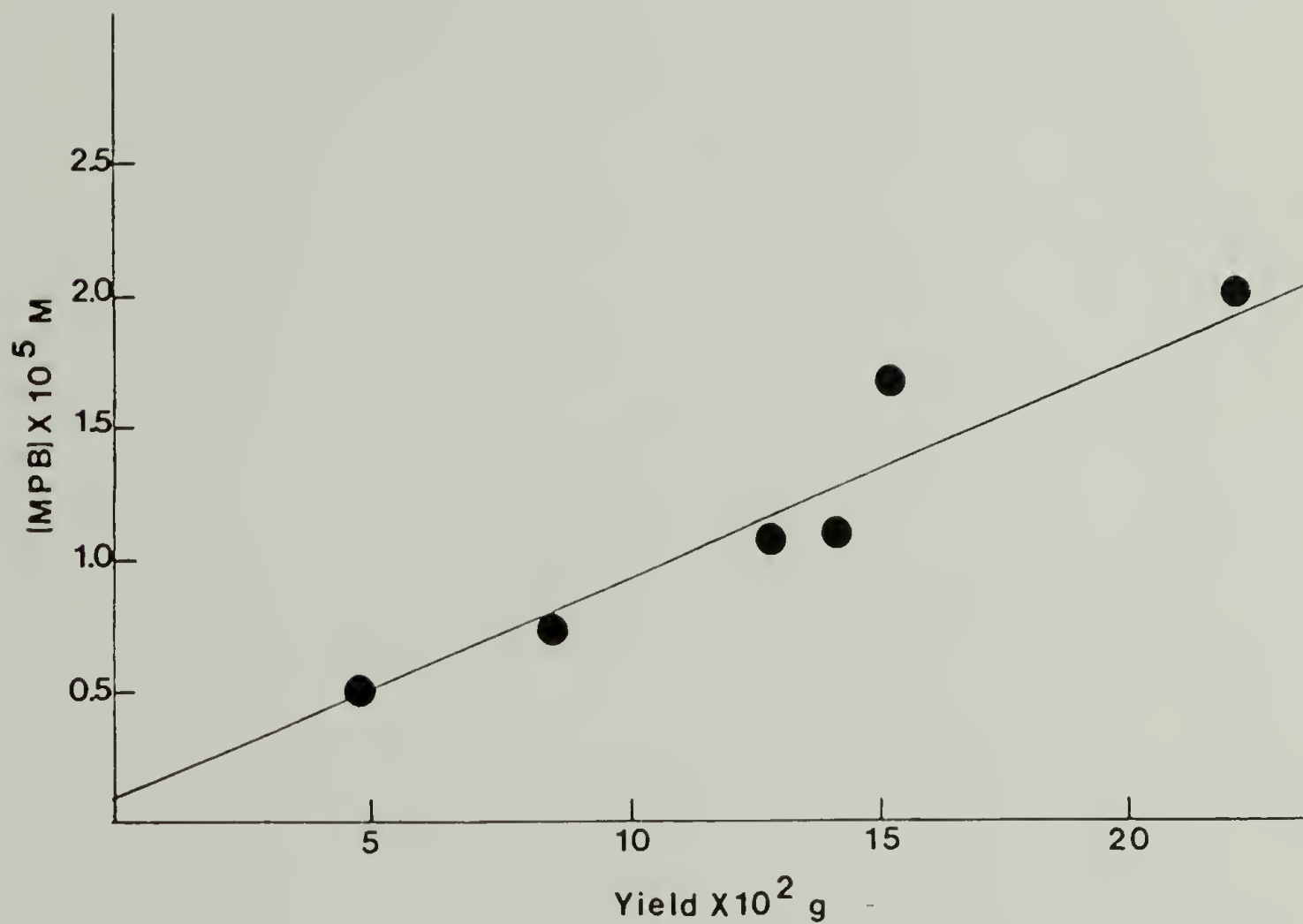


Figure 4.3 Variation of [MPB] Versus Yield for P4MP Obtained with CW(+B<sub>e</sub>) Catalyst. (b) Stereoregular Fraction.



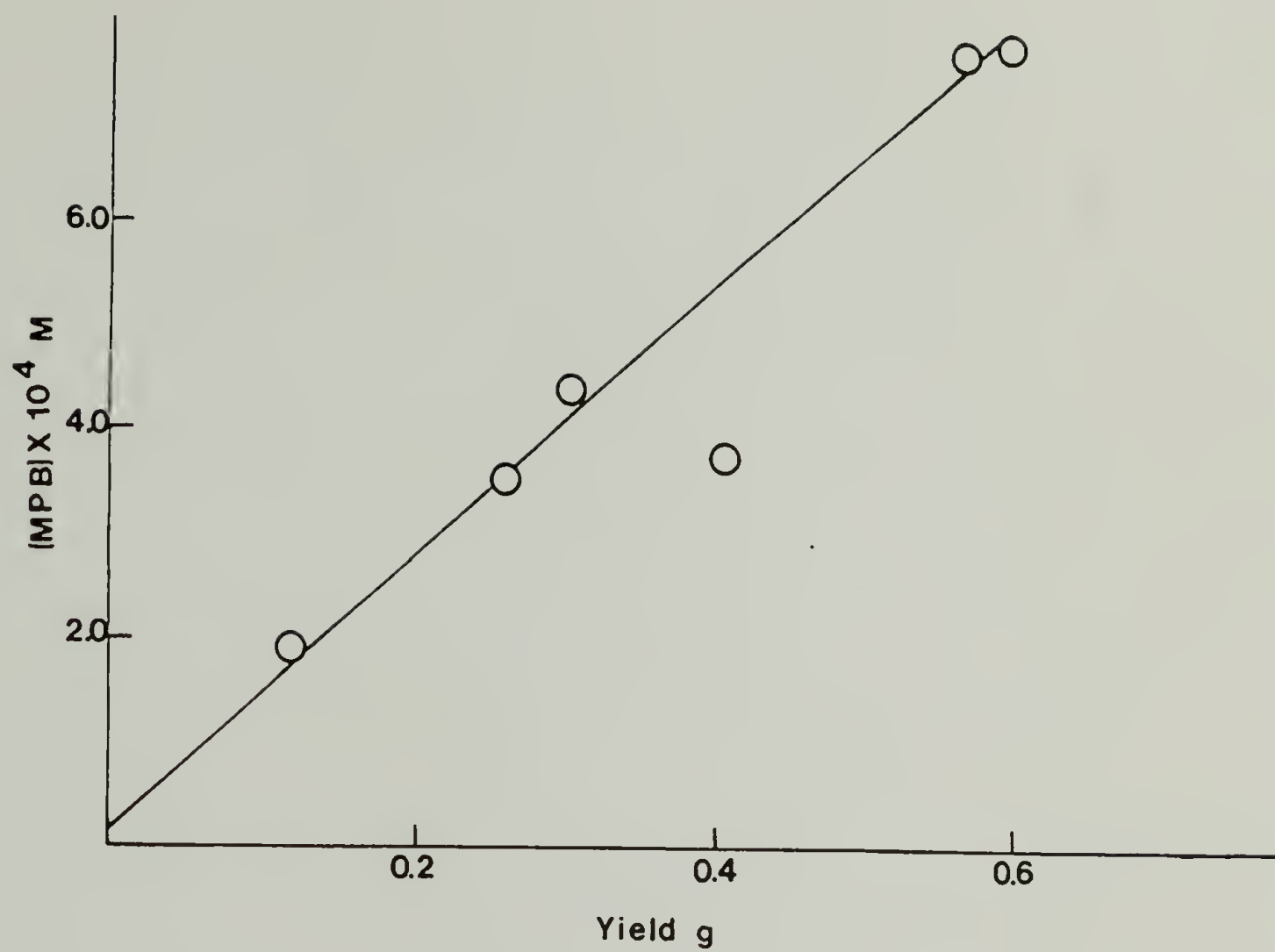


Figure 4.4 Variation of [MPB] Versus Yield for Stereoirregular P4MP. Obtained with: (a) CW(-B<sub>e</sub>).

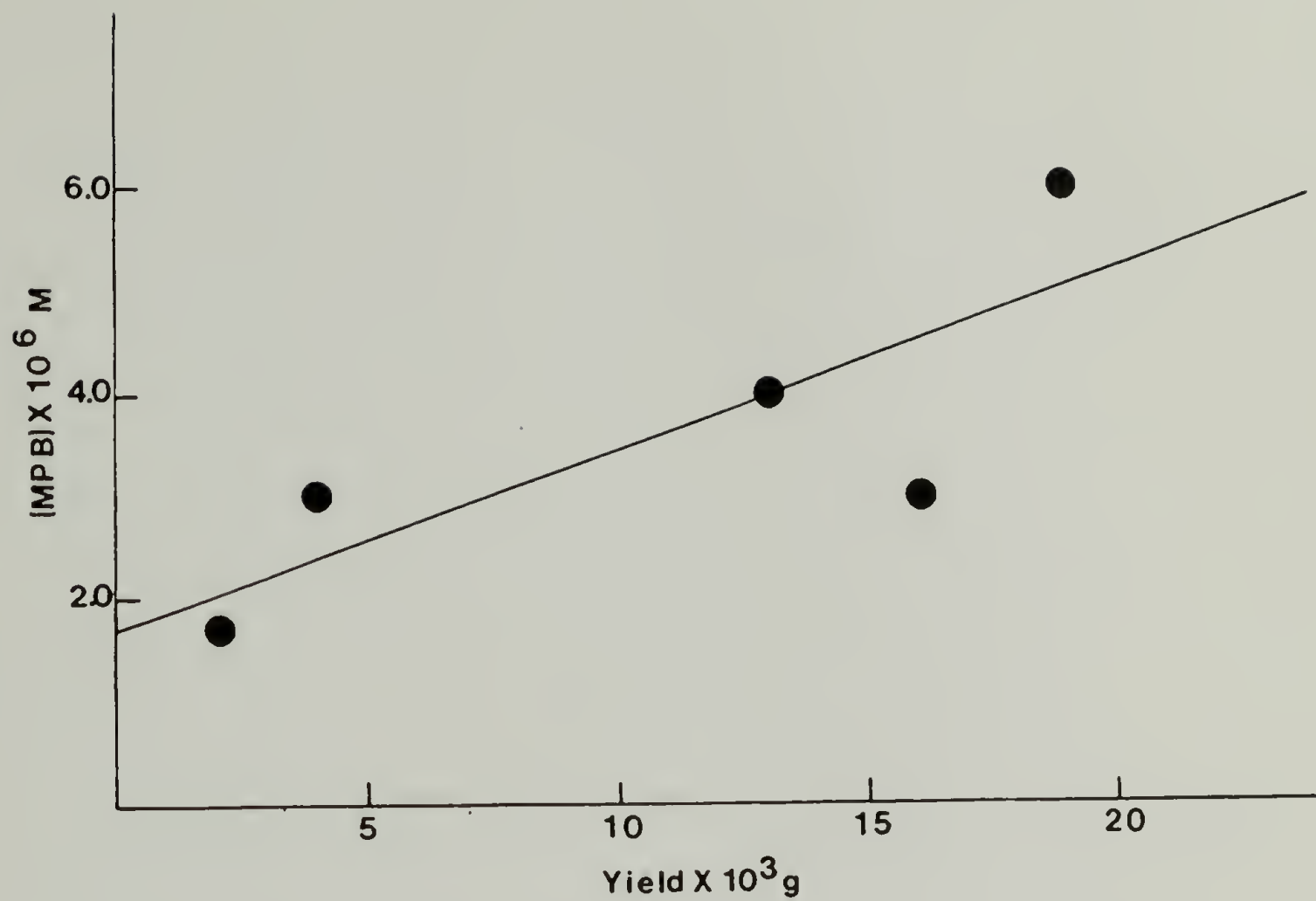


Figure 4.4 Variation of [MPB] Versus Yield for Stereoirregular P4MP. Obtained with: (b)  $CW(+B_e)$ .

Table 4.4 Kinetic Parameters for 4MP and Propylene Polymerization with CW Catalyst

Monomer	4MP	C <sub>3</sub> H <sub>6</sub>	C <sub>3</sub> H <sub>6</sub> <sup>a</sup> 4MP	4MP	C <sub>3</sub> H <sub>6</sub>	C <sub>3</sub> H <sub>6</sub> <sup>a</sup> 4MP
B <sub>e</sub>	none	none	none	MPT	MPT	MPT
R <sub>p</sub> × 10 <sup>4</sup> (Msec <sup>-1</sup> )	3.6	15.0	4.2	0.40	4.6	11.5
IY (%)	59 <sup>b</sup>	55 <sup>c</sup>	0.93	91 <sup>b</sup>	94 <sup>c</sup>	1.0
[C <sub>i</sub> ] (%)	1.7	15	8.8	0.46	6.7	14.6
[C <sub>a</sub> ] (%)	5.4	55	10	0.74	6.5	8.8
[C <sub>d</sub> ] (%)	7.1	70	9.9	1.2	13	11
k <sub>p,i</sub> (Msec) <sup>-1</sup>	68	209	3.1	46	200	4.3
k <sub>p,a</sub> (Msec) <sup>-1</sup>	17	27	1.6	2.4	11	4.6
k <sup>A</sup> <sub>tr,i</sub> × 10 <sup>3</sup> (sec <sup>-1</sup> )	73	1.5	0.02	12	0.17	0.01
k <sup>A</sup> <sub>tr,a</sub> × 10 <sup>3</sup> (sec <sup>-1</sup> )	90	3.1	0.03	14	0.26	0.02

<sup>a</sup>Ratio of kinetic parameters for propylene to 4MP; <sup>b</sup>*n*-pentane insoluble; <sup>c</sup>*n*-heptane insoluble.

4MP. MPT lowers the activities of the non-stereospecific centers for both monomers; the reduction factor is seven for 4MP but only 2.5 for propylene. Finally, the chain transfer to TEA rate constants are very much larger in 4MP than in propylene polymerizations for both stereospecific and nonstereospecific sites, and their values are appreciably lowered by MPT.

The polymerization activities of 3MH and DMO were too small to enable precise determination of  $[C]$ . An estimate of  $[C_t]$  for the polymerization of 3-methyl-1-butene by CW(EB,MPT) is about 4.5% as compared to 7.2% for 4MP polymerization.

### Stereoelective Polymerizations

Stereoelective polymerizations of racemic 4MH, 3MH, and DMO were performed using the  $CH^*((S)-2MBP)$  catalyst. The results in table 4.5 on the total polymers showed that all poly((S)-olefins) have positive  $[\alpha]$ . Thus, it is the S-antipode in the case of 4MH that is preferentially polymerized, and the recovered monomer is enriched in the R-antipode. On the other hand, the preferentially polymerized enantiomers of 3MH and DMO are the R-antipodes. The same overall preference for the opposite antipodes of 4-methyl and 3-methyl substituted olefins was reported before.<sup>1,6</sup> The optical purities of the polymerized



**Table 4.5 Stereoselective Polymerizations of Racemic  $\alpha$ -Olefins**

Catalyst	Monomer	[M] <sup>a</sup> [Ti]	Conv. (%)	Recovered monomer			Total polymer				$\frac{R_p(R)}{R_p(S)}$
				[α] <sup>b</sup>	P <sub>m</sub>	Prev. <sup>c</sup> chir.	[α] <sup>d</sup>	P <sub>p</sub>	Prev. <sup>c</sup> chir.	Eff. <sup>e</sup> (%)	
CH <sup>+</sup> ((S)2MBP)	4MH	3600	37	+0.02	0.66	R	+4.8	1.1	S	1.02	0.98
CW <sup>+</sup> ((- )MBz) <sup>f</sup>	4MH	3600	27.4	+0.01	0.32	R	+3.7	0.85	S	0.03	0.98
CH <sup>+</sup> ((S)2MBP)	3MH	1200	6.4	+0.066	0.33	S	<u>9</u>	4.8	R	4.4	1.10
CH <sup>+</sup> ((S)2MBP)	DMO	300	9.4	+0.157	0.76	S	-3.2	9.3	R	8.6	1.21
CH <sup>+</sup> ((S)2MBP)	DMO	1200	8.4	+0.086	0.52	S	-4.3	5.6	R	5.2	1.12
CW <sup>+</sup> ((- )MBz) <sup>f</sup>	DMO	3600	20.8	+0.13	1.10	S	-3.4	4.0	R	0.14	1.08

<sup>a</sup>[M] is monomer concentration; <sup>b</sup>at 25°C, sodium D line, neat; <sup>c</sup>prevailing chirality; <sup>d</sup>in cyclohexane; <sup>e</sup>efficiency see p.44 ; <sup>f</sup>reference 6 : gP(3MH) is incompletely soluble in cyclohexane at 25°C.

monomer were four to nine times greater for the 3-methyl substituted olefins than 4MH. The chiral catalytic centers can discriminate the antipodes more effectively when the asymmetric carbon is situated closer to the double bond. The stereoelective polymerizations by the  $CW^*((-)\text{MBz})$  catalysts have been previously reported.<sup>6</sup> The efficiency of stereoelection for DMO is about five times greater than it is for 4MH. The absolute magnitudes of stereoelective efficiencies cannot be compared for the  $CW^*$  and the  $CH^*$  catalysts because the former uses about thirty times more optically active Lewis base, internal and external than in the case of the  $CH^*$  catalyst.

P4MH and PDMO were fractionated to investigate in detail the relationship between the stereoelection (as evidenced by the specific optical rotation  $[\alpha]$ ) and the stereoselection (by  $I_S$  as measured by IR).  $^{13}\text{C}$  NMR is not useful in measuring the stereoregularity of the microstructure in these branched higher  $\alpha$ -olefins as it is a really powerful tool for polypropylene studies. The results of  $[\alpha]$  and  $I_S$  are summarized in table 4.6.

Concerning the properties of polyolefin fractions derived from the racemic monomer, the P4MH fractions have isotactic stereoregularity which increases in the order: acetone < ethylacetate < diethylether < cyclohexane. This is the same order as the increase of molecular weights (table 4.2), and  $T_m$  and  $\Delta H_m$  (table 4.3). Therefore, even

**Table 4.6 Microstructure of Stereoselectively Polymerized  
P4MH and PDMO Catalyzed with CH<sup>+</sup>\*(S)2MBP)**

Monomer	[M] <sup>a</sup> [Ti]	Conv. (%)	Fraction											
			Acetone			Ethylacetate			Diethylether			Cyclohexane		
			%	[α] <sup>b</sup>	I <sub>s</sub>	%	[α] <sup>b</sup>	I <sub>s</sub>	%	[α] <sup>b</sup>	I <sub>s</sub>	%	[α] <sup>b</sup>	I <sub>s</sub>
4MH	1200	37	11	+6.2		19	+10		8.9	+21		59	+9.8	
4MH	3600	35	9.0	+5.4	44 <sup>c</sup>	12	+10	73	10	+15	80	67	+9.9	85
DMO	1200	8.2	20	-2.3		29	-3.7		24	-6.3		27	-4.6	
DMO	300	9.1	36	-1.2	28 <sup>d</sup>	41	-5.1	46	16	-4.2	59	6.4	-0.71	67
85%(S)DMO	1200	4.6	9.2	+28	29	20	+59	47	25	+71	59	41	+75	74
3MH	1200	6.4	22	-3.7	-	14	-8.1	-	6.9	-16	-	13	(-) <sup>e</sup>	47
3MH/85% (S)DMO	300	12	40	+7.8	1709 (48) <sup>i</sup>	34	+23	63 (28)	6.1	+22	76 (30)	7.0	(-) <sup>h</sup>	20 (19)

a[M] is monomer concentration; b in cyclohexane d=1, c=1.0 g/dl; cD<sub>997</sub>/D<sub>964</sub> x 100 baseline drawn between 1060 and 935 cm<sup>-1</sup>; e insoluble at 25°C in cyclohexane; f[3MH]/[S-DMO] = 2.9, racemic catalyst used; gD<sub>918</sub>/D<sub>896</sub> x 100 baseline drawn through points 923 and 886 cm<sup>-1</sup>, indicative of [3MH]/[S-DMO] ratio; h not very soluble but in dilute solution shows (-) rotation; i %DMO content determined by comparison with mixtures of two homopolymers.



though solvent extraction fractionates the polyolefins according to both molecular weight and stereoregularity, there is no inversion in the order of the two separations. The PDMO fractions exhibit stereoregularity increase in the same order as the P4MH fractions. The optical rotation of the fractions of P4MH, PDMO and P3MH obtained from the stereoelective polymerization of the racemic monomers increase in the order acetone < ethylacetate < diethylether. However, the cyclohexane soluble fractions have smaller optical rotations than the diethylether fractions (in absolute values).

The stereoelective polymerization of rac-4MH is much more stereospecific than that of rac-DMO. The former (table 4.6) produces more than 60% of cyclohexane soluble, diethylether insoluble, polymers. This fraction was only 6-27% in the case of PDMO, and P3MH. The latter, however, gives also 47% cyclohexane insoluble polymer (probably due to the high melting point and crystallinity of this polymer).

In the case of polymerization of (S)DMO, having 85% optical purity ( $S/R = 12/1$ ), by  $CH^*((S)-2MBP)$ , the polymer fractions have positive rotations. Therefore, it is the S-antipode that is preferentially polymerized, in contrast to the preferred polymerization of the R-antipode from rac-DMO (table 4.5). This is probably due to the larger concentration of the S-antipode. The optical rotation



increases steadily with the increase of solvent power; the cyclohexane fraction has the highest optical rotation. The stereoregularity of the fractions also increases monotonically in the same manner. This polymerization is more stereospecific than the polymerization of the rac-DMO, producing 41% of the cyclohexane fraction.

3MH was copolymerized with 85% (S)DMO to study site stereoselection using the racemic CH((R,S)-2MBP) catalyst. The copolymer was found to be more soluble than P3MH. Only 14% of the copolymer was insoluble in cyclohexane while 47% of the P3MH was insoluble. About 80% of the copolymer was soluble in diethylether while 43% of P3MH was soluble. The IR absorbance ratio ( $D_{918}/D_{896}$ ) was found to be indicative of the [DMO]/[3MH] ratio in the copolymer. Comparison to IR absorbance ratios of standard mixtures of the homopolymers showed that the content of (S)DMO units in the copolymer is 48% in the least stereoregular fraction, 30% in the next two fractions, and only 19% in the most stereoregular fraction.

#### Effect of Optically Active and Racemic Lewis Bases

As previously mentioned, a CH catalyst was synthesized which contained racemic chiral Lewis base, CH((R,S)-2MBP). This catalyst was less active than the CH\* ((S)-2MBP) catalyst. For example, the former has an activity for propylene polymerization ( $[C_3H_6] = 0.73M$ ,

$[C_3H_6]/[Ti] = 3000$ , time = 1 hour, temp. =  $50^\circ C$ ) of 24 kg PP  $(g Ti \cdot [M] \cdot h)^{-1}$  as compared to an activity of 49 kg PP  $(g Ti \cdot [M] \cdot h)^{-1}$  for the latter. The two catalysts exhibit the same stereospecificity (IY = 98% for PP). The difference in activity is even greater for the polymerization of 4MH; the values are 9.3 and 70 g P4MH  $(g Ti \cdot [M] \cdot h)^{-1}$  for CH((R,S)-2MBP) and CH\* ((S)-2MBP) catalysts, respectively.

Those unexpected differences between the optically active and racemic catalysts prompted a more detailed comparison of their kinetics in the polymerization of propylene. Figure 4.5 shows that the CH((R,S)-2MBP) catalyzed polymerization was slow to initiate. The rate of polymerization increased gradually during the first eleven minutes to a maximum rate of  $2 \times 10^{-3} Ms^{-1}$  followed by a modest 50% rate decay. In contrast, the CH\* ((S)-2MBP) catalyzed polymerization reached maximum  $R_p$  of  $6.5 \times 10^{-3} Ms^{-1}$  within a couple of minutes after the activation (figure 4.6) which decayed to about 40% of the maximum rate. This behavior suggests that the number of active sites present initially is smaller for the racemic CH catalyst than in the optically active CH\* catalyst. The kinetic parameters were determined and listed in table 4.7. The main differences between the two catalysts are the number of stereospecific and nonstereospecific active

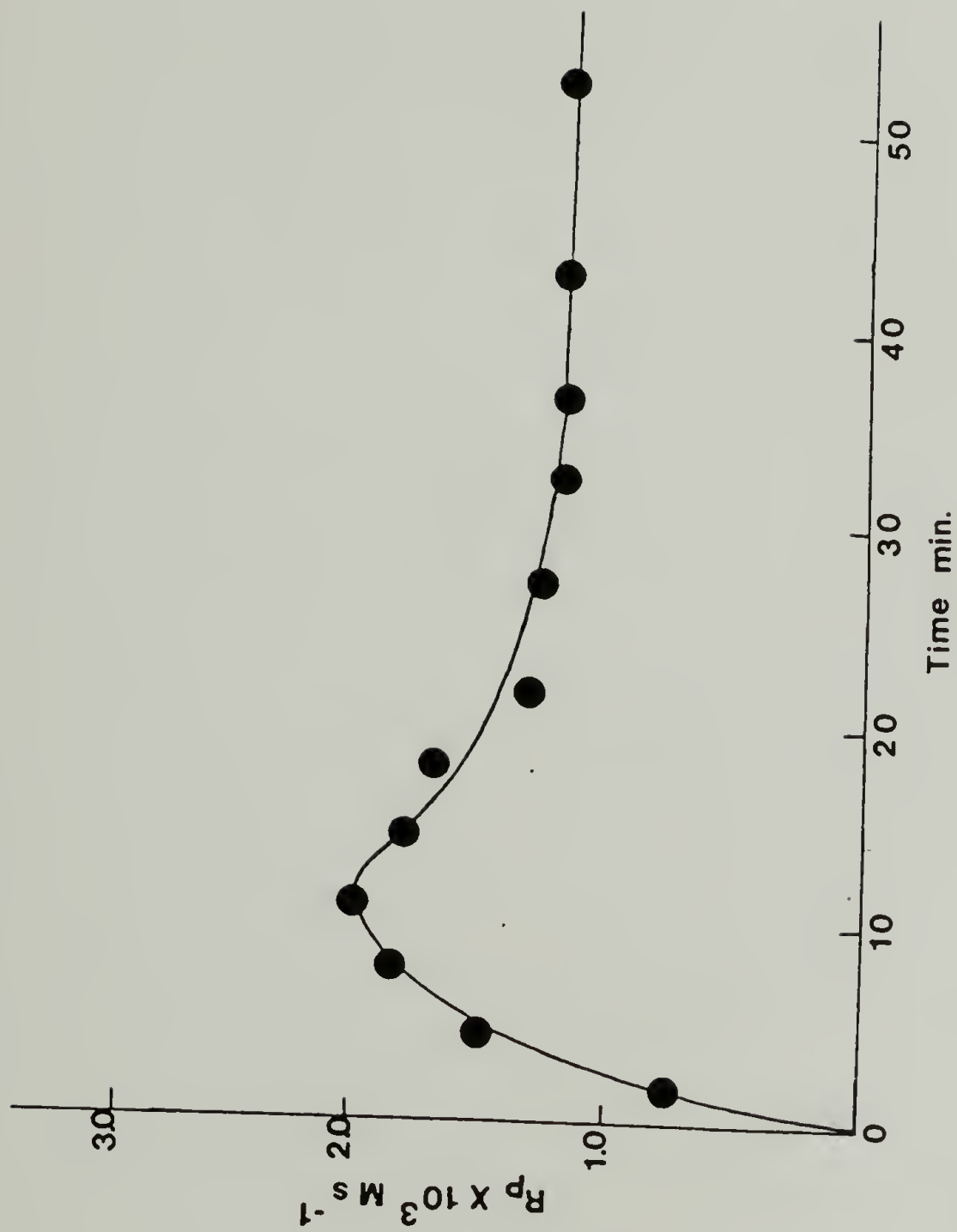


Figure 4.5 Variation of  $R_p$  Versus Time of Propylene Polymerization Catalyzed by  $\text{CH}((R,S)2\text{MBP})$ .

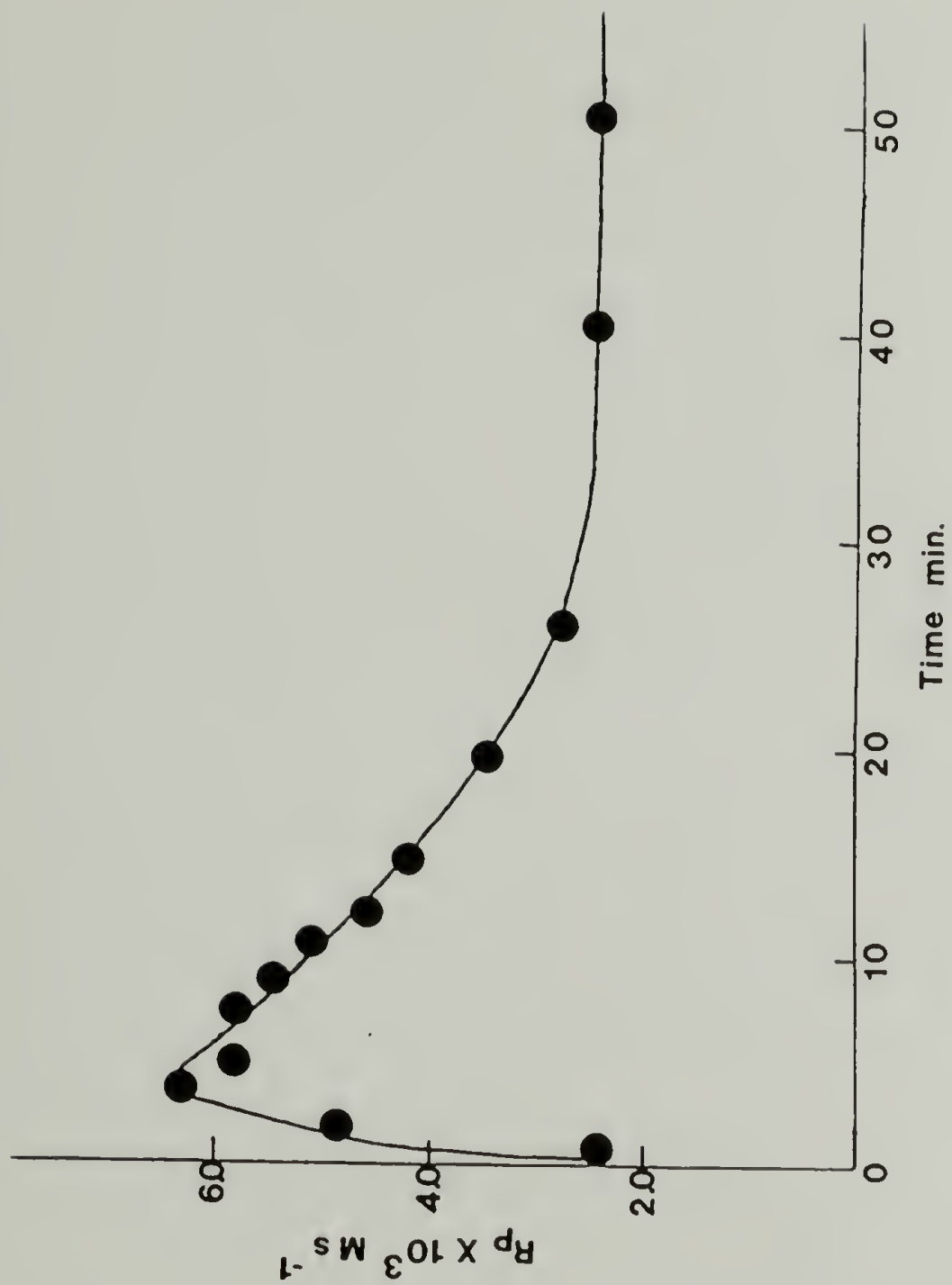


Figure 4.6 Variation of  $R_p$  Versus Time of Propylene Polymerization Catalyzed by  $\text{CH}^*(\text{S})_2\text{MBP}$ .



**Table 4.7 Kinetic Parameters of Propylene Polymerized  
with Various CH Type Catalysts**

catalyst	CH((R,S)2MBP)	CH*((S)2MBP)	CH(EH, BP)
[C <sub>d</sub> ] (mole % of Ti)	7.2	38	40
[C <sub>i</sub> ] (mole % of Ti)	5.0	17	25
[C <sub>a</sub> ] (mole % of Ti)	2.2	21	15
$k_{p,t}$ (Msec) <sup>-1</sup>	158	96	126
$k_{p,i}$ (Msec) <sup>-1</sup>	217	213	206
$k_{p,a}$ (Msec) <sup>-1</sup>	28	3.5	11
$k_{tr,A_i}$ X 10 <sup>3</sup> sec <sup>-1</sup>	1.4	2.2	25
$k_{tr,A_a}$ X 10 <sup>3</sup> sec <sup>-1</sup>	3.1	3.6	23

centers as determined by radiolabeling (figures 4.7 and 4.8), which are 3.4 and 9.5 times greater, respectively in the  $\text{CH}^*((\text{S})\text{-2MBP})$  than there are in the racemic system. The stereospecific sites in the two catalysts have identical  $k_{p,i}$  and  $k_{tr}^{\text{Al}}$  values. It is the nonstereospecific sites in the  $\text{CH}((\text{R,S})\text{-2MBP})$  catalyst which propagates 8 times faster than the  $\text{CH}^*((\text{S})\text{-2MBP})$  catalyst. Previously, the kinetic parameters for the nonchiral  $\text{CH}(\text{EH,BP})$  catalyst had been determined by our group.<sup>11</sup> The values included in table 4.7 (column 4) showed close similarity between this catalyst and the  $\text{CH}^*((\text{S})\text{-2MBP})$  catalyst, except the chain transfer rate constants are more than one order of magnitude greater for the  $\text{CH}(\text{EH,BP})$  system.

### Discussion of Results

The principle concern of this work is the nature of the catalytic sites for the stereospecific and nonstereospecific polymerizations of various  $\alpha$ -olefins. The reference monomer is propylene for the most studies have been made on this monomer. The stereospecific  $\text{MgCl}_2$  supported catalysts comprised of one to two moles of  $\text{B}_i$  for each mole of  $\text{Ti}$ ; the Lewis base is required to complex with the  $\text{MgCl}_2$  to form the active centers.<sup>2b</sup> The bonding interactions between  $\text{B}_i$  and  $\text{MgCl}_2$  have been observed by

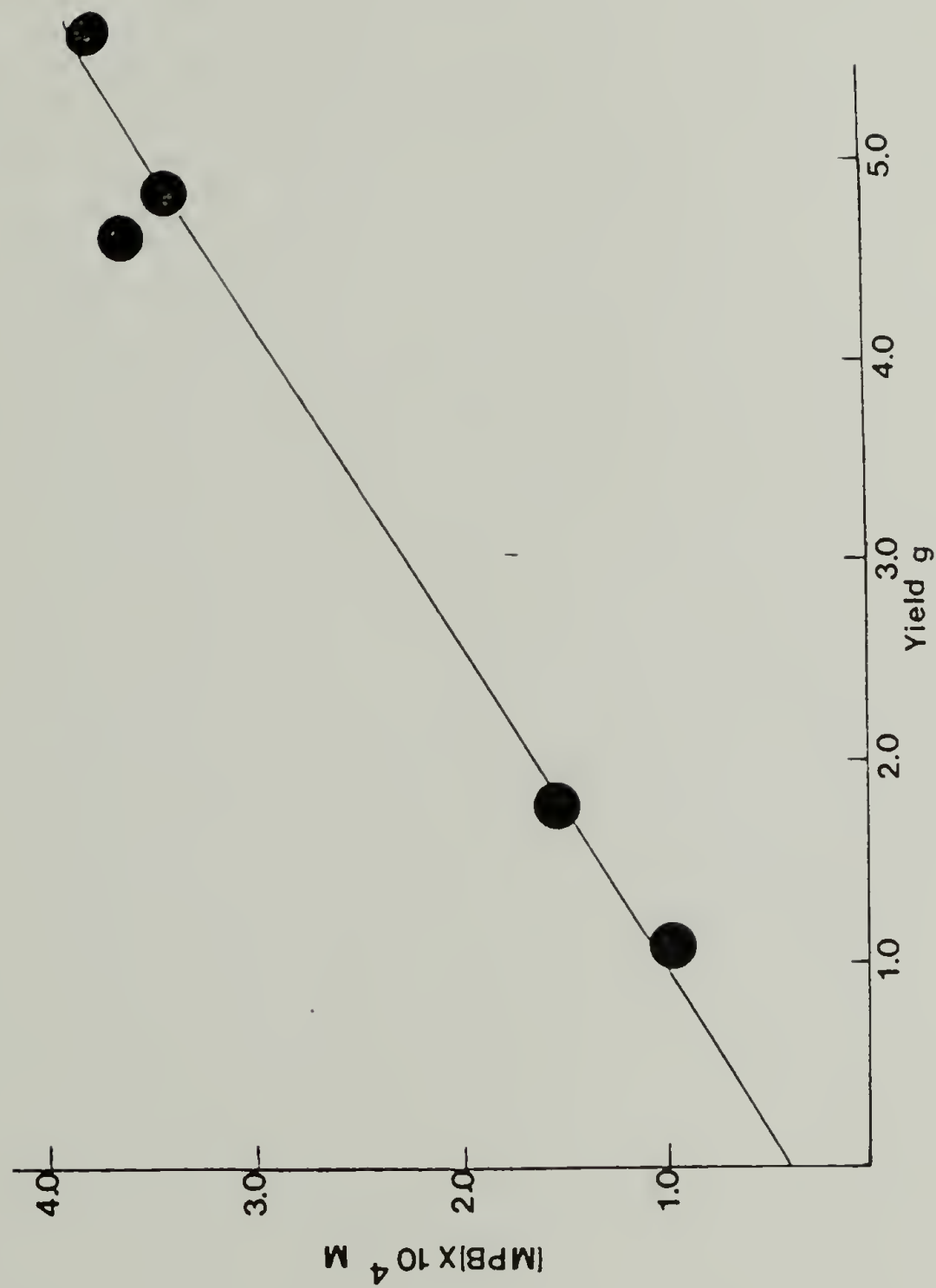


Figure 4.7 Variation of [MPB] Versus Yield of Propylene Polymerization Catalyzed by  $\text{CH}^*(\text{S})_2\text{MBP}$ . (a) Isotactic Fraction.

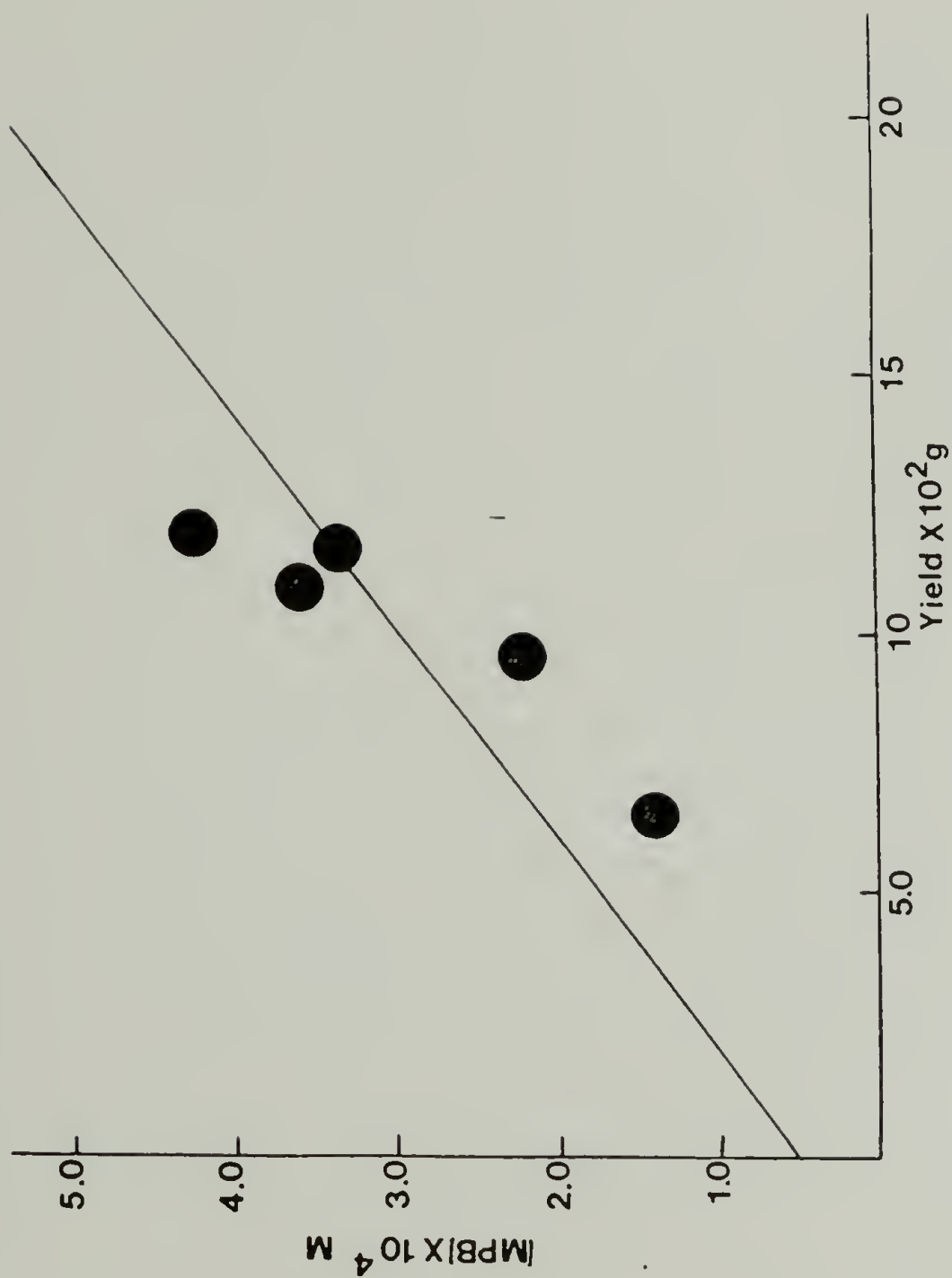


Figure 4.7 Variation of [MPB] Versus Yield of Propylene Polymerization Catalyzed by  $\text{CH}^*$  ((S)2MBP). (b) Atactic Fraction.



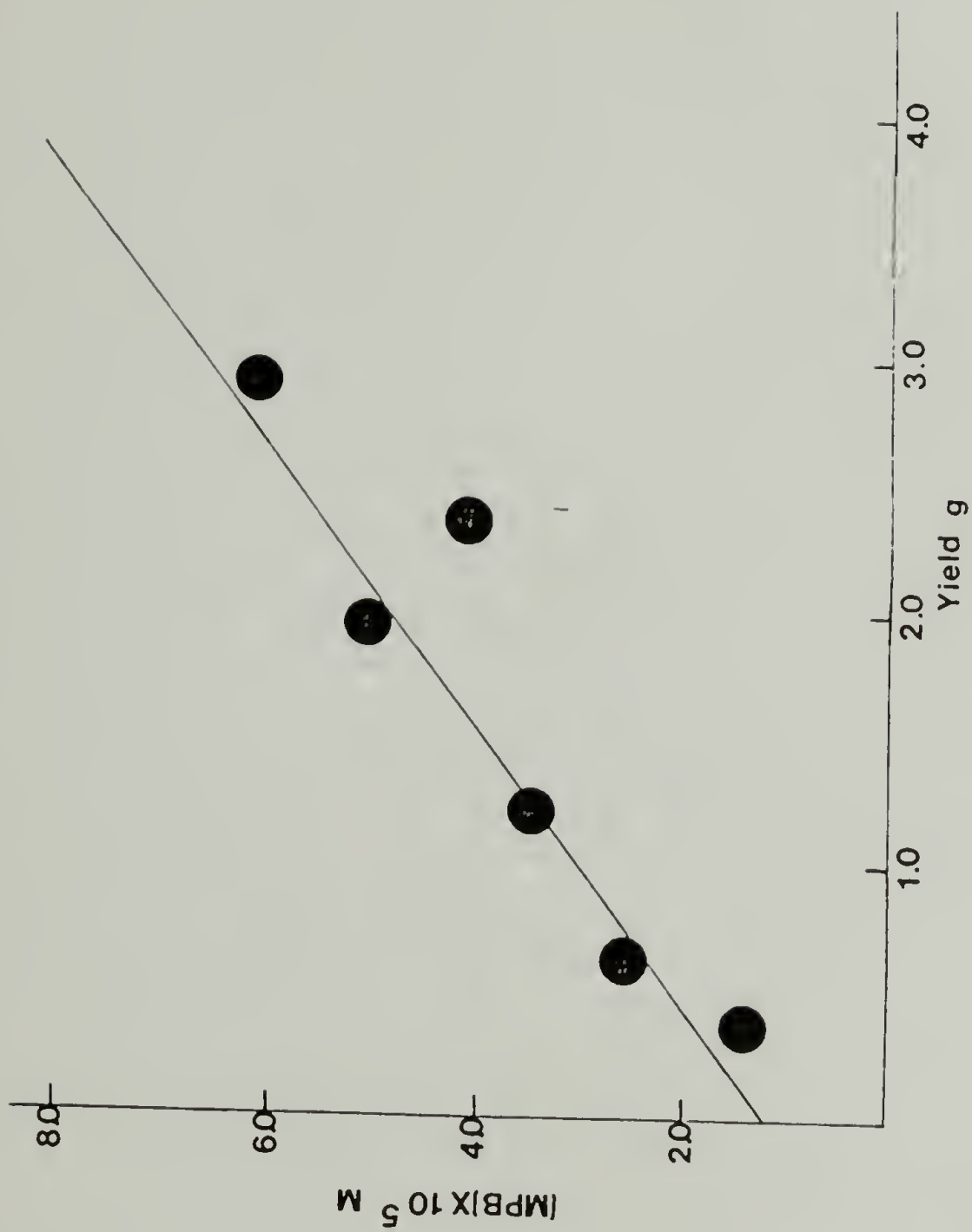


Figure 4.8 Variation of [MPB] Versus Yield of Propylene Polymerization Catalyzed by CH((R,S)2MBP).  
(a) Isotactic Fraction.

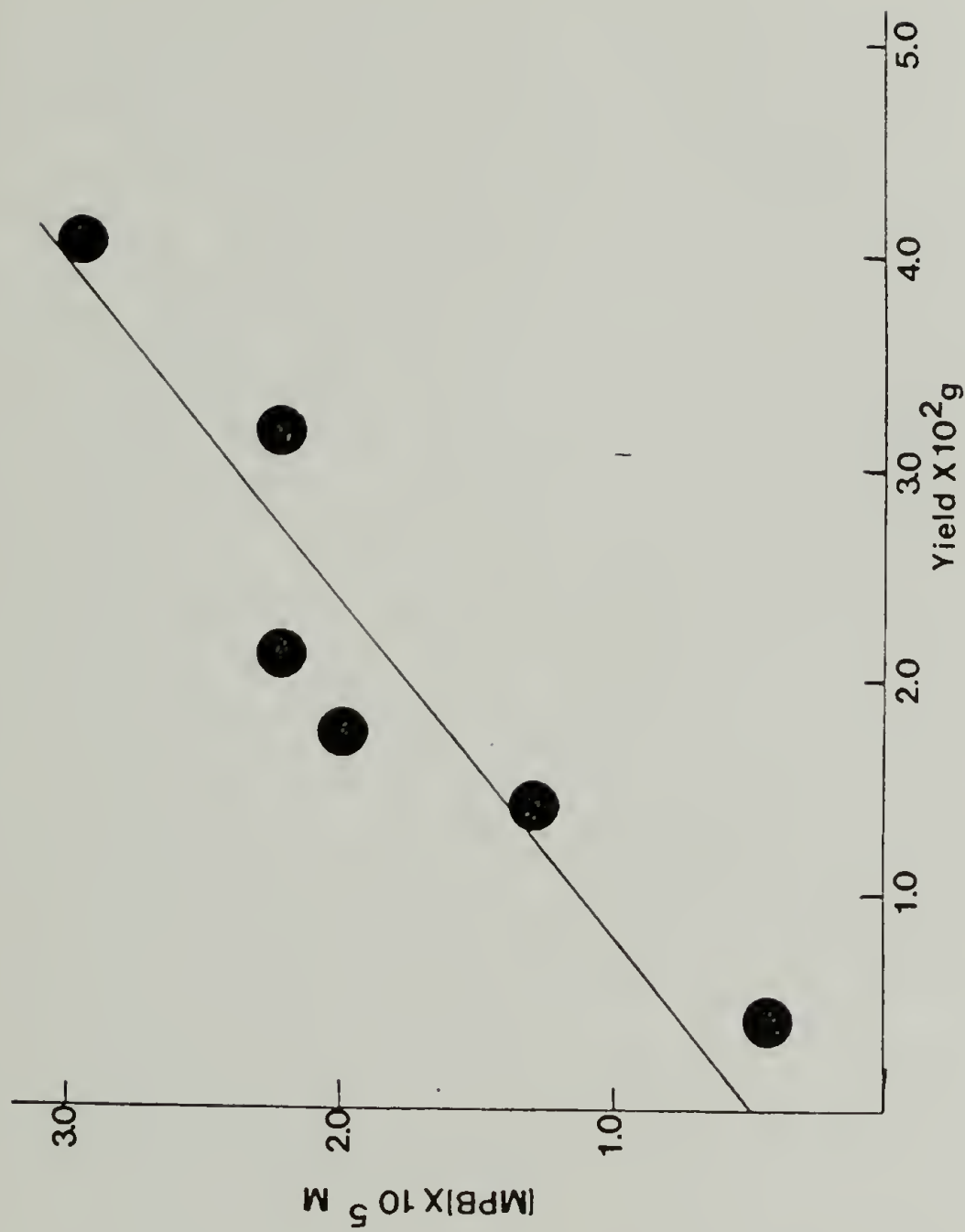
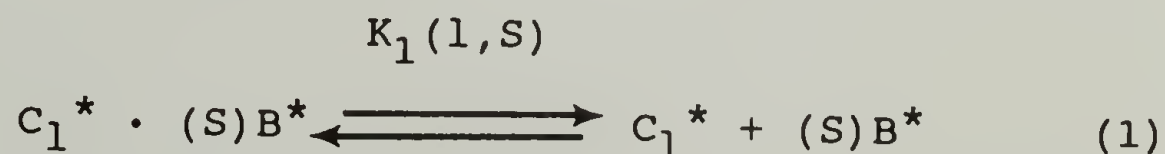


Figure 4.8 Variation of [MPB] versus Yield of Propylene Polymerization Catalyzed by  $\text{CH}((R,S)2\text{MBP})$ .  
(b) Atactic Fraction.

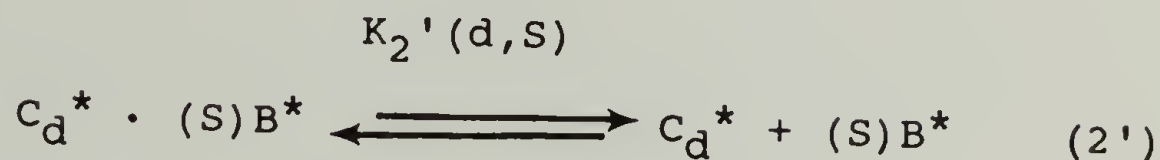
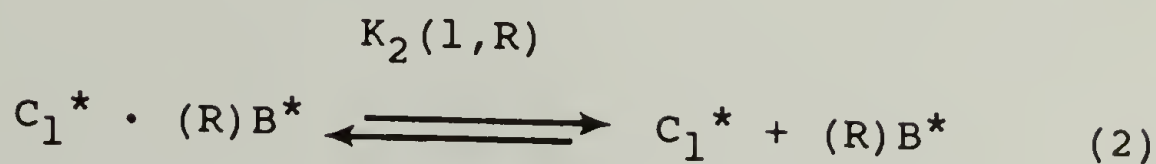
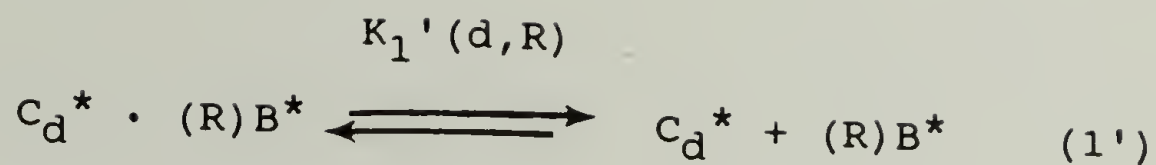
FTIR<sup>12</sup> and solid <sup>13</sup>C-NMR<sup>13</sup>; evidences for bonding between B<sub>i</sub> and Ti(III) were provided by EPR<sup>4</sup> and <sup>13</sup>C-NMR<sup>13</sup>. The structure of B<sub>i</sub> has a pronounced influence on the activity and stereospecificity of the CH type catalysts prepared from it as shown in the work in the previous chapter. The most stereospecific sites are chiral, designated by C<sub>1</sub>·B<sub>i</sub> (s) and C<sub>d</sub>·B<sub>i</sub> (s) by Pino et al<sup>1</sup>, and coordinatively saturated. Activation by TEA may free a vacant coordination position as depicted in figure 4.9. The amount of active centers is dependent upon the concentration of monomeric TEA in equilibrium with the dimeric TEA and the TEA·B<sub>i</sub> complex. It is characterized by large k<sub>p</sub>, (the values of k<sub>p</sub> are about the same for the CW and CH type catalysts), and small k<sub>tr</sub><sup>Al</sup> values. Isotactic polypropylene produced by it has narrow molecular weight distribution (M<sub>w</sub>/M<sub>n</sub> ≈ 2.0).<sup>14</sup> These active centers seem to be too sterically restrictive and inaccessible to higher α-olefins.

The differences between the optically active and racemic CH(2MBP) catalysts in olefin polymerizations may be explained by the relative stability of the diastereomeric complexes of C<sub>1</sub> or C<sub>d</sub> with either antipode of B<sub>i</sub><sup>\*</sup>,









The equilibria may involve TEA and all the species are attached to the  $MgCl_2$  surface as in figure 4.9. The  $C^*$  species on the left hand side of the equilibria are in the resting states; the  $C^*$  species on the right hand side of the equilibria are catalytically active. One set of diastereomers is more stable than the other set; it can be assumed that  $K_1 \gg K_2$  without loss of generality. In the  $CH^*((S)-2MBP)$  system, the  $C_l^*$  is present largely in the dissociated state which is catalytically active, while the more stable  $C_d^* \cdot (S)B^*$  is not. In the racemic system, both  $C_l^*$  and  $C_d^*$  form stable complexes with the preferred antipode  $(R)B^*$  and  $(S)B^*$ , respectively. Dissociation of these stable complexes has to occur before they can initiate polymerization (figure 4.9). The racemic catalyst has only one-eighth of the 4MH polymerization activity of the  $CH^*((S)-2MBP)$  system. The latter also has 5 times more active sites for propylene polymerization than the

CH((R,S)-2MBP) catalyst (table 4.7). It seems that the rac- $B_i$  complexes both  $C_d^*$  and  $C_l^*$ , whereas the optically active  $B_i^*$  complexes probably preferentially with either  $C_d^*$  and  $C_l^*$ , thus both have stereoselection.

The n-heptane soluble polypropylenes are formed by several kinds of active centers. They probably differ in the number of coordinative bonds between the Ti(III) ion and the support, or in coordinate alkylaluminum if any, or in the number of Lewis base molecules either in the inner coordination sphere as depicted by  $(C_l \cdot B_i)_s$  and/or the outer coordination sphere as represented by  $(C_l)_s \cdot (B_i) \cdot TEA$  in figure 4.9. The ability of a site to polymerize a monomer with more steric bulk at the double bond increased with lower state of ligation but also has less stereochemical control in the selection of a particular enantioface of the monomer. In propylene polymerizations the nonstereospecific centers have high Lewis acidity, associate with  $B_i$  more strongly, and exists mostly in the resting state. The apparent  $k_{p,a}$  is 1/10 to 1/60 as large as  $k_{p,i}$  for the stereospecific sites suggesting a correspondingly larger ratio of resting state to active state (table 4.7).

In CW(EB,MPT) catalyst there are about 1.2% of the Ti which catalyze polymerization of 4MP, which is about one-fifth the amount of low stereospecific sites for propylene

polymerization. The former has  $k_{tr}^{Al}$  values 30 to 100 times larger than the later. This means the 4MP polymerization sites have low steric constraints and are accessible to TEA. In the case of P4MH even the most stereoregular polymer was soluble in cyclohexane and has IR  $I_S$  of only 85%. More than a third of the P4MH is soluble in diethylether. The catalytic centers for the polymerization of 3-methyl- $\alpha$ -olefins have the lowest activity and stereospecificity. Table 4.6 shows that less than one-fifth of the PDMO was insoluble in diethylether which has a low  $I_S$  of 67%. As much as one-fifth to one-third of the PDMO is soluble in acetone and has an  $I_S$  value of only 28%. These active centers have very little steric hindrance and stereochemical control, yet they show high stereoelective efficiencies (table 4.5)

The  $CH^*$  catalyst polymerizes 4MH and 3-methyl- $\alpha$ -olefins with 2.5% and  $2.7 \times 10^{-3}\%$  of the polymerization activity, they are 1.5% and 0.2% respectively for the  $CW^*$  and  $\alpha-TiCl_3$  catalysts. The differences indicate that the most stereospecific CH catalyst contains very few active centers having little steric constraint.

Previously, the CW type catalyst prepared with non-chiral  $B_i$  (ethylbenzoate) and chiral  $B_e$  had been compared.<sup>6</sup> When the latter is (-)-dimenthylterephthalate, the catalyst is 7.5 times more stereoelective in the polymerization of racemic DMO than the catalyst with (-)-



menthylbenzoate as the  $B_e$ . The diester is expected to be more strongly complexed with the chiral center resulting in more effective site stereoselection.

The activities of 3MH polymerization are nearly the same for the optically active and racemic CH catalysts. This lack of difference may be explained by the assumption<sup>1</sup> that the catalytic centers for the 3-methyl substituted monomers are highest in Lewis acidity. The dissociation constants are so small that the contribution from the preference of an enantiomeric active center of one chirality or the other for a particular antipode of  $B^*$  is insignificant. In all polymerizations carried to less than 30% conversion, the polymer produced and the monomer recovered exhibit opposite chirality (Table 4.3) as expected for a stereoselective process. With the same enantiomer of the Lewis base for either the  $CW^*$  or  $CH^*$  type catalyst, the (S)4MH is preferentially polymerized to produce P4MH having positive optical rotation. The converse is true for DMO and 3MH. Polymerization of the R antipode was preferred and the resulting polymer has negative optical rotation. This suggests that the active site possesses very strict steric requirements which may involve a precise conformation of the side chain of the monomer. The minimum energy conformations for 4MH and DMO are shown in figure 4.10. The propagation preference of one antipode over another is best expressed by the ratio



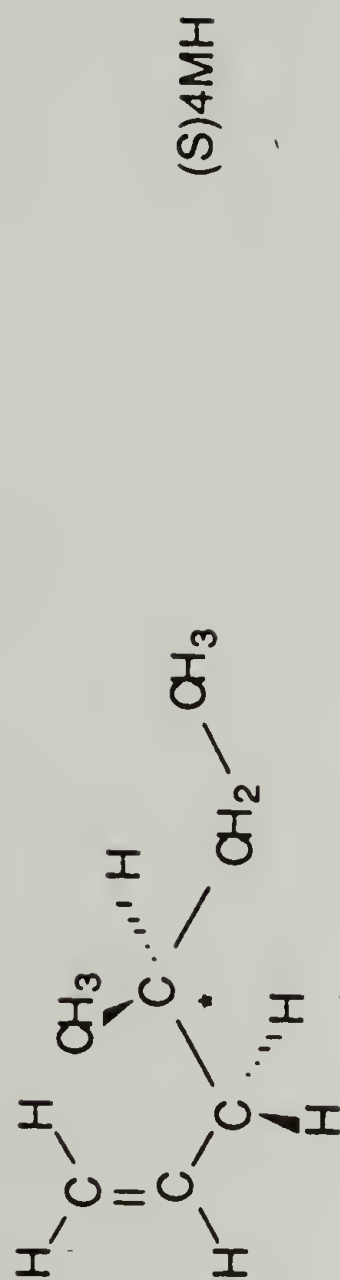
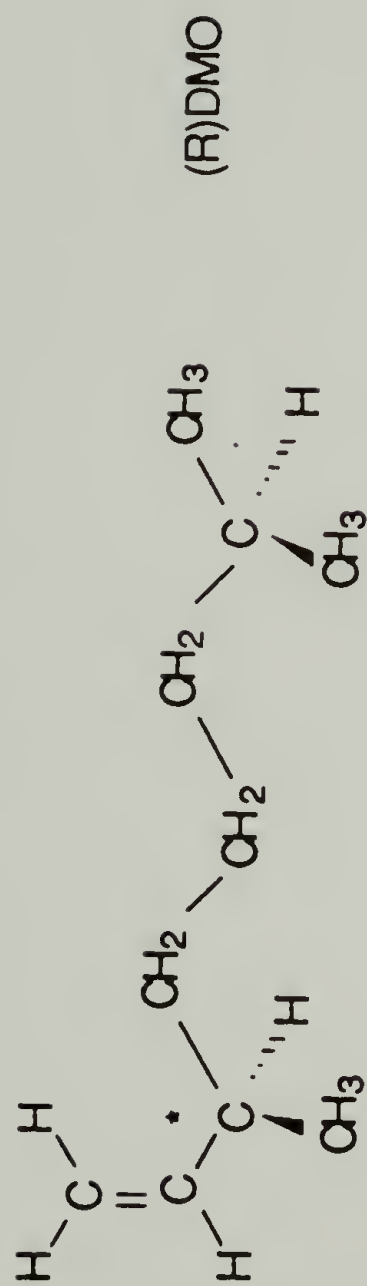


Figure 4.10 Minimum Energy Conformations for (R)DMO and (S)4MH.

of the rates of polymerization  $R_p(S)/R_p(R)$  which can be calculated with the knowledge of  $P_p$ ; which is the percent content of the prevalent enantiomer in the polymer,

$$\frac{R_p(S)}{R_p(R)} = \frac{50 + 0.5 P_p}{50 - 0.5 P_p} \quad (3)$$

At low conversion this is also equal to  $k_p(S)/k_p(R)$ . Changing monomer composition will affect the  $k_p(S)$  or  $k_p(R)$ .  $R_p(R)/R_p(S)$  given in the last column of table 4.5 shows that the stereoelective efficiency is lower for 4MH than DMO. This is as expected, because the substitute is further removed from the double bond in the former. Polymerization of 5-substituted olefins is nonster-eoelective.<sup>15</sup> This difference is diminished for active centers which are less sterically hindered. For instance low stereospecificity sites produce P4MH and PDMO of low stereoregularity with the same handedness.<sup>6</sup>

When 85%(S)DMO was used as the monomer, the PDMO produced exhibited large positive rotation regardless of the stereoregularity of the polymer (table 4.6). Therefore, the (S)DMO was polymerized in this case even though the opposite antipode was favored for the ster-eoelective polymerization of the racemic monomer. This may be explained by a small energy difference between the coor-

dination of one enantiomer over another. An alternative explanation is that the active centers have two vacant coordinative positions, and that Ti(III) of either chirality can complex with (S)2MBP molecules. The results observed with 85%(S)DMO would mean that it is the chirality of the titanium which determines the stereoelection process and that the chiral influence of the base is weak.

Finally, the stereospecificity and stereoelectivity are not associated phenomena. The optical rotation of the polymer increases with increasing stereoregularity for the acetone, ethylacetate, and diethylether fractions (table 4.5), however, the most stereoregular cyclohexane fraction has a smaller optical rotation than the ether fraction. In the case of the copolymer of 3MH with 85%(S)DMO, this rotation changes sign. In other words the low and high stereospecific active centers seem to prefer the opposite antipodes. This was also found to be the case for P4MH obtained with CW catalysts containing either chiral  $B_i$  or  $B_e$  or both.<sup>6</sup> The fractions with intermediate stereoregularity possess highest optical purity. The PDMO produced by these catalysts exhibit opposite optical rotation for the stereoregular and stereoirregular fractions. Using the catalyst  $MgCl_2/(-)$ -menthylanisate/ $TiCl_4$ //TBA, Pino et al<sup>1</sup> found the stereoirregular and stereoregular P4MH to contain monomers with prevalent S and R chirality, respectively. These observations cannot

be attributed to polymerization of prevailing antipode in the unpolymerized monomer. In fact, when the amount of Lewis base is small,  $[(-)\text{-menthylanisate}]/([Ti]/[Al]) = 0.13$ , the catalyst polymerized the (S)DMO preferentially in both stereoirregular and stereoregular products,<sup>1</sup> also, the optical purity of the DMO polymerized to stereoirregular polymer is larger than that of the unpolymerized monomer. Therefore, the synthesis of the stereoirregular ethylacetate soluble PDMO is also stereoelective. Pino et al<sup>1</sup> had suggested that the active center for the polymerization of branched  $\alpha$ -olefins have two free coordination sites one of which is occupied by the optically active Lewis base as also proposed above. The stability of the complexed  $B^*$  would depend upon the chirality of the Ti ion, i.e.  $C_1 \cdot (S)2MBP$ . If the former complex is stable, it will be stereospecific and polymerize one antipode stereoelectively. The complex of the opposite chirality may be less stable; the Lewis base can dissociate and reassociate. It will polymerize the opposite antipode with lower stereoregularity.



## Conclusions

It has been demonstrated for the superactive CH catalyst that the active sites are chiral, activities of catalyst complexed with optically pure Lewis base and racemic Lewis base are different. Each site possibly has a preference for one enantiomer over the other. Also, it is seen that a variety of active sites with different steric hindrance and therefore different stereoelective abilities are present as evidenced by the fractionated polymers of the stereoelective polymerizations. Active site counting has shown that the number of active centers is dependent upon the steric structure of the monomer.

## References

1. P. Pino, G. Guastalla, B. Rotzinger, and R. Mülhaupt in **"Transition Catalyzed Polymerizations"**, R.P. Quirk, Ed., Harwood Acad. Pub., N.Y., 435 (1983).
2. a) J.C.W. Chien and C.I. Kuo, *J. Polym. Sci., Polym. Chem. Ed.*, **23**, 731 (1985). b) J.C.W. Chien and Y. Hu, *J. Polym. Sci., Polym. Chem. Ed.*, **25**, 2847 (1987).
3. J.C.W. Chien, S. Weber, and Y. Hu, *J. Polym. Sci., Polym. Chem. Ed.*, **27**, 1514 (1989).
4. J.C.W. Chien and Y. Hu, *J. Polym. Sci., Polym. Chem. Ed.*, **27**, 897 (1989).
5. P. Pino, F. Ciardelli, G.P. Lorenzi, and G. Natta, *J. Am. Chem. Soc.*, **84**, 1487 (1962).
6. F. Ciardelli, C. Carlini, A. Altomare, F. Menconi and J.C.W. Chien in **"Transition Metal Catalyzed Polymerizations, Ziegler-Natta and Metathesis Polymerization Catalysts"**, R.P. Quirk, Ed., Cambridge Univ. Press, Cambridge, 25 (1988).
7. P. Pino, G. Fochi, O. Piccolo, and U. Giannini, *J. Am. Chem. Soc.*, **104**, 7381 (1982).
8. J.C.W. Chien, T. Ang, and C.I. Kuo, *J. Polym. Sci., Polym. Chem. Ed.*, **23**, 723 (1985).
9. J.C.W. Chien and B.M. Gong, unpublished results.
10. J.C.W. Chien and Y. Hu, *J. Polym. Sci., Polym. Chem. Ed.*, **25**, 2847 (1987).
11. J.C.W. Chien and Y. Hu, *J. Polym. Sci., Polym. Chem. Ed.*, **26**, 2973 (1988).
12. J.C.W. Chien, J.C. Wu, and C.I. Kuo, *J. Polym. Sci., Polym. Chem. Ed.*, **21**, 726 (1983).
13. J.C.W. Chien, L.C. Dickinson, and J. Vizzini, *J. Polym. Sci., Polym. Chem. Ed.*, **28**, 2321 (1990).
14. J.C.W. Chien and C.I. Kuo, *J. Polym. Sci., Polym. Chem. Ed.*, **24**, 1779 (1986).
15. F. Ciardelli, G. Montagnoli, D. Pini, O. Pieroni, C. Carlini, and E. Benedette, *Makromol. Chem.*, **147**, 53 (1971).

## CHAPTER V

# MgCl<sub>2</sub> SUPPORTED HIGH MILEAGE CATALYSTS FOR OLEFIN POLYMERIZATION, AN NMR STUDY

### Introduction

As can be seen in the previous chapters, there is now a fairly quantitative knowledge about the kinds of active sites and the numbers in the MgCl<sub>2</sub> catalysts, which can account for the thousand fold increase in the productivity of isotactic polypropylene over the previous Ziegler-Natta catalysts. This improvement is achieved by the careful preparation of the MgCl<sub>2</sub> support so as to maximize the number of chiral active sites of one kind and to minimize the intrinsic activities of the achiral active sites. Previously, our laboratories have extensively studied the CW type catalyst. FTIR and hydrolysis-GC have been used to characterize the organic components in these materials.<sup>1</sup> The CH system has also been characterized, but no FTIR had been performed on it.

In the study of the CW catalyst by FTIR, it was found that the  $\nu$  C=O for ethylbenzoate (EB) shifted from 1719 cm<sup>-1</sup> to 1683 cm<sup>-1</sup> upon complexation with MgCl<sub>2</sub>. Accompanying this was the shift of the  $\nu$  C-O vibrations from

1279  $\text{cm}^{-1}$  and 1109  $\text{cm}^{-1}$  to 1329  $\text{cm}^{-1}$  and 1306  $\text{cm}^{-1}$ . Treatment of the support with  $\text{TiCl}_4$  resulted in no significant changes in the vibrational spectra except for a broadening of the C=O peak. These results were confirmed by Spitz et al.<sup>2</sup> Sevini et al.<sup>3</sup> had detected an intermediate peak between that of  $\text{MgCl}_2 \cdot \text{EB}$  and  $\text{TiCl}_4 \cdot \text{EB}$ . Peaks attributable to both species in the supported catalysts were observed by Guyot et al.<sup>4</sup> who supported the view of a ternary complex between  $\text{MgCl}_2$ , EB, and  $\text{TiCl}_4$ . Keszler and Simon<sup>5</sup> also assumed that ternary species were present from the existence of constant EB/ $\text{TiCl}_4$  ratios with grinding time. As seen in chapter IV, there is an equimolar ratio between the ester and Ti which is typical for both CH and CW catalysts.

The opposing view was put forth by Terano et al.<sup>6</sup> who made an in depth study on supported catalysts by thermal and FTIR analysis. No endotherms corresponding to the decomposition of  $\text{TiCl}_4 \cdot \text{EB}$  complex were detected after long grinding times of the complex with  $\text{MgCl}_2$ . Also, they saw no distinguishing peaks in the IR of  $\text{TiCl}_4$  and EB complex on the supported catalyst. Yano et al.<sup>7</sup> found that there is a competitive reaction between  $\text{TiCl}_4$  and EB in the coordination on a support created from a Grignard and  $\text{AlCl}_3$ .

There is also the idea that the external Lewis base may convert the atactic sites to isotactic sites.



Kashiwa<sup>8</sup> has claimed an enhancement of isotactic yield by the external base. This has support from Soga et al<sup>9</sup> who converted an aspecific system ( $\text{MgCl}_2/\text{TiCl}_3$ ) to an isospecific system through the treatment with EB.

To shed further light upon the nature of the coordination of the organic components in the CH and CW catalysts, a study utilizing magic angle spinning cross-polarization solid state NMR was performed. This is a novel technique in the analysis of supported catalysts. Abis et al<sup>10</sup>, however, had demonstrated the utility of NMR for catalysts through the study of model compounds ( $\text{MgCl}_2$  and  $\text{TiCl}_4$  ester complexes). In this chapter are presented the results of chemical shift and relaxation measurements of the support at different stages of the catalyst synthesis.

### Experimental

Catalyst samples were prepared as previously described in chapter II. All materials were handled under argon by Schlenk techniques. Aliquots were taken at each step of the support formation and modification, washed with 4 X 100 ml of heptane, and vacuum dried for NMR analysis. Solution NMR of the adduct was performed in  $\text{CDCl}_3$  on a Varian XL-300 spectrometer.

Samples for solid NMR were loaded into 6 mm i.d. sapphire NMR cells equipped with double viton "O"-ring

fitted ceramic end caps (Doty Scientific, 600 Clemson Rd., Columbia, SC 29223) in a dry box also under argon. High purity nitrogen was used as the spinning gas to avoid any reaction with air. The samples were only exposed to the atmosphere from Schlenk tube to the NMR probe.

$^{13}\text{C}$ -NMR spectra were measured at 50.13 MHz with 5  $\mu\text{s}$   $90^\circ$  pulses for both carbon and protons on an IBM 200 AF instrument equipped with an IBM solids accessory. Samples were spun at 4 kHz. The number of scans for the model compounds was 400 while for the procatalyst synthesis steps it was 3000-4000. Cross polarization spectra were obtained with a proton  $90^\circ$  pulse followed by 1-2 ms simultaneous  $^1\text{H}$  and  $^{13}\text{C}$  spin-lock and 50 ms acquisition with simultaneous high power proton decoupling. The phase of the pulse was alternated between the x and -x axes to eliminate baseline irregularities. The cross-polarization constant  $T_{\text{CH}}^{-1}$  was estimated from the initial exponential rise of signal as a function of spin-lock time. The spin lattice relaxation rate of the protons in the rotating frame ( $T_{1\rho}^{-1}$ ) was estimated from the decay of the  $^{13}\text{C}$  signal with spin-lock time. The spin lattice relaxation rate of the protons in the laboratory frame ( $T_1$ ) was measured by a  $180^\circ$   $^1\text{H}$  pulse followed by a variable delay, a  $^1\text{H}$   $90^\circ$  pulse, and then by the above spin-lock and acquisition sequence.

For the study of the CH system, three model supports were created to aid in the characterization. One was formed by the ball-milling of  $\text{MgCl}_2$  with diisobutylphthalate (BP) (6.25:1) for 72 hrs. The second was formed by the reaction of  $\text{TiCl}_4$  with an equimolar amount of BP at room temperature in heptane. And the third was synthesized by ball-milling the  $\text{TiCl}_4 \cdot \text{BP}$  complex with  $\text{MgCl}_2$  for 72 hr in a ratio of 1:10. In all cases the resulting solids were washed with 4 X 100 ml of heptane and vacuum dried.

## Results

### CW System

Magnesium Chloride/Ethylbenzoate. Figure 5.1 shows the MAS-CP  $^{13}\text{C}$  spectrum of  $\text{MgCl}_2/\text{EB}$  (1:0.015). The intensities were low because of the broad linewidths of 300 to 570 Hz. The side bands at 3 kHz are marked with an asterisk. The chemical shift values of the EB in  $\text{MgCl}_2$  are compared with those of neat EB in table 5.1.

$\text{MgCl}_2/\text{EB}/p\text{-Cresol}$ . Figure 5.2 is the MAS-CP  $^{13}\text{C}$ -NMR spectrum of PC and EB adsorbed on  $\text{MgCl}_2$ . The dominant features are due to PC which is present in an amount 3.3 times greater than EB and because the PC resonances have narrower linewidths than those of EB. In fact, because of the lower concentration and broader linewidth only the

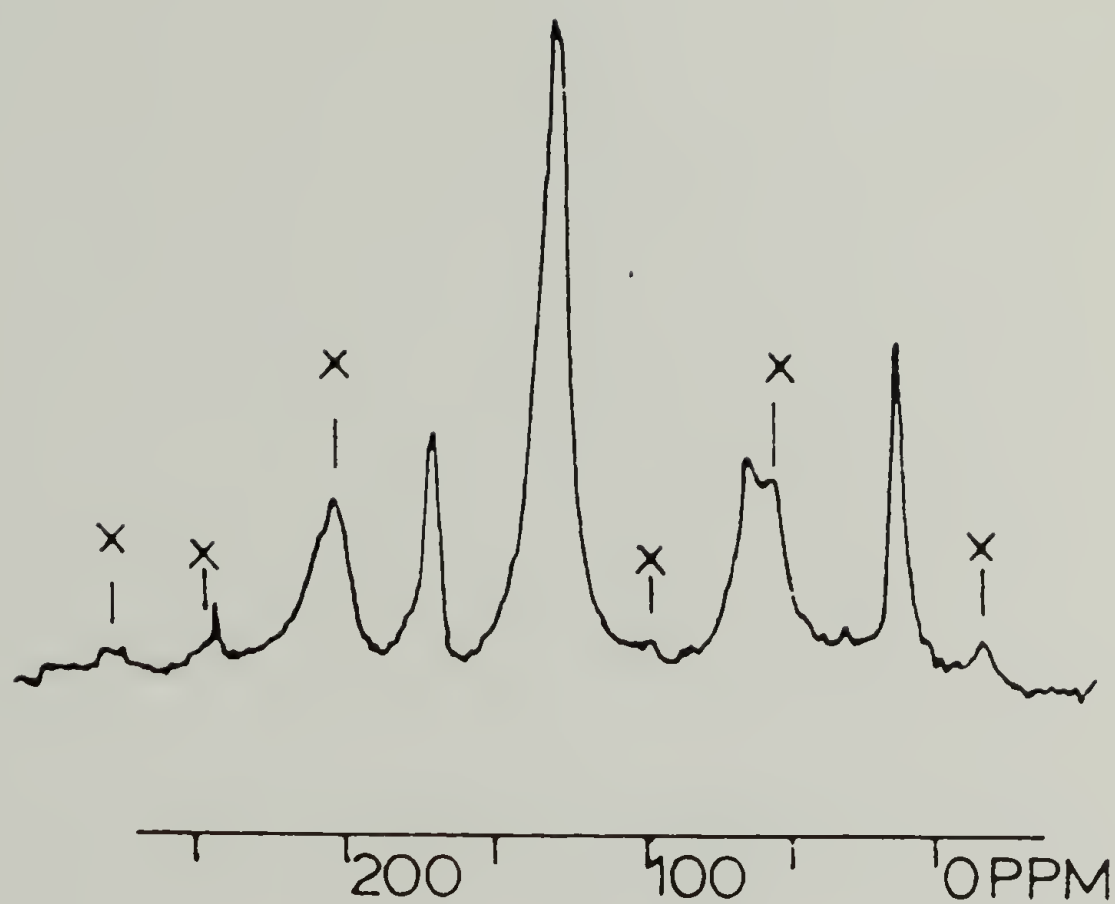


Figure 5.1 MAS-CP  $^{13}\text{C}$  NMR Spectrum of  $\text{MgCl}_2/\text{EB}$ . Sidebands Marked with X.



**Table 5.1  $^{13}\text{C}$  NMR Parameters for  $\text{MgCl}_2/\text{EB}$**

	$\text{C}_{\text{ar}}$	$-\text{CO}_2$	$-\text{OCH}_2$	$\text{CH}_3$
Chemical shift obsd, ppm	128.9	171.0	65.2	14.2
liq. EB	129	166.3	60.8	14.4
Linewidth, Hz	570	300		300
$T_1^H$ , ms	36	31		
$T_{1\rho}^H$ , ms	5.3	8.7		7.3
$T_{\text{CH}}$ , ms	0.12	0.47		0.11
Relative intensity	6.4	0.7		1.0

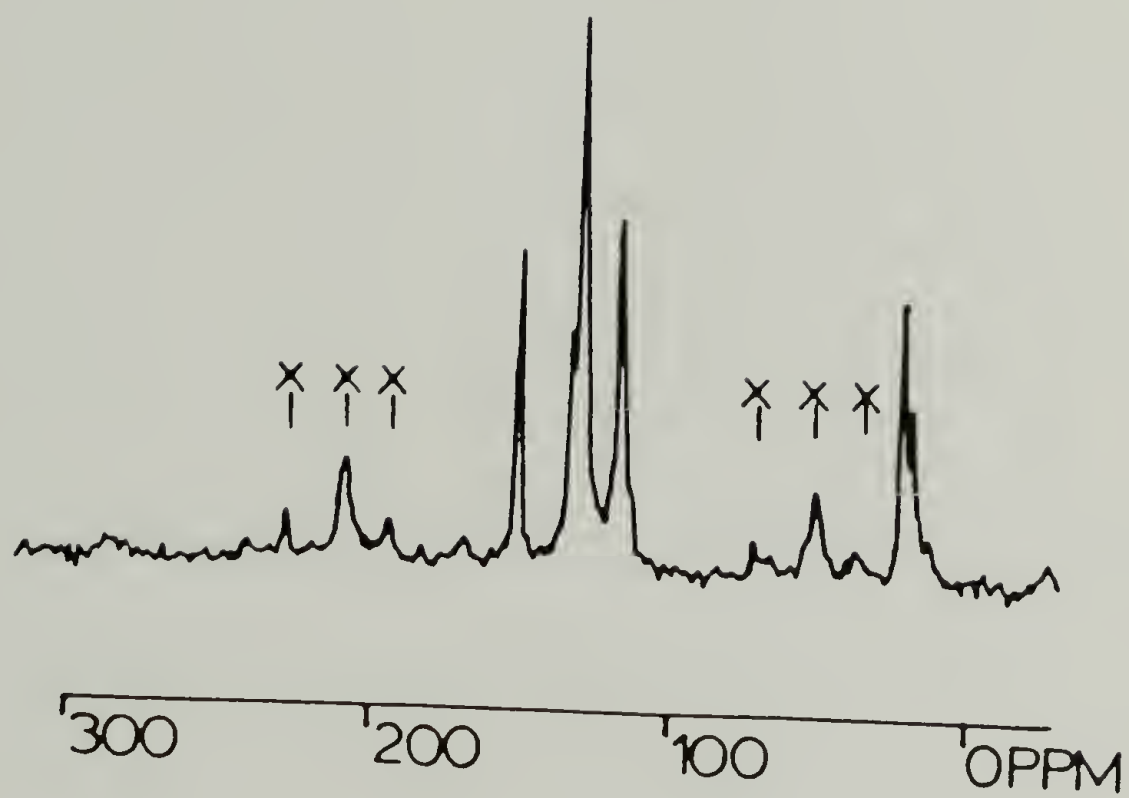


Figure 5.2 MAS-CP  $^{13}\text{C}$  NMR Spectrum of  $\text{MgCl}_2/\text{EB}/\text{p-Cresol}$ . Sidebands Marked with X.

carbonyl and oxymethylene carbons of EB are weakly observable in figure 5.2; its other resonances are unresolved under the dominant PC lines.

All the carbon nuclei in PC on  $\text{MgCl}_2$  have chemical shifts nearly the same as PC dissolved in  $\text{CDCl}_3$  or DMSO (table 5.2). Only the unprotonated  $\text{OC}_1$  carbon shows a small upfield shift. The interesting difference is that there are two peaks for the methyl resonance in figure 5.2 situated 2 ppm above and below the methyl position in solution.

The chemical shifts of the ethylbenzoate peaks simultaneously present in the sample with the PC are also of interest. Comparing tables 5.1 and 5.2, it is seen that the carbonyl of the EB in the  $\text{MgCl}_2/\text{EB}/\text{PC}$  sample is displaced about 4 ppm upfield approximately back to the liquid NMR position, but that the oxymethylene peak is unchanged.

According to the method of preparation, the elemental analysis, and hydrolysis GC, the material should contain PC:EB in a 1:0.3 ratio. However, as seen in table 5.2 the MAS-CP NMR spectra give the ratio of about 1:0.16. Some possible reasons for this discrepancy are the following: the relative CP efficiencies of detecting EB and PC are not known; more mobile EB could reduce EB intensity. The signal to noise for EB peaks in  $\text{MgCl}_2/\text{EB}/\text{PC}$  also contributes to the error. The EB linewidths in  $\text{MgCl}_2/\text{EB}$

**Table 5.2  $^{13}\text{C}$  NMR Parameters for  $\text{MgCl}_2/\text{EB}/p\text{-Cresol}$**

	$\text{PC}^a$					$\text{EB}$	
	$\text{C}_1$	$\text{C}_p$	$\text{C}_o$	$\text{C}_m$	$\text{CH}_3$	$\text{CO}_2$	$\text{OCH}_2$
Chemical shift							
obsd., ppm	150.2	133	129.7	116.3	22.2, 18.6	167.1	64.1
in DMSO	160	131	129	119	20.0		
in $\text{CDCl}_3$	158.3		130.2	115.6	20.4		
Linewidth, Hz	140		230	195	140		
$T_1^H$ , ms	189		161	168	187, 147		
$T_{1\rho}^H$ , ms	10.1		8.5	9.2	10.3, 12.8		
$T_{CH}$ , ms	0.18		0.08	0.04	0.08, 0.69		
Relative intensity							
per carbon	1.0		0.9	0.9	1.1	0.17	0.15

<sup>a</sup>  $O$  = ortho,  $p$  = para,  $m$  = meta carbon,  $\text{C}_1$  = unprotonated PC carbon.



are about two times broader than those of PC in this sample. If the linewidths of EB are further increased in the  $\text{MgCl}_2/\text{EB}/\text{PC}$ , it could contribute toward reduction in signal intensity. A combination of the above factors may account for the low EB:PC intensity ratios in the MAS-CP NMR for this sample.

The relaxation times were obtained and are presented in table 5.2.

The cross polarization times for PC are very short for all its carbons indicating that the PC molecules maintain rigid positions on the  $\text{MgCl}_2$ . The relatively longer  $T_{\text{CH}}$  for the aromatic  $\text{C}_1$  is a consequence of the absence of directly bonded protons for that carbon. The virtually uniform  $T_{1\text{p}}^{\text{H}}$  values shows rapid spin diffusion among protons as found in the EB case.

An attempt was made to measure the  $T_1^{\text{C}}$  and it was found to be longer than 30 s which is inconveniently long for accurate measurement in these low signal to noise samples. Such a long carbon spin lattice relaxation time argues further for a rigid adsorption of the PC onto  $\text{MgCl}_2$  at room temperature.  $T_2^{\text{H}}$  is not exponential and intensity decays away entirely within 25  $\mu\text{s}$ . This is much shorter than  $T_2^{\text{H}}$  in simple organic crystals. The cause is not likely to be rigid close packing of proton magnetic dipoles, but it may be ascribed to proton coupling to the rapidly relaxing chloride nuclei.

MgCl<sub>2</sub>/EB/PC/Triethylaluminum. The addition of triethylaluminum (TEA) to the PC/EB/MgCl<sub>2</sub> causes some definite shift and linewidth changes in the PC carbons as is evident from figure 5.3. The NMR parameters for this sample are listed in table 5.3.

The clearest change upon TEA binding is in shift of the position of C<sub>m</sub> peak downfield from 116.3 to 120.3 ppm. There is now a shoulder evident at 154 ppm on the C<sub>1</sub> peak of PC. The cross polarization spectrum shows no peaks ascribable to the ethyl groups of TEA. Pure TEA has carbon resonances at 0.75 and 8.74 ppm. A characteristic of alkyl aluminum compounds is that the alkyl groups are in rapid exchange. The fact that the ethyl resonances of Et<sub>n</sub>Al(OC<sub>6</sub>H<sub>4</sub>Me)<sub>3-n</sub> were unobservable in figure 5.3 means that there is too much motion for the proton magnetization to be transferred to the carbon nuclei.

The aliphatic region of the NMR spectrum of this sample undergoes some evolution even when stored in a very reliable inert atmosphere as shown in figure 5.4. The two samples compared to the freshly prepared are: (1) sample examined left in the NMR rotor kept in the dry box for about a week, during which it was taken in and out of the box several times, and (2) preparation of the sample stored in the dry box for 1 week. The two show nearly identical changes in the aliphatic region suggesting that

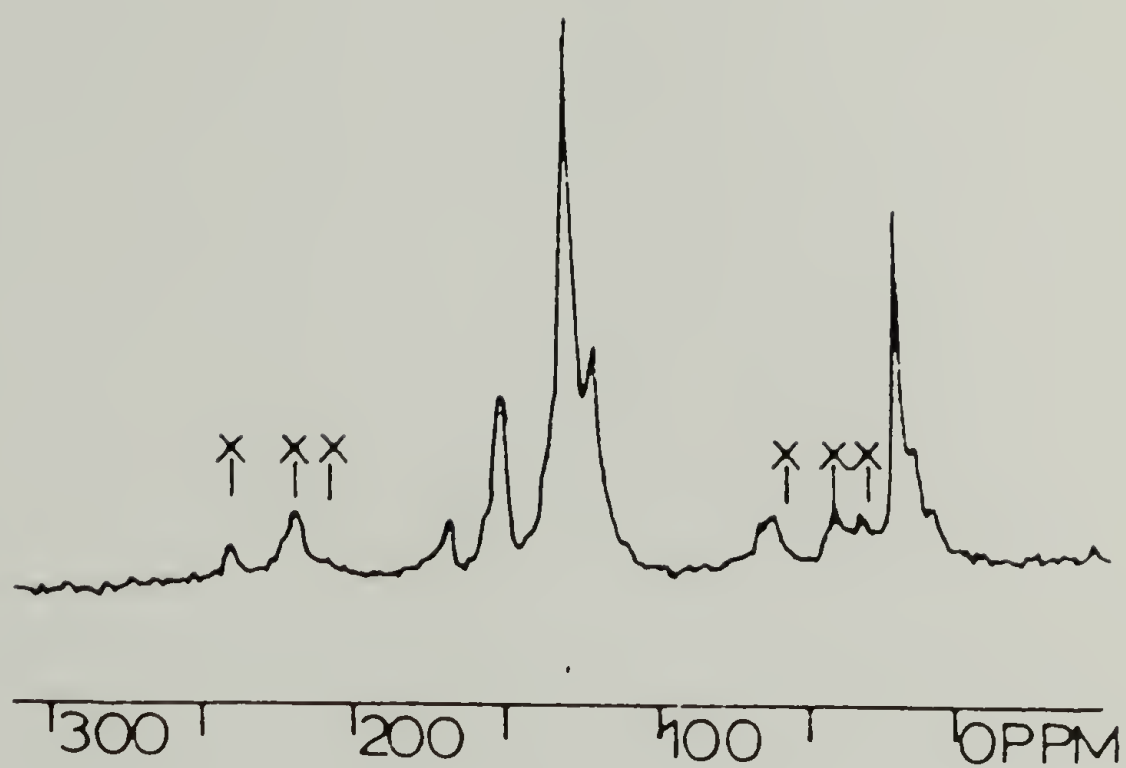
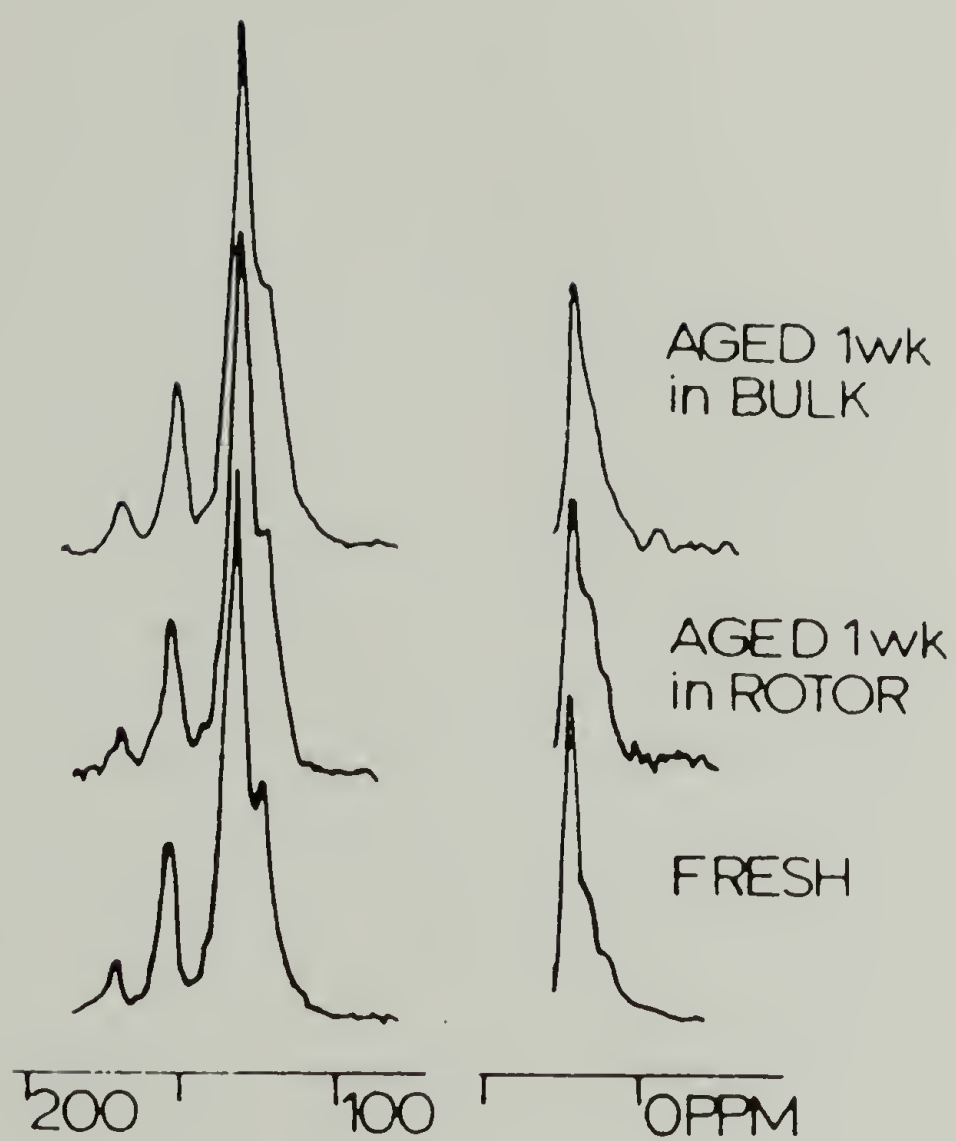


Figure 5.3 MAS-CP  $^{13}\text{C}$  NMR Spectrum of  $\text{MgCl}_2/\text{EB}/\text{p-Cresol}/\text{TEA}$ . Sidebands Marked with X.

**Table 5.3  $^{13}\text{C}$  NMR Parameters for  $\text{MgCl}_2/\text{EB}/\text{p-Cresol}/\text{TEA}$**

	$\text{Et}_n\text{Al}(\text{OC}_6\text{H}_4\text{Me})_{3-n}$				EB	
	$\text{C}_1$	$\text{C}_{o,p}$	$\text{C}_m$	$\text{CH}_3$	$\text{CO}_2$	$\text{OCH}_2$
Chemical shift, ppm	151	129	120	20.2	167	66
$T_1^H$ , ms	150	100	90	121	74	80
$T_{1\rho}^H$ , ms	7.9	5.8	4.0	6.7	13	3.7
$T_{\text{CH}}$ , ms	0.20	0.05	0.03	0.10	0.2	0.03





**Figure 5.4** Comparison of MAS-CP  $^{13}\text{NMR}$  Spectra for Differently Aged  $\text{MgCl}_2/\text{EB}/\text{PC}/\text{TEA}$  Catalyst.

some chemistry is taking place not attributable to possible exposure to the atmosphere.

MgCl<sub>2</sub>/EB/PC/TEA/TiCl<sub>4</sub>. The reaction of the support in the previous section with TiCl<sub>4</sub> produces the CW procatalyst, the MAS-CP NMR spectrum of which is shown in figure 5.5. The poor quality of the spectrum is partly due to the fact that the rotor could only be spun at low angular velocity despite several tries at repacking. This resulted in more sideband problems with the lineshapes and lowering of spectral intensity. In addition paramagnetic Ti ions that are present can compound these difficulties. The NMR parameters are given in table 5.4. It must be noted that some of the contact shifts are possible and much of the carbon present is unobservable due to paramagnetic shortening of T<sub>1</sub> beyond observability.

The C=O, C<sub>Ar</sub>, -OCH<sub>2</sub>, and CH<sub>3</sub> carbons of EB are found as in the MgCl<sub>2</sub>/EB sample at 172, 128., 68, and 13.9 ppm, respectively. Their linewidths are generally greater than the corresponding peaks in figure 5.1 (table 5.1) even considering the low accuracy. There is a shoulder at 20 ppm, which is attributable to the p-CH<sub>3</sub> carbon of PC derivatives. However, the other carbons were buried beneath the sidebands.

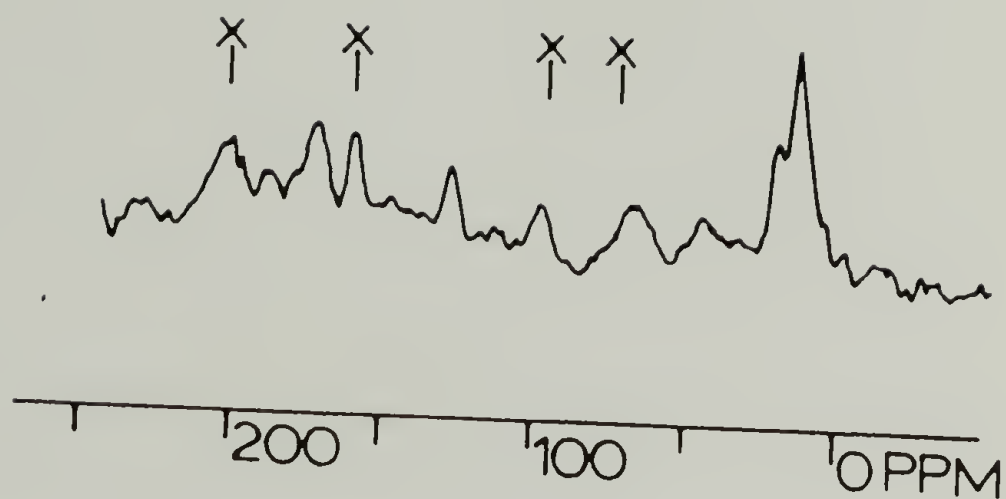
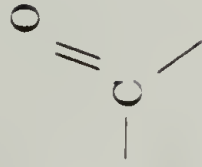


Figure 5.5 MAS-CP  $^{13}\text{C}$  NMR Spectrum of  $\text{MgCl}_2/\text{EB}/\text{PC}/\text{TEA}/\text{TiCl}_4$ . Sidebands Marked with X.

**Table 5.4**  $^{13}\text{C}$  NMR Parameters for  $\text{MgCl}_2/\text{EB}/\text{PC}/\text{TEA}/\text{TiCl}_4$

Carbons	Chemical shift (ppm)	Linewidth (Hz)
EB: 	172	500
$\text{C}_{ar}$	128	
$\text{OCH}_2$	$\sim 68$	
$\text{CH}_3$	13.9	400
PC: $p\text{-CH}_3$	20	



## CH System

MgCl<sub>2</sub>·EH/PA. The liquid NMR spectrum of the ester free adduct is similar to that of the free 2-ethyl-1-hexanol (EH) except for the chemical shifts. The downfield shift from 65.2 ppm to 66.8 ppm is indicative of the coordination of the alcohol to MgCl<sub>2</sub>. Nothing can be elucidated of the other peaks in the alkyl region for they are masked by the decane solvent of the adduct solution.

The addition of phthalic anhydride in a ratio of 1:6.25 MgCl<sub>2</sub>/PA created an adduct containing a coordinated dioctylphthalate (DOP) ester (the reaction product of PA and EH). Because of the insolubility of this adduct, only low concentration samples of the compound could be used. But because of the weak signal of the C=O, this could not be detected. With a concentration of approximately 80% adduct in CDCl<sub>3</sub>, a spectrum with poor signal to noise was obtained in which two C=O peaks were evident at 170.6 and 176.5 ppm (the liquid C=O was 167.1 ppm) (figure 5.6 and Table 5.5). The oxymethylene was seen at 70.1 ppm, 2.5 ppm downfield from the free dioctylphthalate. This suggests that two states of the ester carbonyls exist. Possibly they are that of being coordinated and that of being uncoordinated. The appearance of almost equal intensities seems to suggest that only one carbonyl coordinates with the Mg metal.

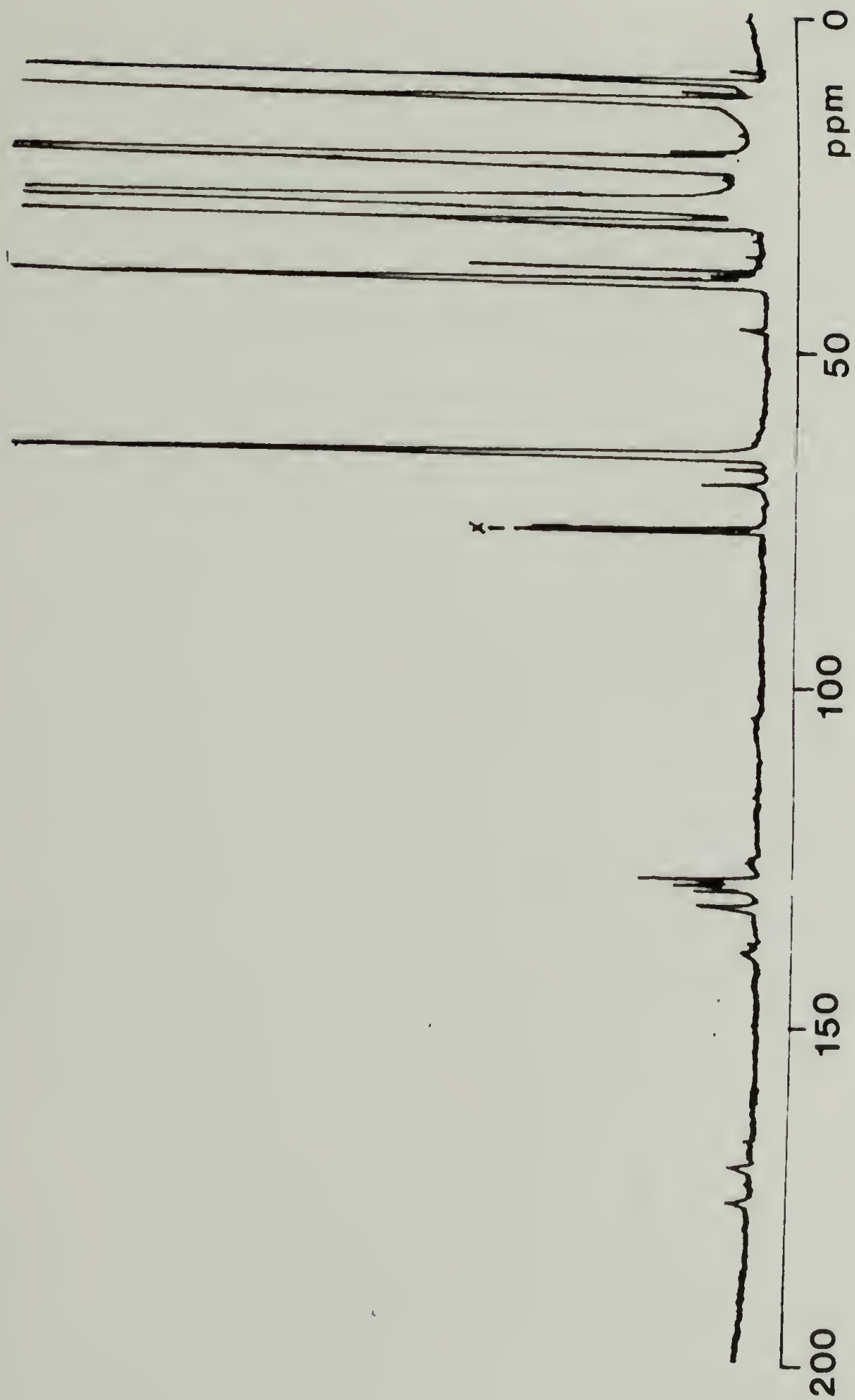


Figure 5.6 Liquid  $^{13}\text{C}$  NMR spectrum of  $\text{MgCl}_2\cdot\text{EH/PA}$  in  $\text{CDCl}_3$ .

Table 5.5  $^{13}\text{C}$  NMR Parameters for  $\text{MgCl}_2 \cdot \text{EH/PA}$

Chemical Shift Obsvd. (ppm)	$^{13}\text{C}$	
	C=O	C <sub>Ar</sub> -OCH <sub>2</sub> -
	170.6, 176.5	128.3, 129.8, 70.1, 67.5 132.2
Liq. dioctylphthalate*	167.6	128.9, 130.9, 68.1 132.8
Liq. EH*	-	- 65.2-65.6

\* liquid NMR run in  $\text{CDCl}_3$

TiCl<sub>4</sub>·BP. The model compound spectrum had a clear separation of peaks (figure 5.7). The methylene carbon is 7 ppm further downfield (table 5.6) than what was seen in the MgCl<sub>2</sub>·EH·PA spectrum. The aromatic carbons as well are shifted further downfield from 128-132 to 129-135 ppm. But the carbonyl is almost at the same chemical shift. So clearly there is a lower density of electrons in the vicinity of the aromatic carbons. T<sub>1</sub><sup>H</sup> values are shorter and in the same range as found the ethylbenzoate(EB)·MgCl<sub>2</sub> complex. This was said to be indicative of rigidity because of the increased polarization efficiency. This is to be expected as this is a discreet complex.

Relaxation experiments revealed that the carbonyl peak was in reality two peaks. It is possible that because of steric restrictions within the coordination sphere of the Ti, Only one of the ester carbons are closely coordinated in the complex.

MgCl<sub>2</sub>·BP. This spectrum of the model complex is clearly defined as was that of the previous compound (figure 5.8). The surprising result is the clear existence of three carbonyl peaks and two methoxy carbon peaks (table 5.7). In the previous study of co-ground EB·MgCl<sub>2</sub> only one carbonyl peak was clearly defined. The T<sub>1</sub><sup>H</sup>'s are all around 0.6 s about half of that observed in the TiCl<sub>4</sub>·BP complex. This may be due to quadrupolar interaction of the ester nuclei with the lattice chlorides.



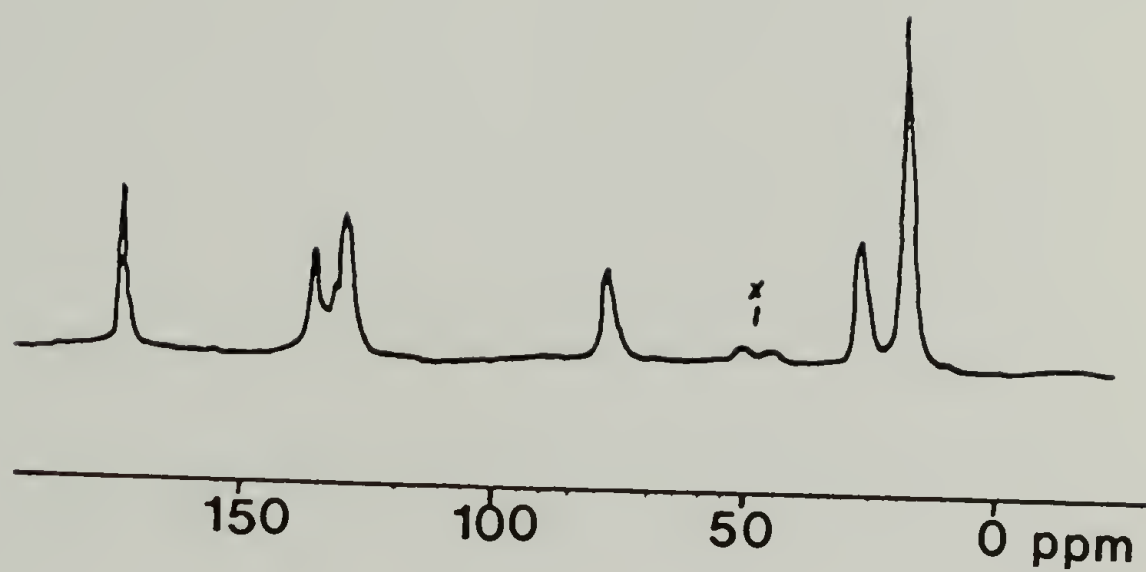


Figure 5.7 MAS-CP  $^{13}\text{C}$  NMR Spectrum of  $\text{TiCl}_4\cdot\text{BP}$ .  
Sidebands Marked with X.

Table 5.6  $^{13}\text{C}$  NMR Parameters for  $\text{TiCl}_4\cdot\text{BP}$

	C=O	C <sub>Ar</sub>	-OCH <sub>2</sub> -
Chemical Shift Obsvd. (ppm)	173.4	129.2, 131.3, 135.0	77.4
$T_1^H$ (s)	1.5	1.3	1.3

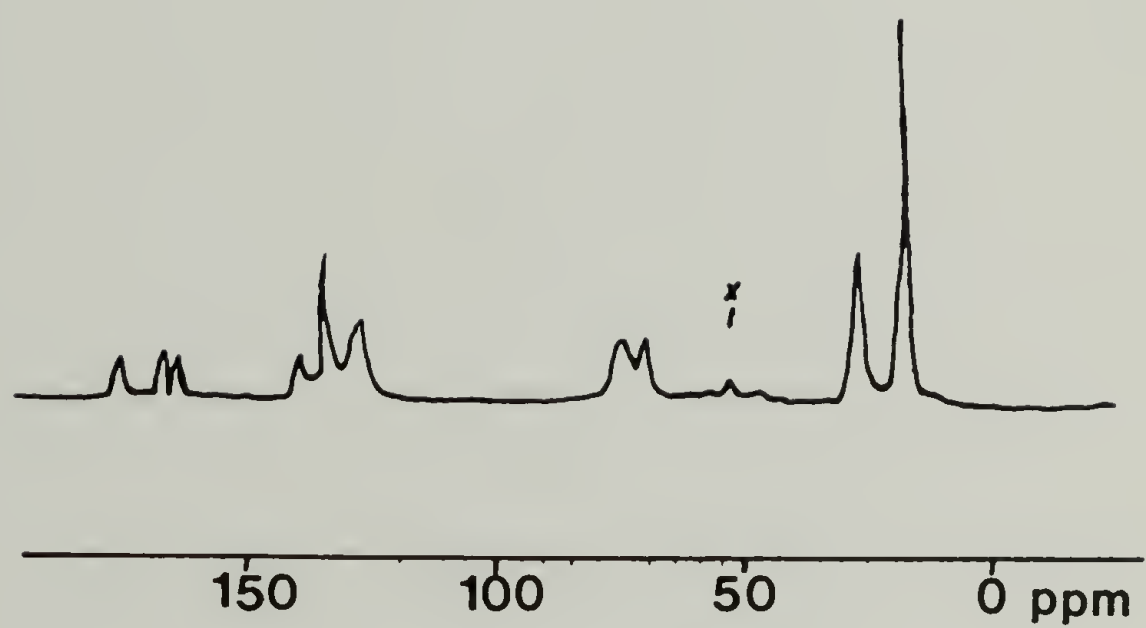


Figure 5.8 MAS-CP  $^{13}\text{C}$  NMR Spectrum of  $\text{MgCl}_2 \cdot \text{BP}$ .  
Sidebands Marked with X.

Table 5.7  $^{13}\text{C}$  NMR Parameters for  $\text{MgCl}_2 \cdot \text{BP}$

Chemical Shift Obsvd. (ppm)	$^{13}\text{C}$		
	C=O	C <sub>Ar</sub>	-OCH <sub>2</sub> -
	163.5, 166.5, 175.0	126.1, 133.7, 138.5	70.2, 75.0
Liq. BP	167.4	128.8, 130.9, 132.6	71.6
$T_1^H$ (s)	0.60	0.60	0.60



These values are twenty times larger than that found for the  $\text{MgCl}_2 \cdot \text{EB}$  complex. Possibly the interaction with the  $\text{MgCl}_2$  is not as strong as when EB is used. The solution value for the BP carbonyl is 167.4 ppm. Two of the peaks seen in this spectrum are close to this value, indicating the presence of loosely bound or unbound carbonyls.

$\text{MgCl}_2 \cdot \text{TiCl}_4 \cdot \text{BP}$ . The spectrum is broader than that of the previous (figure 5.9). On the surface there appears to be simply an addition of the two previous spectra. The carbonyls for the  $\text{MgCl}_2 \cdot \text{BP}$  complex are apparent (table 5.8) showing the partial dissociation of the  $\text{TiCl}_4 \cdot \text{BP}$  complex. Those carbonyl peaks due to the latter complex are quite broad and overlap.

$\text{MgCl}_2 \cdot \text{EH/PA/TiCl}_4$ . In this reaction the support is formed from precipitation of  $\text{MgCl}_2$  by the reaction of the solvating alcohol with  $\text{TiCl}_4$ . Because of the large excess of the  $\text{TiCl}_4$  used the support contains both  $\text{TiCl}_4$  and  $\text{TiCl}_3\text{OR}$ . Unlike the previous spectra, the intensities are low and the peaks are broad (figure 5.10). No longer are the aromatic carbons resolved. The alkyl region is more intense than the aromatic region. The  $T_1^{\text{H}}$ 's (table 5.9) are the same order of magnitude as that of the model support which is indicative of the same degree of interaction between the components.

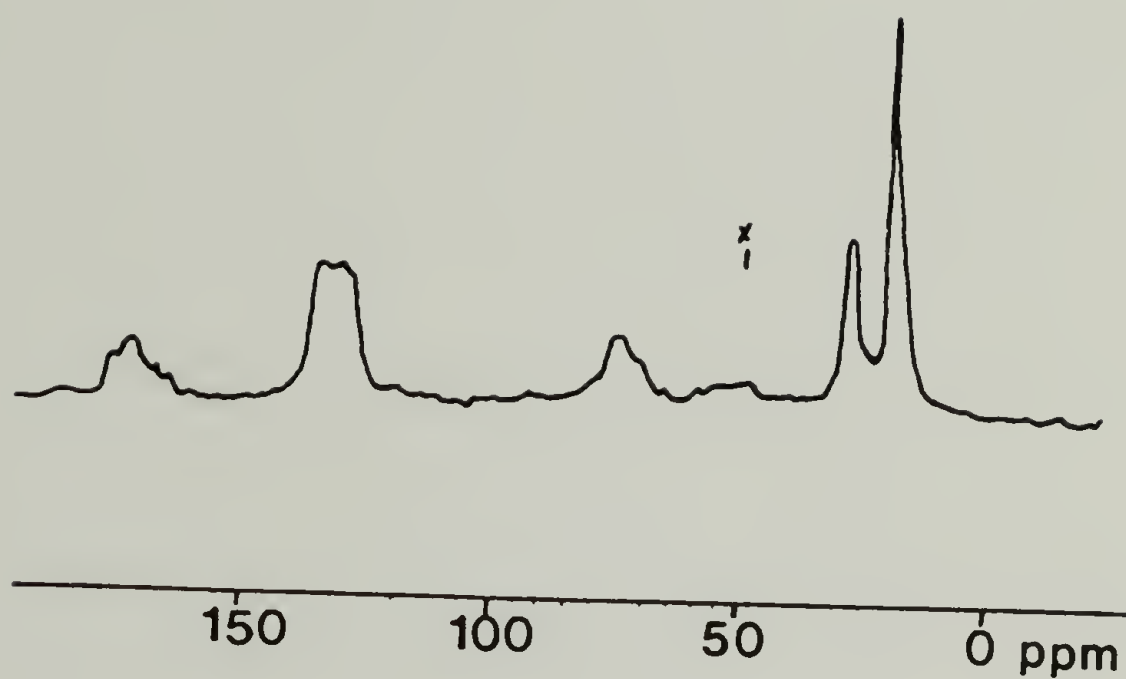


Figure 5.9 MAS-CP  $^{13}\text{C}$  NMR Spectrum of  $\text{MgCl}_2 \cdot \text{TiCl}_4 \cdot \text{BP}$ . Sidebands Marked with X.

Table 5.8  $^{13}\text{C}$  NMR Parameters for  $\text{MgCl}_2 \cdot \text{TiCl}_4 \cdot \text{BP}$

	C=O	C <sub>Ar</sub>	-OCH <sub>2</sub> -
Chemical Shift Obsvd. (ppm)	163.5-175.0	126.1-138.5	70.2-77.4
T <sub>1</sub> <sup>H</sup> (s)	0.5	0.4	*

\* not sufficiently resolved for meaningful measurement

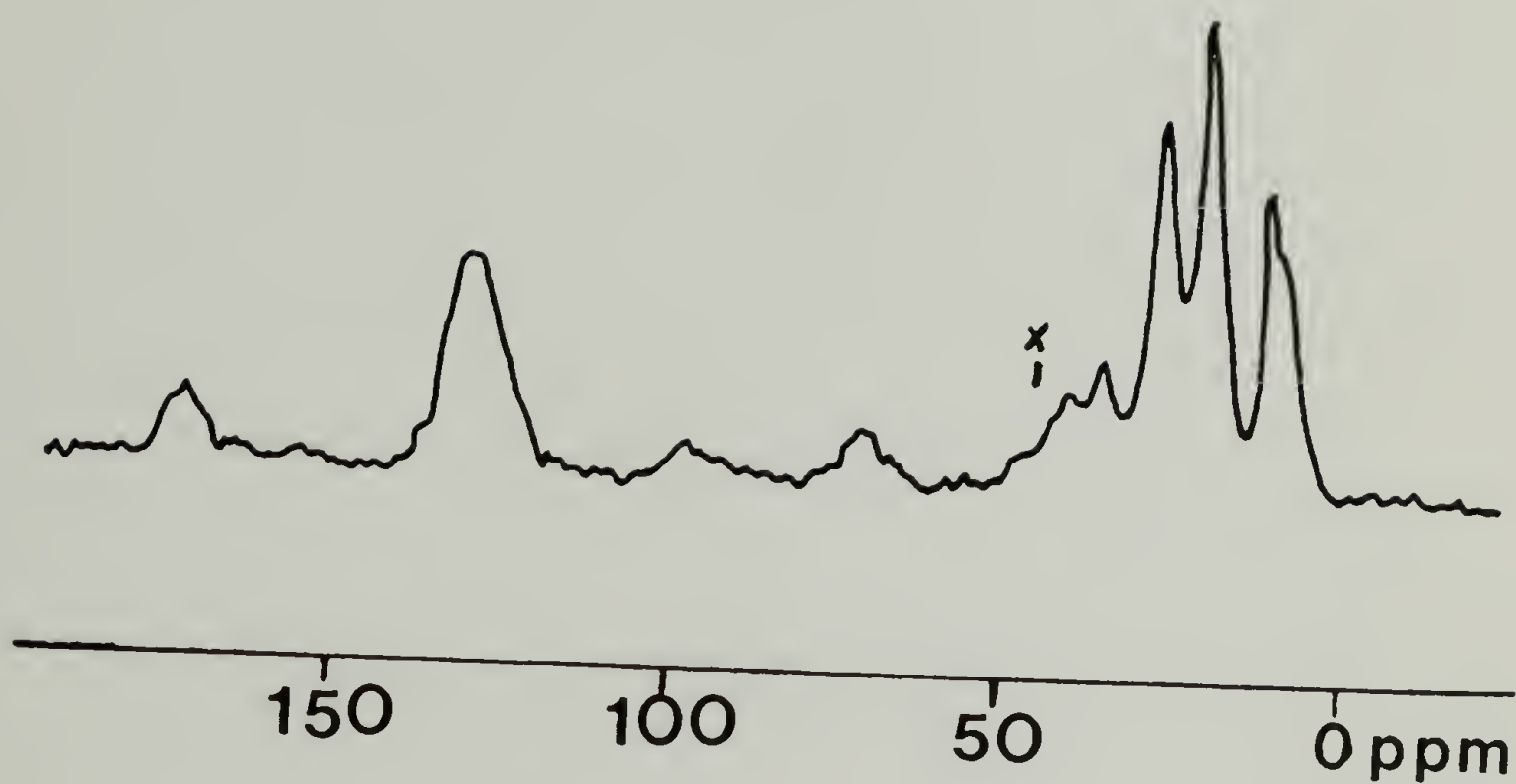


Figure 5.10 MAS-CP  $^{13}\text{C}$  NMR Spectrum of  $\text{MgCl}_2\cdot\text{EH/PA/TiCl}_4$ . Sidebands Marked with X.

Table 5.9  $^{13}\text{C}$  NMR Parameters for  $\text{MgCl}_2\cdot\text{EH}/\text{PA}/\text{TiCl}_4$

	C=O	C <sub>Ar</sub>	-OCH <sub>2</sub> -
Chemical Shift Obsvd. (ppm)	173.8	131.3	74.3
T <sub>CH</sub> (μs)	455	17	*
T <sub>1ρ</sub> <sup>H</sup> (ms)	41	7.9	*
T <sub>1</sub> <sup>H</sup> (s)	0.48	0.48	*

\* not sufficiently resolved for meaningful measurement



The chemical shift of the carbonyl is 7 ppm downfield from the solution value. It is surprisingly close to that of the  $\text{TiCl}_4/\text{BP}$  complex. (That for the  $\text{MgCl}_2/\text{BP}$  was 163.5, 166.5 and 175.0 ppm.) But the  $T_1^H$  is longer suggesting that the chelation is not as strong as in the  $\text{TiCl}_4/\text{BP}$ , that is, the mobility is greater. The  $T_{\text{CH}}$  is close to the same value as that of  $\text{MgCl}_2/\text{EB}$ , however.

$\text{MgCl}_2 \cdot \text{EH}/\text{PA}/\text{TiCl}_4/\text{BP}$ . On addition of the BP ester, a large displacement of the alcoholate occurs. New peaks due to the BP appear at 26.7 and 17.6 ppm in the alkyl region (figure 5.11). No differentiating peaks can be seen in the aromatic or the carbonyl region. But this spectrum is more resolved than the previous in these areas. Also, the  $\text{OCH}_2$  has a narrower line width.

The chemical shift of the carbonyl moves 2 ppm upfield toward the solution value (table 5.10). The  $\text{OCH}_2$  and the aromatic peaks occur at about the same chemical shifts.

$\text{MgCl}_2 \cdot \text{EH}/\text{PA}/\text{TiCl}_4/\text{BP} + \text{TiCl}_4$  Wash. The purpose of the wash is to eliminate any loosely bound species. The Ti alcoholate is almost eliminated. The content of both of the esters on the support is reduced 50%.

The decrease in the DOP content is evident by the stronger dominance of the BP peaks in the alkyl region (figure 5.12). Essentially no shifts in the peak positions occur. Both the  $T_{1p}^H$  and  $T_1^H$  (table 5.11) values

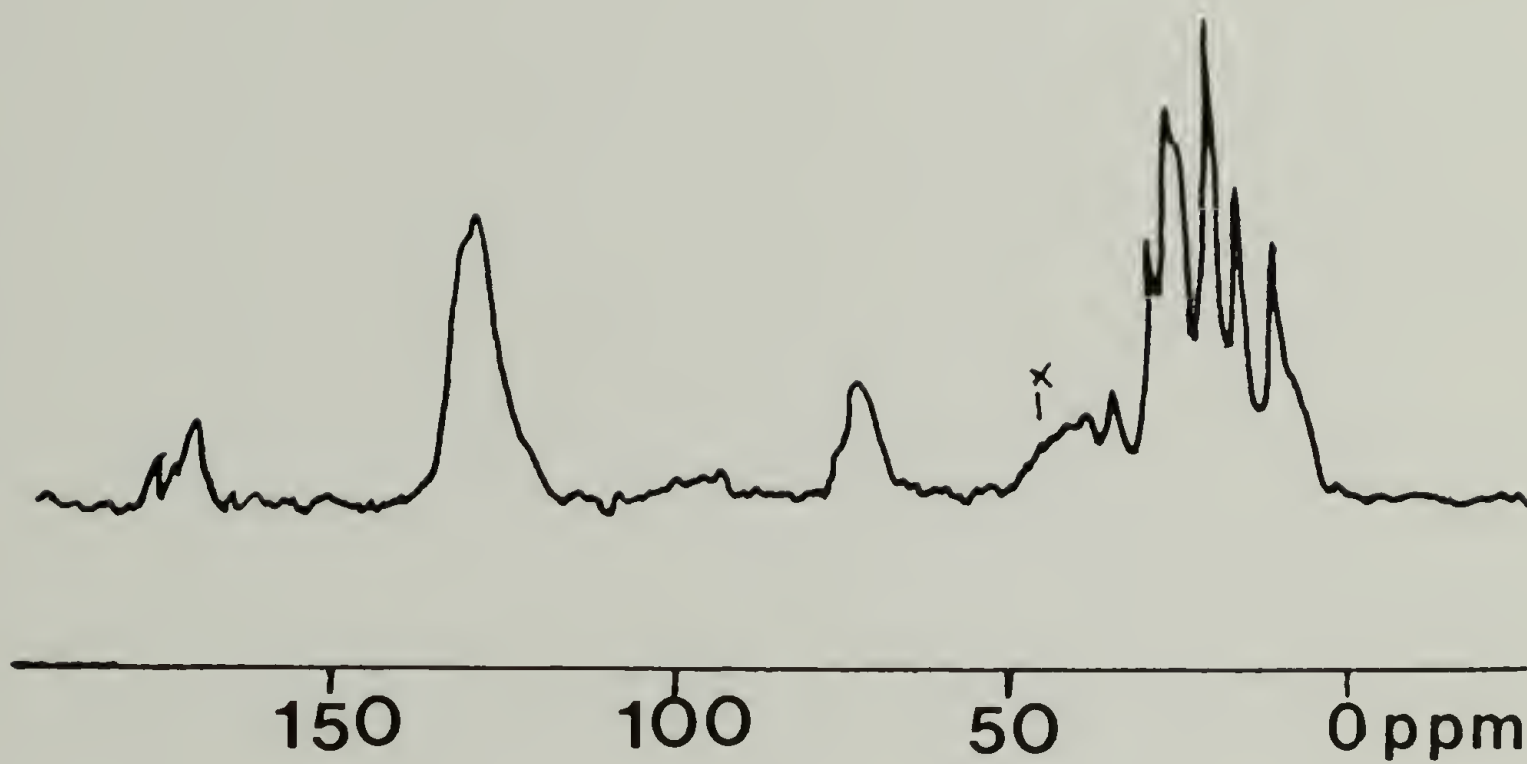


Figure 5.11 MAS-CP  $^{13}\text{C}$  NMR Spectrum of  $\text{MgCl}_2\cdot\text{EH}/\text{PA}/\text{TiCl}_4/\text{BP}$ . Sidebands Marked with X.

Table 5.10  $^{13}\text{C}$  NMR Parameters for  $\text{MgCl}_2 \cdot \text{EH}/\text{PA}/\text{TiCl}_4/\text{BP}$

	C=O	C <sub>Ar</sub>	-OCH <sub>2</sub> -
Chemical Shift Obsvd. (ppm)	171.7	130.7	74.4
T <sub>CH</sub> (μs)	534	15.7	10.7
T <sub>1ρ<sup>H</sup></sub> (ms)	13.1	10.7	13.5
T <sub>1<sup>H</sup></sub> (s)	0.39	0.45	0.46

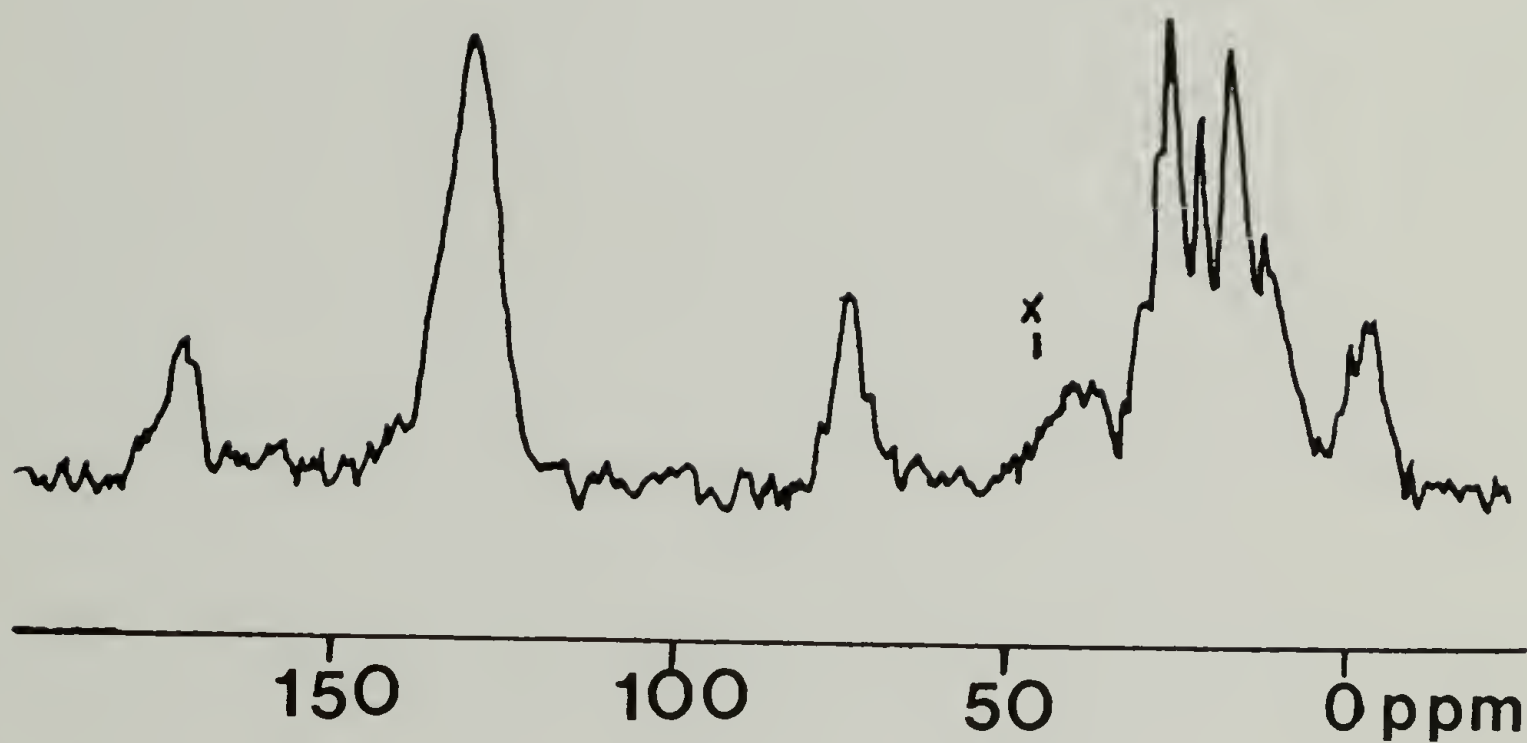


Figure 5.12 MAS-CP  $^{13}\text{C}$  NMR Spectrum of  $\text{MgCl}_2\cdot\text{EH/PA/}$   
 $\text{TiCl}_4\text{/BP} + \text{TiCl}_4$  Wash. Sidebands Marked with  
X.

Table 5.11  $^{13}\text{C}$  NMR Parameters for  $\text{MgCl}_2 \cdot \text{EH/PA/TiCl}_4/\text{BP} + \text{TiCl}_4$  Wash

	C=O	C <sub>Ar</sub>	-OCH <sub>2</sub> -
Chemical Shift Obsvd. (ppm)	171.3	129.7	74.0
T <sub>CH</sub> (μs)	523	21.4	14.0
T <sub>1ρ</sub> <sup>H</sup> (ms)	12.7	10.1	9.2
T <sub>1</sub> <sup>H</sup> (s)	0.19	0.23	0.20



are about 50% of those found in the previous two stages of the reactions. A closer interaction of the ester with the support may be occurring.

### Discussion

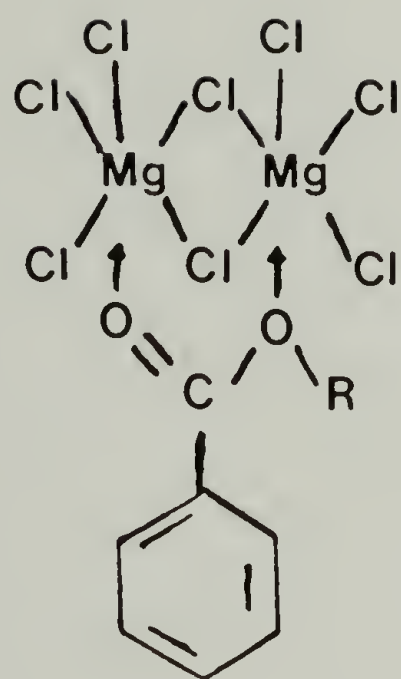
Ball-milling of 0.15 mol of EB with 1 mol of anhydrous  $\text{MgCl}_2$  affixed the EB strongly on the surface of  $\text{MgCl}_2$  with disordered crystal structure. In fact, this adsorbed EB remained throughout the subsequent steps of catalyst preparation. FTIR showed that the C=O and C-O stretching vibrations of  $\text{MgCl}_2/\text{EB}$  have values of  $1683\text{ cm}^{-1}$  and  $1329, 1306\text{ cm}^{-1}$ , respectively.<sup>1</sup> The corresponding frequencies for neat EB are  $1719\text{ cm}^{-1}$  and  $1109, 1279\text{ cm}^{-1}$ . Therefore, the C=O vibration has decreased in frequency and C-O vibrations have increased in frequency upon complexation with  $\text{MgCl}_2$ .

The indirect referencing of chemical shift in the solid state by MAS-CP NMR has a typical error of  $\pm 0.5\text{ ppm}$ . The chemical shifts for the neat EB are compared to those of  $\text{MgCl}_2/\text{EB}$  in table 5.1. The methyl carbon resonances have the same chemical shift value in both physical states, thus, serving as the internal reference. One can be confident that both the  $\text{OCH}_2$  and C=O carbons are approximately 5 ppm downfield shifted as a result of complexation with  $\text{MgCl}_2$ . Such downfield shifts correspond to

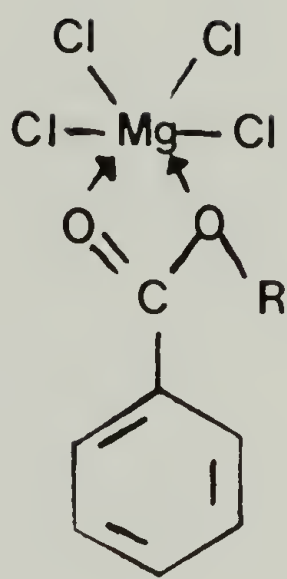
deshielding or loss of electron density at these nuclei and suggest coordination of EB molecules to  $\text{Mg}^{+2}$  ions. In the (100) and (110) faces of  $\text{MgCl}_2$  there are exposed 5- and 4- coordinate  $\text{Mg}^{+2}$  ions,<sup>11</sup> respectively, EB could complex with both of them. The deshielding effect should be smaller for EB complexed on the (100) face than that adsorbed on the (110) face. Since the ball-milled  $\text{MgCl}_2$  has a highly disordered crystal structure,<sup>12</sup> there are probably additional  $\text{Mg}^{+2}$  ions having electronegativities different from above. The differently coordinated EB should have different chemical shifts and consequently broad MAS-CP NMR linewidths.

If both the carbonyl and ester oxygens are coordinated to  $\text{Mg}^{+2}$  ions having electronegativities different from above. The differently coordinated EB should have different chemical shifts and consequently broad MAS-CP NMR linewidths.

If both the carbonyl and ester oxygens are coordinated to  $\text{Mg}^{+2}$  ions, as indicated by both the FTIR and MAS-CP NMR, then the EB molecules are bound to the  $\text{MgCl}_2$  surface very rigidly. This is in agreement with the short  $T_{\text{CH}}$  times and the high cross polarization efficiencies. The structure of EB complexed to the (100) face may be suggested as in I, whereas the structure of EB on the (110) face may be as in II (figure 5.13).



I



II

Figure 5.13 Possible Structures of Monoester/Metal Complex.

Typical proton spin lattice relaxation times,  $T_1^H$ , in rigid organic compounds are on the order of seconds, but the presence of rapid motion such as rotating methyl groups can shorten  $T_1^H$ . The value in p-di-t-butyl benzene is 0.5 s; in this case the molecule has six methyl groups which are effective in promoting spin-lattice relaxation. One might expect EB to have comparable or longer  $T_1^H$ . Instead, the EB in  $MgCl_2/EB$  has  $T_1^H$  on the order of 35 ms. This probably reflects the contribution of electric quadrupole relaxation of the  $^{35}Cl$  and  $^{37}Cl$  nuclei which have large quadrupole moments. Furthermore, these magnetic nuclei on the surface of  $MgCl_2$  would be in a highly anisotropic electric field and thus would have very short relaxation times.

The  $T_1^H$  values are about equal for all the protons at different EB carbons. This indicates rapid intramolecular proton spin diffusion. In EB complexed to  $MgCl_2$  the Cl ions would be in close proximity to the  $CH_2$  protons as depicted in structures I and II. The rapidly relaxing  $Cl^-$  ions would cause fast relaxation of these  $CH_2$  protons through modulation of either dipolar interaction. Then by spin diffusion the rapid relaxation of the  $CH_2$  protons would be transmitted to the other protons of the EB molecule. This explanation would also account for the very short  $T_2$  of the protons.



The reaction of  $\text{MgCl}_2/\text{EB}$ , containing 1 mol of  $\text{MgCl}_2$ , with PC at  $50^\circ\text{C}$  resulted in the adsorption of all 0.5 mol of PC without appreciable loss of EB in the process. FTIR results suggest the complexation of PC with mainly the (001) face of  $\text{MgCl}_2$  through the hydrogen bonding between the hydroxyl group of PC with a  $\text{Cl}^-$ .<sup>1</sup> This is consistent with the small upfield shift of the oxyaromatic  $\text{C}_1$  resonance of PC in the second step of the support synthesis as compared to PC from the liquid NMR. This is indicative of increased electron density. The shifts of the other aromatic carbons are smaller and within experimental error.

The  $^{13}\text{C}$  NMR linewidths of PC are narrower than those for EB indicating less dispersity in chemical shifts for the adsorbed PC than the latter. In fact, splitting of the methyl resonance of PC into two peaks of unequal intensities  $\pm 2$  ppm from the methyl position in solution suggests two discrete types of adsorbed PC. There is also the possibility of ring current shifts between adjacent PC differently affecting the axial methyl carbon chemical shift.

The complexation of PC to  $\text{MgCl}_2/\text{EB}$  caused an upfield shift of the carbonyl carbon resonance of EB to the value for the neat compound. On the other hand, neither the chemical shift of  $\text{OCH}_2$  nor for the other carbon nuclei of EB differ in the support before and after complexation of the EB. If PC is adsorbed solely in the (001) face, then



any effect on EB would require transmission through the bulk of  $\text{MgCl}_2$ . In that event, it seems unlikely that there should be a shift of only the carbonyl carbon resonance but not the ester carbon resonance. The results may be interpreted as adsorption of the PC weakening the carbonyl- $\text{MgCl}_2$  coordination. Possibly, in that case coordination of the EB is through the other oxygen of the ester. The resulting freedom for molecular rotation of EB in that material could contribute to the poor cross polarization efficiency and thus lower NMR intensity as discussed previously. According to this interpretation, the two methyl carbon resonances would correspond to PC molecules adsorbed on two faces of  $\text{MgCl}_2$ . The particular sites that PC is most likely displace EB are those that are weakly basic. PC would not be expected to compete with EB for the strongly Lewis acidic sites.

The above interpretation is consistent with the broadly held view regarding the functions of EB. By active site counting it has been found that the Lewis base greatly reduces the number of the nonstereospecific sites.<sup>12</sup> The complexed EB would prevent the attachment of  $\text{TiCl}_4$  onto these  $\text{MgCl}_2$  sites. Furthermore, it has been shown that the nonstereospecific sites which have been formed have rate constants of propagation which are one-tenth to one-sixteenth of those of the stereospecific sites. this may be explained by the assumption that  $\text{TiCl}_4$

attached to strongly acidic Lewis  $\text{MgCl}_2$  become themselves strongly Lewis acidic. EB or an additional Lewis base introduced with TEA (in the case of the CW catalyst, it is methyl-p-toluate) will complex with these Ti ions. Propagation is prevented by virtue of lacking in vacant coordination position. If there is dissociation-association equilibrium of Ti-EB species (see previous chapter), then propagation is possible during the dissociated phase for  $\pi$ -complexation of a monomer molecule and subsequent migratory insertion.

It is noteworthy that the spin-lattice relaxation times of PC in  $\text{MgCl}_2/\text{EB}/\text{PC}$  are much longer than those of EB in the PC free support. The  $T_1^{\text{H}}$  and  $T_{1\rho}^{\text{H}}$  values are about six fold and two fold greater, respectively, for PC than EB (compare tables 5.1 and 5.2). The short  $T_1$ 's for adsorbed EB had been attributed to quadrupolar relaxation of the  $\text{Cl}^-$  ions in an asymmetric electric field. Therefore, the longer  $T_1$ 's for the adsorbed PC suggests that this contribution is not as important for PC. Two explanations may be suggested. The carbons of the complexed PC may be situated away from the  $\text{Cl}^-$  ions of the surface. Secondly, the  $\text{Cl}^-$  ions on the face which complexes the PC may be of relatively low electric field gradient.

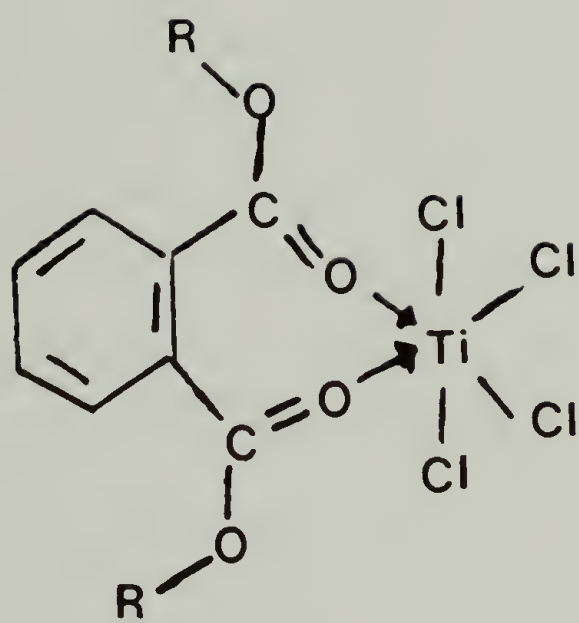
Relaxation times of PC shorten upon reaction with TEA. Either the quadrupolar interaction of the Al is contributing or the carbons of the reaction product are in

a more favorable position to interact with the surface of the support. The  $T_1^H$  values of EB are longer in the support containing the TEA than for  $MgCl_2/EB$  suggesting that the EB is in a different coordination state.

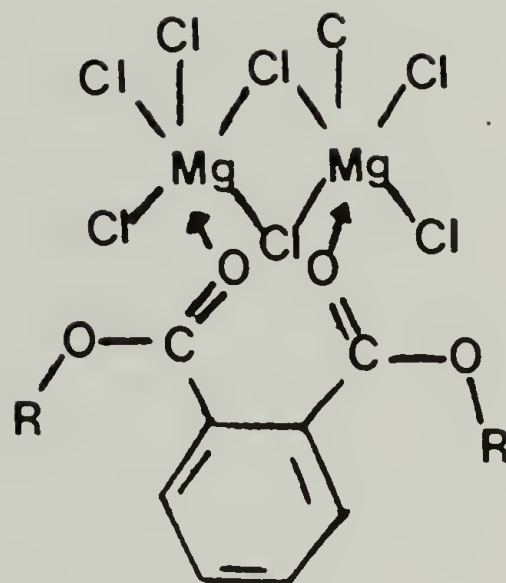
The results for the CH system correspond to those previously obtained with the CW catalyst system. That is, the  $T_{CH}$  values are short indicating rigidity of the ester complex and  $T_1^H$  values are extremely short for an organic molecule in the solid state suggesting nuclear relaxation of the protons with the lattice Cl ions. But there are distinct differences in the line shapes and widths between the monoester and diester complexes on  $MgCl_2$  supports.

In the  $MgCl_2 \cdot EB$  complex a broad single line of about 300 MHz width was observed for the carbonyl carbon. But in the  $MgCl_2 \cdot BP$  spectra there is noticeable splitting of that peak. At least three overlapping peaks are evident suggesting the existence of different discrete chemical environments for the carbonyl.

In the previous study of the  $MgCl_2 \cdot EB$  system, two states of binding of the EB to the  $MgCl_2$  surface were proposed, I and II. Similar types of complexation with  $TiCl_4$  have been postulated. In addition to the complexation modes depicted, it is possible with a dicarboxylic ester to have a free carbonyl, complexing of two carbonyls to a single metal center (III), and bridging complexes between two metal centers (IV) (figure 5.14).



III



IV

Figure 5.14 Possible Structures of Diester/Metal Complex.



Because of bond distances, the modes most observable in NMR would probably be that of (II), free carbonyl, and complexation of two carbonyls on a single metal center.

In a study of dicarboxylic ester·TiCl<sub>4</sub> complexes by Rivet et al,<sup>13</sup> elemental and IR analyses revealed that two types of complexation occurs, carbonyl-ester oxygen coordination with the metal center as in (II) and coordination by two carbonyls with the metal center (III). The factor which seems to determine what the complexation will be is the strain energy of the metallocycle formed. Seven member rings have less strain energy than the four member ring. Even the bridging of two metal centers (IV) should be more stable than (II) as shown by the results of Rivet.

This last fact may be the reason that the monoesters are not effective in this system. EB may only coordinate with one metal center, therefore, if it decoordinates, it is removed from the support. But for the dicarboxylic ester to be removed, both ester groups must be decoordinated from the support.

It is seen in the NMR results that the carbonyl is shifted upfield when the support is treated with BP. It is known that 75% of DOP is replaced by BP in the synthesis. The bulkiness of the 2-ethylhexyl radical of DOP may prevent the coordination of the type of (I), so the coordination of type (III) and (IV) may be prevalent. But



the smaller isobutyl radical of BP may permit such complex formation.

In a previous paper, our laboratories performed EPR on the CH system.<sup>14</sup> A signal was observed which was assigned to an organic radical. This was explained as being due to the electron of the  $Ti^{3+}$  radical moving around the aryl ring in a complex of type (III) in resonance. In the  $TiCl_4 \cdot BP$  complex where the structure of (III) would be dominant, the ring current of the complex may be responsible for the 173.4 ppm shift for the carbonyl observed ( the shift for the carbonyl in  $MgCl_2 \cdot EB$  is 171.0 ppm). The close interaction of the aryl ring with  $MgCl_2$  may also explain the 175.0 ppm shift that is observed.

So the upfield shift of the carbonyl may be due to the replacement of DOP in type (III) and (IV) structures with BP in a type (I) structure. The absence of a corresponding shift of the methoxy carbon throughout the preparation shows that the ester oxygen tends to have a close interaction with the metal centers. The ester oxygen may form a stronger complex with the metal than the carbonyl. A similar phenomenon is seen with EB in the CW preparation.

## Conclusions

It is seen from the results that the Lewis basic organic components are rigidly bound to the surface of  $\text{MgCl}_2$  in both the CH and CW catalyst systems. The state of coordination changes throughout the catalyst synthesis, but the ester remains rigid. Unusually short  $T_1^H$ 's are measured in these systems and may be a result of quadrupolar interactions with the  $\text{Cl}^-$  of the support. The CH system clearly shows that several types of coordination occurs on the surface of the support. This may be a result of the different coordinations of the diester to sites of differing Lewis acidity. There is no direct evidence that the base is coordinated to  $\text{TiCl}_4$  in the procatalyst. The NMR spectrum of  $\text{TiCl}_4 \cdot \text{BP}$  complex ball-milled with  $\text{MgCl}_2$ , however, contains carbonyl peaks corresponding to both  $\text{TiCl}_4 \cdot \text{BP}$  and  $\text{MgCl}_2 \cdot \text{BP}$  complexes.

MAS-CP NMR is a useful tool in the analysis of the organic components in supported Ziegler-Natta systems. States of complexation and mobility of the components may be deduced from chemical shifts and relaxation measurements. Coupled with other analytical techniques a more complete understanding of the roles of the catalyst components may be achieved.

### References

1. J.C.W. Chien, J.C. Wu, and C.I. Kuo, *J. Polym. Sci., Polym. Chem. Ed.*, **21**, 725 (1983).
2. R. Spitz, J.L. Lacombe, and A. Guyot, *J. Polym. Sci., Polym. Chem. Ed.*, **22**, 2641 (1984).
3. P.C. Barbé, G. Cecchin, and L. Noristi, *Adv. in Polym. Sci.*, **81**, 16 (1987).
4. A. Guyot, R. Spitz, L. Duranel, and J.L. Lacombe in *"Catalytic Polymerization of Olefins"*, T. Keii and K. Soga, Eds., Kodansha, Tokyo, 147 (1986).
5. B. Keszler and A. Simon, *Polymer*, **23**, 916 (1982).
6. M. Terano, T. Katakao, and T. Keii, *J. Polym. Sci., Polym. Chem. Ed.*, **28**, 2035 (1990).
7. T. Yano, T. Inoue, S. Ikai, M. Shimasu, Y. Kai, and M. Tamura, *J. Polym. Sci., Polym. Chem. Ed.*, **26**, 477 (1988).
8. N. Kashiwa, J. Yoshitake, and A. Toyota, *Polymer Bulletin*, **19**, 333 (1988).
9. K. Soga, J.R. Park, and T. Shiona, *Makromol. Chem., Rapid Comm.*, **11**, 117 (1990).
10. L. Abis, E. Albizatti, U. Giannini, G. Guinchi, E. Santoro, and L. Noristi, *Makromol. Chem.*, **189**, 1595 (1988).
11. J.C.W. Chien, S. Weber, and Y. Hu, *J. Polym. Sci., Polym. Chem. Ed.*, **27**, 1499 (1989).
12. J.C.W. Chien and Y. Hu, *J. Polym. Sci., Polym. Chem. Ed.*, **25**, 2847 (1987).
13. E. Rivet, R. Aublin, and R. Rivest, *Can. J. Chem.*, **39**, 2343 (1961).
14. J.C.W. Chien and Y. Hu, *J. Polym. Sci., Polym. Chem. Ed.*, **27**, 897 (1989).



## CHAPTER VI

# STEREOSPECIFICITY AND STEREOELECTIVITY OF HOMOGENEOUS OLEFIN POLYMERIZATION CATALYSTS

### Introduction

Interest in the polymerization of propylene with homogeneous catalysts was expanded by the invention of the chiral metallocene catalysts, ethylenebis( $\eta^5$ -indenyl)-zirconiumdichloride (ETIZC) and ethylenebis( $\eta^5$ -tetrahydroindenyl)zirconiumdichloride (ETHIZC), by Brintzinger and co-workers.<sup>1</sup> Since that time, there has been much activity in the development of new catalysts for the stereospecific polymerization of pro-chiral monomers.<sup>2,3,4</sup> Attempts have been made to elucidate the mechanism of stereospecific polymerization in these systems.<sup>5,6</sup>

The homogeneous catalyst has been in existence for thirty years. The first catalysts studied exhibited low activity in the polymerization of ethylene and no activity with propylene when activated with aluminumalkyl.<sup>7</sup> It was suspected that the active species was cationic in nature. A major advancement came with the discovery by Kaminsky that alkylaluminumoxane (specifically methylaluminumoxane (MAO)) produced systems which had activities of  $10^6$  g

polymer/mol metal·atm·hr.<sup>8</sup> And for the first time, polymerization of propylene with these systems was possible.

The role of the MAO was believed to be of both alkylation and complexation. The increased activity is thought to result from this complexation for the mode of deactivation in the absence of MAO is bimolecular with respect to catalyst.<sup>9</sup> MAO may prevent this deactivation route.

But the discovery of the MAO free cationic alkyl-zirconocene which polymerized ethylene by Jordon<sup>10</sup> and subsequent advances by Hlatkey et al<sup>11</sup> has changed the view of the role and the necessity of MAO. It is now believed that MAO forms a stable counterion, thus, providing the high activity. Indeed, Zambelli has shown that dimethylaluminumfluoride (DMAF) activates metallocenes which have the same stereochemical control as in the presence of MAO.<sup>12</sup>

Seemingly, the role of MAO is small as far as steric influence on the metal center. Corradini has demonstrated that the stereospecific nature of the ETHIZC/MAO could be explained by near neighbor interactions involving only the bridged ligand and the polymer chain.<sup>5</sup> Also, the work of Pino et al in the hydro-oligomerization of propylene with an enantiomerically pure ETHIZC showed that the ligands could direct the preferential insertion of one enantioface



of the monomer in agreement with the calculations of Corradini.<sup>13</sup>

The study presented here explores the influence of solvent polarity on the ETIZC/MAO system in the polymerization of propylene. If the active species is indeed a cation, changes in the polarity of the medium should have a noticeable influence on the polymerization. Also, the polymerization of racemic 4-methyl-1-hexene (4MH) is studied with the (S)-ethylenebis(tetrahydroindenyl)zirconiumbis(O-acetyl-(R)-madalate) ((S)-ETHIZ)/MAO system to determine the stereoelective efficiency.

### Experimental

All materials were handled under dry argon by Schlenk techniques. Toluene and chlorobenzene solvents were distilled from Na prior to use. Monomers were purified as described in chapter II.

#### Catalyst

ETIZC was prepared by previously published procedures in our laboratories.<sup>14</sup> (S)-ETHIZ was prepared by published procedures and provided by W. Kaminsky, University of Hamburg, FRG.<sup>15</sup>

## MAO

MAO was prepared from the reaction of  $\text{Al}_2(\text{SO}_4)_3 \cdot 15\text{H}_2\text{O}$  with TMA.<sup>9</sup> Al content of the product was 42%. A 30 mM stock solution was made with toluene.

## Polymerization of Propylene

Polymerizations were run in three different solvents, toluene, 1:1 toluene/chlorobenzene v/v, and chlorobenzene. In a typical polymerization 50 ml of the solvent was introduced to a 250 ml argon filled crown cap reactor. MAO (7.2 mmol in Al) was introduced via syringe. The vessel was heated to 50°C and the Argon was removed and replaced by 2.5 atm propylene. 2.4  $\mu\text{mol}$  of the ETIZC was introduced to initiate the polymerization ( $[\text{MAO}]/[\text{Zr}] = 3000$ ). The polymerizations proceeded for 1 hr and were terminated by the introduction of 2% HCl/MeOH. The polymer was filtered and washed with MeOH and vacuum dried.

## Polymerization of 4MH

50 ml of toluene was introduced into the glass reactor. 5 ml of 4MH was syringed in followed by MAO (7.2 mmol in Al). 2.4  $\mu\text{mol}$  of the (S)-ETHIZ was then introduced to initiate the reaction ( $[\text{MAO}]/[\text{Zr}] = 3000$ ). Polymerizations were run at 25° and 50° C for 23 and 5 hrs. respectively. Polymerizations were quenched with HCl/MeOH and filtered. The polymer was then washed with MeOH. The

monomer was recovered by isolation of the dibromide derivative followed by regeneration with Zn.

### Polymer Characterization

The polymers were fractionated with various boiling solvents using a soxhlet extractor. Thermal data was obtained on a Perkin Elmer DSC 4. Intrinsic viscosities were obtained for polypropylene in decalin at 135° C and for Poly(4MH) in cyclohexane at 30° C. The following relationships were used to obtain Mw:

$$\text{polypropylene,} \quad [\eta] = 1 \times 10^{-4} M_w^{0.8} \quad 16a$$

$$\text{poly(4MH),} \quad [\eta] = 5.75 \times 10^{-5} M_w^{0.78} \quad 16b$$

Optical rotations for both the recovered monomer were measured on an Adolph Research Autopol III on the neat solutions at 25° C using the sodium D wavelength with an accuracy of  $\pm 0.002^\circ$ . The optical purity of the recovered and polymerized monomer and IR spectroscopic stereoregularity ( $I_s$ ) was determined as described in chapter II.

## Results

### Effect of Polarity of the Solvent

There was essentially no change in the activity in the polymerization of propylene in toluene ( $\epsilon=2.284$ ), toluene/chlorobenzene 1:1 ( $\epsilon=4.205$ ), and chlorobenzene ( $\epsilon=5.708$ ) with ETIZC/MAO. Activities of the polymerizations were  $1.1 \times 10^4$ ,  $8.7 \times 10^3$ , and  $8.7 \times 10^3$  Kg/mol Zr·[M]·hr for toluene, toluene/chlorobenzene, and chlorobenzene solvents respectively. It was important to measure the activity in terms of solubility of propylene as the solubility was twice as high in chlorobenzene as it was in toluene. The difference in activities is within experimental error. Also, the rate profiles are very similar (figure 6.1) in the induction period to reach maximum rate and the decay.

The fractional distribution (table 6.1) was drastically changed becoming more stereoirregular with the increase of the polarity of the medium. But the thermal properties and molecular weights did not vary within the respective fractions (table 6.2). Seemingly, the only difference between the polymers produced in the polymerizations is their fractional make up.



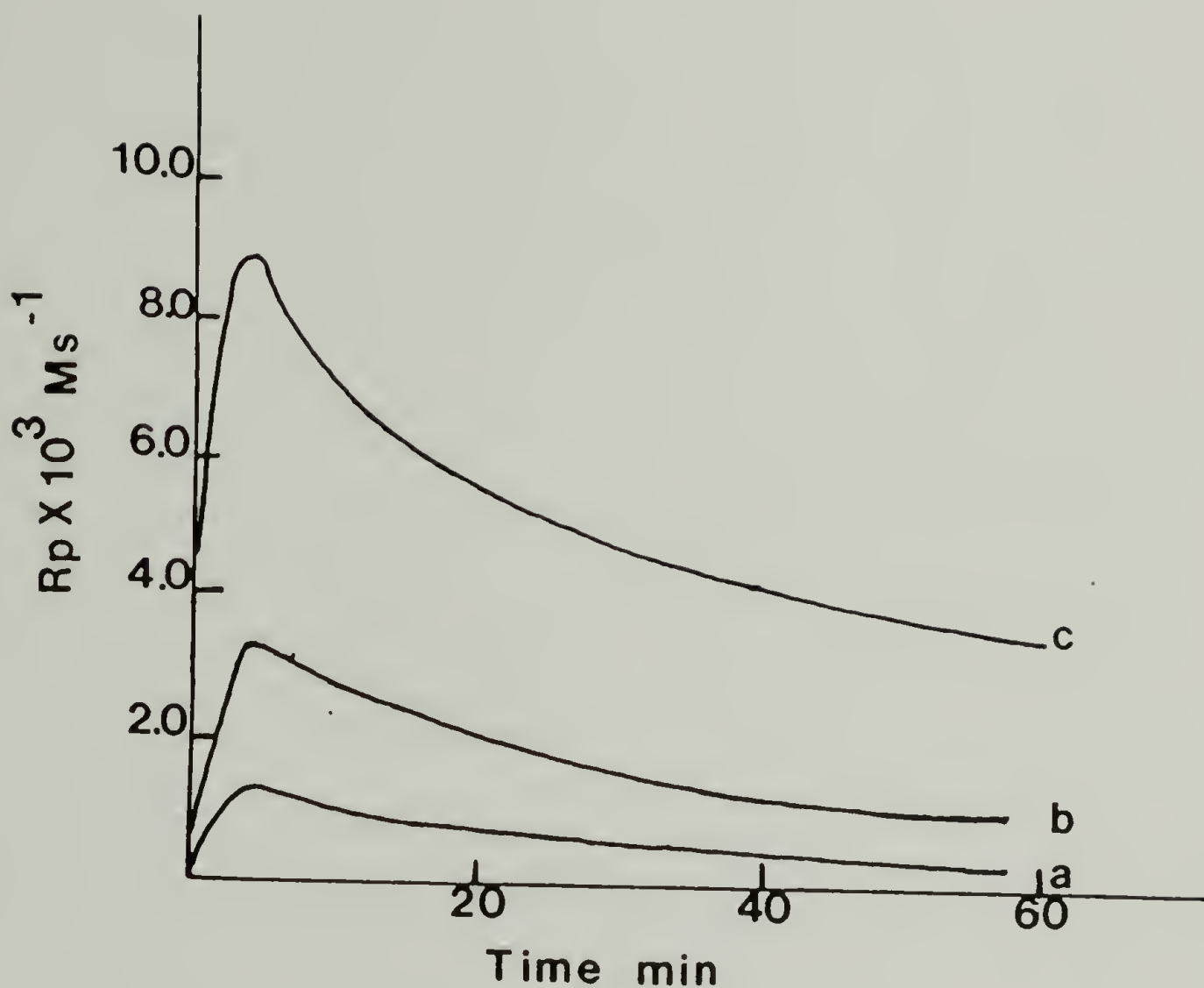


Figure 6.1 Profiles of Propylene Polymerization Catalyzed with ETIZC/MAO in Various Solvents. a) Toluene, b) Toluene/Chlorobenzene 1:1, and c) Chlorobenzene.



**Table 6.1 Fractional Distribution of Polypropylene  
Polymerized with ETIZC/MAO**

Polym. Solvent	Fraction wt%			
	Acetone	Ethylether	Hexane	Heptane
Toluene	5.4	22	39	33
Toluene/Chlorbenzene	10	26	56	8.4
Chlorobenzene	19	46	33	1.8

Conditions:  $[Zr] = 4.8 \times 10^{-5}$ ;  $[MAO]/[Zr] = 3000$ ; Temp. = 50°C

Table 6.2 DSC Melt Endotherms and Molecular Weights for Polypropylene Fractions

Polym. Solvent	Fraction									
	Acetone		Ethylether		Hexane		Heptane			
	T <sub>m</sub> <sup>max</sup> °C	ΔH (cal/g)	MW X10 <sup>-3</sup>	T <sub>m</sub> <sup>max</sup> °C	ΔH X10 <sup>-3</sup>	MW X10 <sup>-3</sup>	T <sub>m</sub> <sup>max</sup> °C	ΔH X10 <sup>-3</sup>	MW X10 <sup>-3</sup>	ΔH X10 <sup>-3</sup>
Toluene	--	--	4.3	104	9.8	4.3	122	15	12	15
Toluene/chorobenz.	--	--	4.3	101	9.6	6.3	117	15	11	16
Chlorobenzene	--	--	1.8	97	11	4.4	117	14	11	15

<sup>1</sup> Perkin Elmer DSC 4 Scan rate 20 °C z in decalin at 135 °C

### Stereoelective Polymerization of 4MH

The polymerizations at the different temperatures produced polymers of very different properties. That produced from the 25° C polymerization was powdery, whereas, that produced at 50° C was a waxy material. Table 6.3 lists the  $P_m$  and the  $P_p$  for the polymerizations. The  $P_p$  is higher for this monomer than as was seen before for the heterogeneous systems. Especially at 25°C, where it is 17%. Unexpected is that the optical rotations for the total polymers is almost the same despite a difference in the  $P_p$ . Also, one can see that in the polymerizations the activity of the 25°C is an order of magnitude lower than the higher temperature polymerization.

Table 6.4 lists the fractionation data. Unlike the heterogeneous catalyst, no ethyl ether insoluble fraction is present. This is most likely due to the low molecular weights (table 6.5). But in the acetone (lowest molecular weight fraction) the opposite antipode is present in a sizable quantity as evidenced by the large optical rotation. Also, unlike what was seen before, the optical rotation continues to increase with the solving power of the solvent and with no drop in rotary power in the highest boiling solvent.

The fractions of the homogeneous polymerized P4MH, except for the acetone fraction which has MW too low to

Table 6.3 Stereoselective Polymerizations of 4MH with (S)-ETHIZ/MAO

Polymerization Temp °C	Conversion %	Monomer		Prev. chir.	Polymer		Prev. chir.	$\frac{Rp(S)}{Rp(R)}$
		[ $\alpha$ ]	Pm		[ $\alpha$ ]	Pp		
25	9.0	+0.052	1.7	R	+17	17	S	1.4
50	27	+0.065	2.0	R	+19	6.0	S	1.1

**Table 6.4 Microstructure of Stereoselectively Polymerized  
4MH Catalyzed by (S)-ETHIZ/MAO**

Polymerization Temp °C	%	Acetone		Fraction Ethylacetate		Ethylether	
		[ $\alpha$ ]	I <sub>D</sub>	%	[ $\alpha$ ]	%	I <sub>D</sub>
25	21	-13	94	42	+10	37	+31 97
50	20	-7.8	74	76	+22	4.0	+31 96



Table 6.5 Molecular Weights of Poly(4MH) from  
Polymerization with (S)-ETHIZ/MAO

Polym. Temp. / °C	fraction	Mw X 10 <sup>3</sup>	
		Acetone	Ethylacetate
25		7.1	19
			26
50		0.84	9.0
			22

" from intrinsic viscosity; in cyclohexane at 30°C

Ethylether

crystallize, have much larger  $\Delta H$  and  $X_c$  (table 6.6) than that produced from the heterogeneous system. Most significant and interesting is that all the fractions of the polymer produced at 25°C have the same  $I_s$  of > 94%. The 50°C polymer varies in  $I_s$  of the fractions in similar manner as the heterogeneous produced polymer.

### Discussion

It was thought that the changing of the solvent polarity would drastically affect the catalyst behavior, if indeed the active species was a cation. It is known that a change in solvent polarity can change the polymer productivity several orders of magnitude in anionic and cationic polymerizations.<sup>17</sup> Of course, in these polymerizations the insertion reaction should not be ionic in nature so the only increase in productivity would be due to the more efficient formation of the cationic active species. But the productivities and the rate profiles show that the formation of the active species occurs at the same rate in each of the polymerizations. The difference in magnitude of the profiles may be attributed to the greater solubility of propylene in chlorobenzene than in toluene.

But there was an effect on the fractional stereochemical distribution. One may think that this could be

Table 6.6 Comparison of P4MH Melt Transitions

Catalyst	Fraction					
	Ethylacetate		Ethylether		Cyclohexane	
	Tmax(°C)	$\Delta H$ (Cal/g)	%X <sup>a</sup>	Tmax	$\Delta H$	%X
CH((S)-2mBP) <sup>†</sup>	121	1.02	7.8	191	2.37	18
				214	7.29	56
(S)-ETHIZ25	136	6.02	46	177	7.49	58
				-	-	-
(S)-ETHIZ50	120	1.58	12	165	5.15	40
				-	-	-

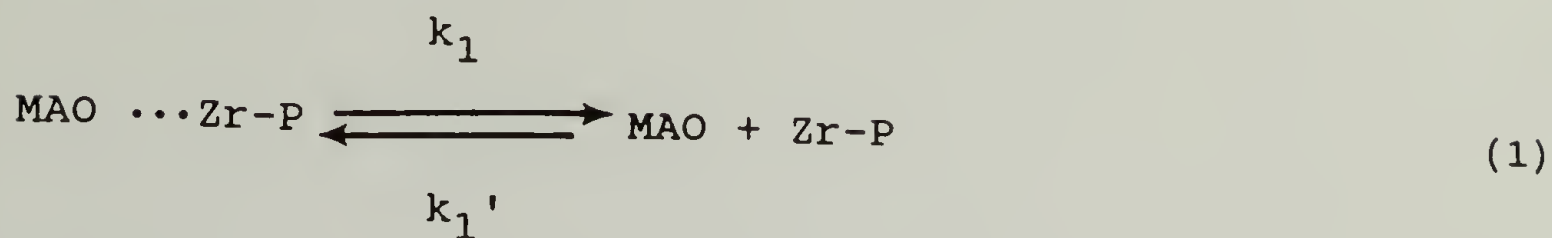
<sup>†</sup>MgCl<sub>2</sub> supported Ti catalyst modified with di((S)-2-methylbutyl)phthalate <sup>a</sup>%X =  $\Delta H / \Delta H^{\circ}$ .  
 Using  $\Delta H^{\circ} = 13$  cal/g ref. O. Bonsignori, P. Pino, G. Manzini, and V. Crescenzi, Die Makromol. Chem., Suppl., 1, 317 (1975).

ascribed to the dissociation of MAO from the active center creating centers that are relatively less sterically crowded. But not only the microstructure is changed but the molecular weight distribution is changed as evidenced by the elimination of a hexane insoluble fraction. The change in the solvent increases both misinsertions and the termination reactions.

Previous studies on both ETIZC/MAO and ETHIZC/MAO of propylene have shown that there is a narrowing of molecular weight distribution and a slight increase in the isotactic sequence length with increase in the MAO concentration.<sup>18,19</sup> Radiolabeling experiments indicated that the active site concentration for ETHIZC at 30° C decreased 80% when [MAO]/[Zr] was decreased from 3500 to 350.<sup>18</sup> So change in the nature of the binding of MAO to the active center could affect the stereoregularity.

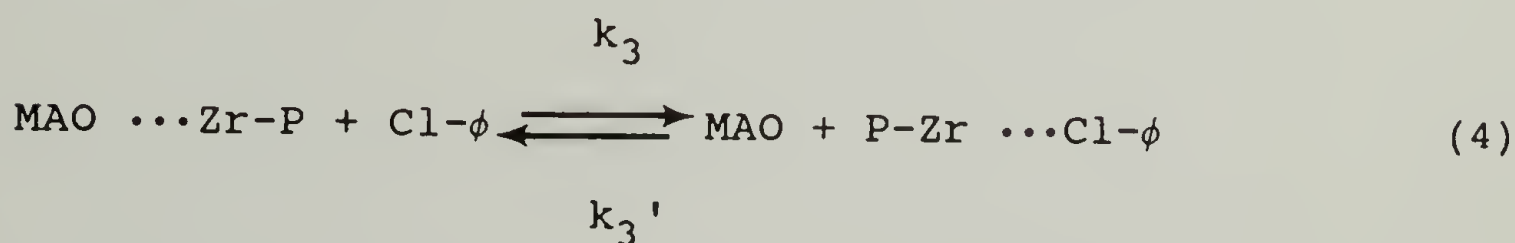
We have proposed that in the polymerization of propylene by these homogeneous systems a single misinsertion occurs which is not immediately corrected.<sup>19</sup> This gives rise to anisotactic polymer (isotactic sequences in the same polymer chain of opposite chirality). A novel catalyst produced in our laboratories takes advantage of such a site switching mechanism to produce elastomeric polypropylene (containing isotactic and atactic sequences in the same chain).<sup>20</sup>

In view of these results, the following equilibria may be envisioned:



If  $K_1$  is large, than the switching depicted in equation 2 would be likely to occur. A lower concentration of MAO would promote such site switching.

A solvent such as chlorobenzene should also modify this behavior:



It is possible that the chlorobenzene is more labile than the MAO so that the switching would be more prevalent.



Not enough data has been collected to provide insight into any of these possible processes.

More insight into the stereochemical situation is provided by the polymerization of a racemic monomer with the optically pure (S)-ETHIZ. This system was used because the isolation of a pure diastereomer is possible. The polymerization of 4MH with (S)-ETHIZ/MAO gives polymers of different stereochemical distribution and molecular weight according to the polymerization temperature used.

Interestingly, at 25° C there is not a difference between the stereoregularity of the fractions as determined by IR. This method measures the helical content of the polymers, specifically sequence lengths of 11-12 in the case of propylene.<sup>21</sup> Of course, if a non-corrected error occurs, a polymer chain may contain a number of helical segments that may not crystallize well. On the other hand, at such low molecular weights ( < 25,000), the molecular weight will become a factor.<sup>22</sup> The decrease in the melt temperature with solubility may be due to either of these factors or both.

The polymer produced at 50° C does have variable isotactic composition similar to that produced from a heterogeneous system.<sup>23</sup> Differences in the solubility will also be due to this tacticity difference.

The higher stereoregularity of these polymers than that of the heterogeneous systems may be the result of a single type of active site in the homogeneous catalyst with a rigid stereochemical environment for the monomer. The surprising result of such a one site system is the production of the polymer of opposite enantiomeric preference prevalent in the acetone soluble fraction.

If the equilibria described before are considered, there could be two states available for the preferential coordination of the Si and the Re enantiomeric faces. In the case of racemic monomers this also means the differentiation between enantiomers. In an ideal system one would expect that high stereoregularity would translate to high stereoelectivity (the preference of one antipode over another). The optical purities are indeed high as compared to that in optically active heterogeneous catalyst products, but it is obvious that enantiomeric misinsertions occur. For example, it is thought to be preferred in this system to have the coordination of the (S)-enantiomer on the Si face, but it must be also possible to have coordination of the (R)-enantiomer on either the Re or Si face.

The existence of an abundance of the less preferred antipode in the low molecular weight fraction suggests that the state of the catalyst that permits the polymerization of this enantiomer is also more facile to termi-

nation reactions. In the homogeneous catalysts the chain termination reactions (transfer to monomer, transfer to aluminum, and  $\beta$ -hydride) elimination are several orders of magnitude higher than in the heterogeneous catalysts.  $\beta$ -hydride elimination the major process involved in the homogeneous polymerizations.<sup>24</sup>

Corradini and co-workers performed calculations on the insertion of propylene with a metallocene catalyst.<sup>25</sup> The focus was on the prefinal product. That is the conformation of the polymer immediately following the insertion step. In the calculation the assumption made was that the polymer was relatively immobile during the insertion process (in agreement with the condition of least motion insertion proposed by Hines<sup>26</sup> and Cossee<sup>27</sup>) with the exception of the rotation around the third and fourth bonds of the polymer (figure 6.2).

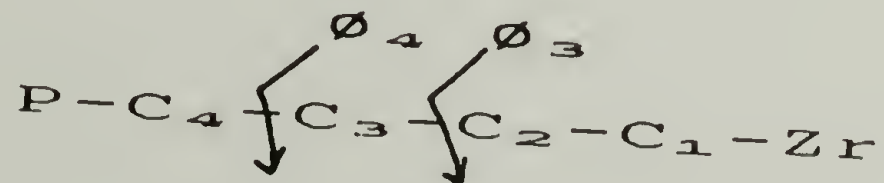


Figure 6.2 Considered Bond Rotations in Insertion Models.

It is useful to look at the problem of the stereoselection of the ETHIZ in a similar way. Because of complexities, propylene is considered with the results applicable to 4MH. Figure 6.3 illustrates the insertion on the Si face of propylene. Insertion involves only small perturbation of the polymer chain. In the insertions on the Re face of the propylene (figure 6.4), the polymer chain would have to be directed away from the insertion direction for continuous Re insertion to be favored. Note that in this conformation the  $\beta$ -hydrogen of the polymer chain is directed toward the metal center making it susceptible to transfer to the metal with subsequent termination of the polymer chain. In the insertion step the first methyl group in the polymer chain is directed toward the metal center making this mode unfavorable. For the continued insertion on a given face, migration of the polymer chain to the initial coordination site with resumption of the previous conformation is required.

The preceding model seems to indicate that the coordination of the monomer to the (S)-ETHIZ is highly dependent upon the conformation of the polymer chain in the vicinity of the active center. In this case, the Si coordination (and in the case of 4MH, the coordination of the (S)-enantiomer) should be preferred. The sequential coordination of the Re face should occur at relatively short periods because of energetic considerations. It may ex-



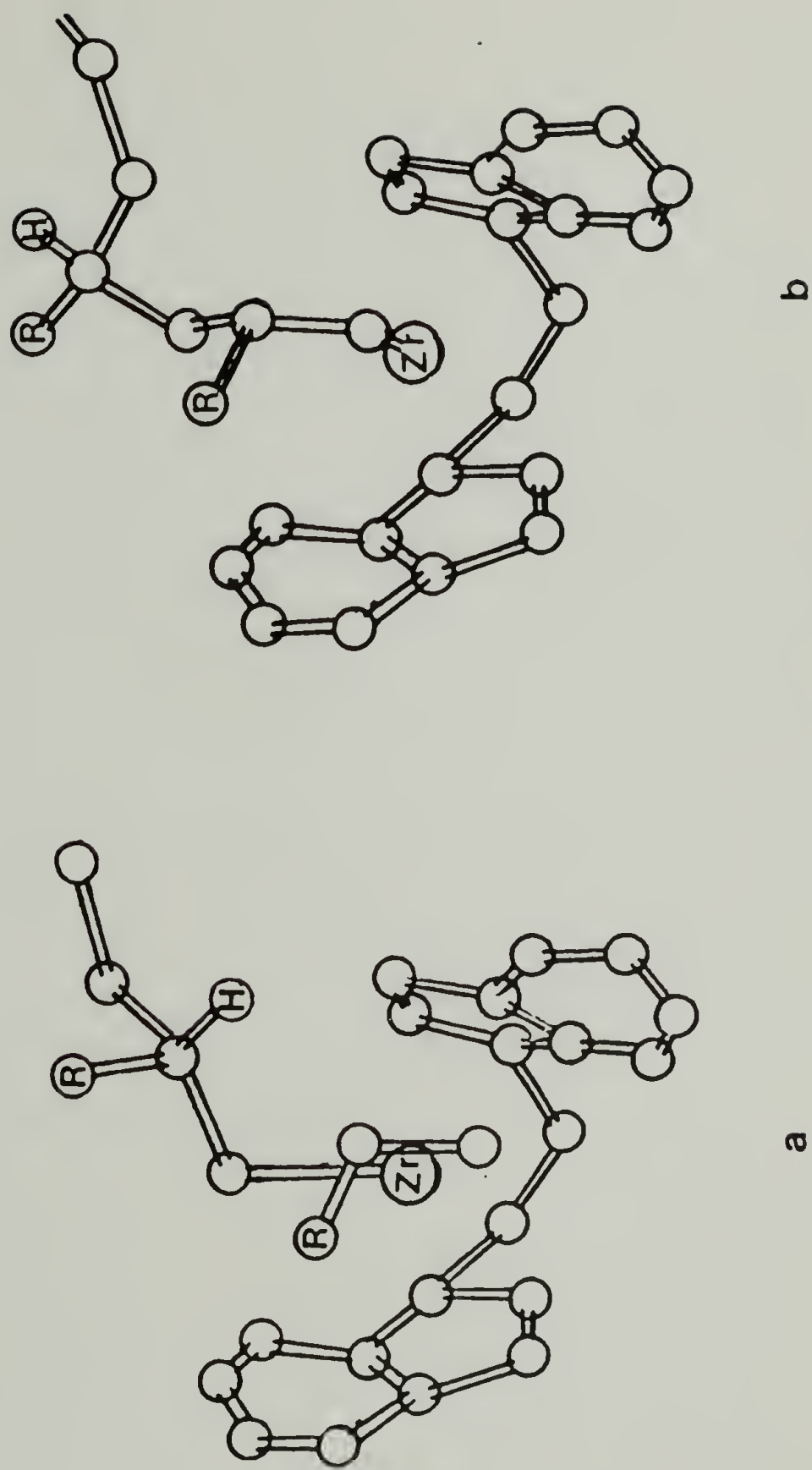


Figure 6.3 Possible Path for Continuous Si Insertion. a) Prior to Insertion and b) After Insertion.



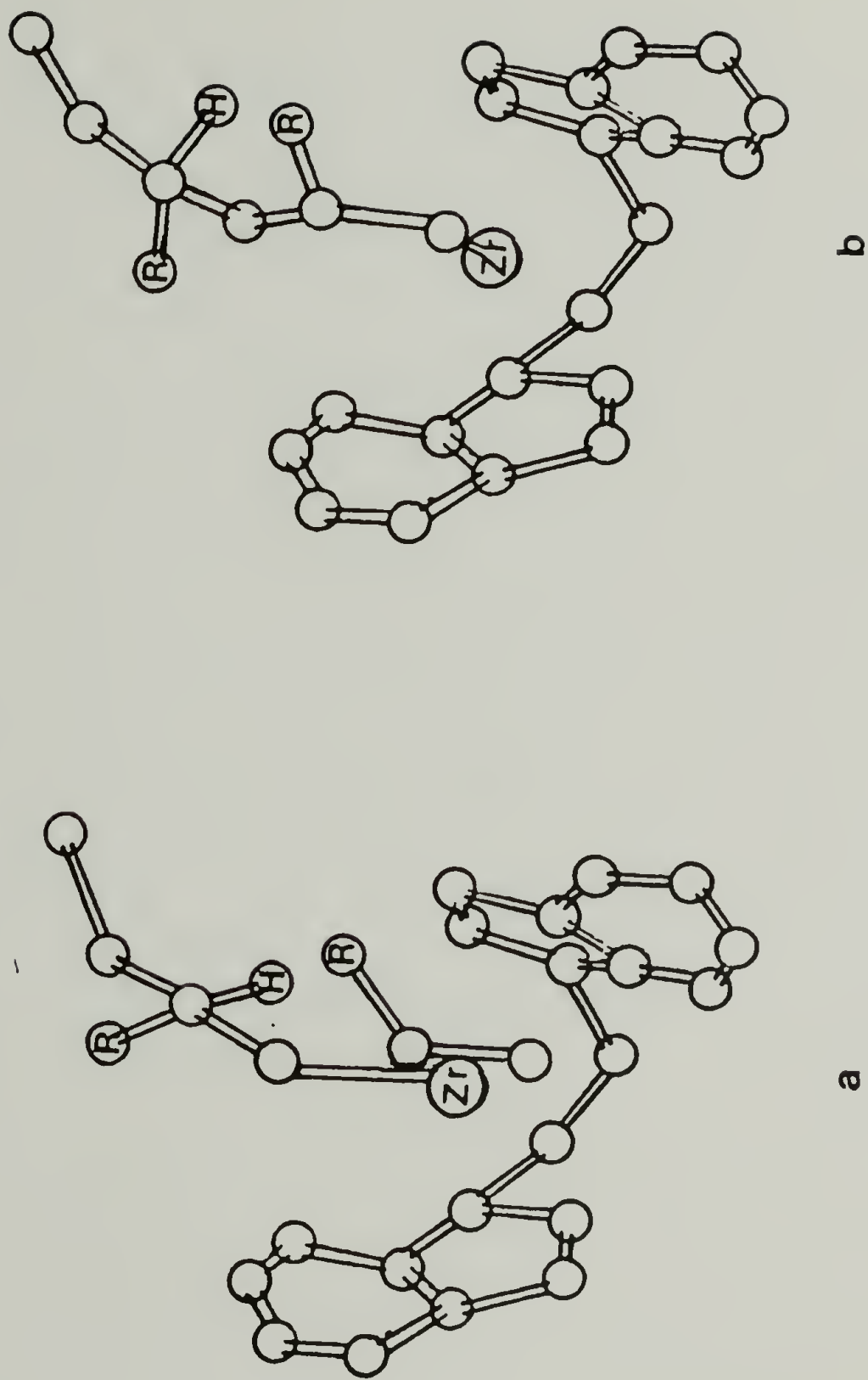


Figure 6.4 Possible Path for Continuous Re Insertion. a) Prior to Insertion and b) After Insertion.

plain the existence of the predominance of the (R)-4MH in the low molecular weight material due to the  $\beta$ -hydride elimination, but the enantiomeric preference in that fraction is not clear from the accepted model.

It is assumed in this model that the metallocene ligands are static in nature. But it has been shown recently that very bulky monomers such as norbornene and 1,4,5,8-dimethano-octahydronaphthalene are homo and copolymerized by ETIZC/MAO. The previously described model would not sterically allow for this.

It is known that  $\eta^5$  - indenyl transition metal complexes have enhanced reactivity toward ligand substitution and related reactions compared to their  $\eta^5$ -C<sub>5</sub>R<sub>5</sub> analogues.<sup>28-30</sup> This is believed to be related to the relative ease of ring slippage from  $\eta^5$  to  $\eta^3$ . Ground state slip fold distortion of  $\pi$ -bound indenyl ligands has been established by dynamic NMR and X-ray crystallography.<sup>31-35</sup> It is possible that changes through ring slippage affecting the hinge angle may create a catalyst environment which would promote coordination of the opposite antipode than that preferred by the initial catalyst.

### Conclusions

It has been shown that the ansa metallocene systems discussed in this chapter are not as stereochemically rig-

id as previously thought. In addition to changing the polymerization temperature and MAO concentration, one may change the stereochemical distribution of the polymer by changing the polymerization solvent. It is not clear whether this is a result of changes in dielectric of the medium or greater coordination ability of the solvent. Stereoelective polymerization of racemic monomer with optically pure catalyst has revealed that the catalyst exists in at least two states as evidenced by the existence of fractions of opposite optical rotation. The static model of these systems presented in past literature can not explain such results. In such models one must consider change in position of the polymer chain and a change in its conformation. Also, fluctuation of the ring ligands is a possibility.

### References

1. F.R.W.P. Wild, L. Zsolnai, G. Huttner, and H.H. Brintzinger, *J. Organomet. Chem.*, **232**, 233 (1982).
2. J.A. Ewen, "Catalytic Polymerization of Olefins", T. Keii and K. Soga, Eds., Elsevier, New York, 271 (1986).
3. J.A. Ewen, R.L. Jones, A. Razavi, and J.D. Ferrara. *J. Am. Chem. Soc.*, **110**, 6256 (1988).
4. N. Ishihara, T. Seimiya, M. Kuramoto, and M. Uoi, *Macromol.*, **19**, 2465 (1986).
5. P. Corradini, G. Guerra, M. Vacatello, and V. Villani, *Gazz. Chim. Ital.*, **118**, 173 (1988).
6. L. Cavallo, G. Guerra, L. Oliva, M. Vacatello, and P. Corradini, *Polym. Comm.*, **30**, 16 (1989).
7. D.S. Breslow and N.R. Newburgh, *J. Am. Chem. Soc.*, **79**, 5072 (1957).
8. H. Sinn and W. Kaminsky, *Adv. Organomet. Chem.*, **18**, 99 (1980).
9. J.C.W. Chien and B.P. Wang, *J. Polym. Sci., Polym. Chem Ed.*, **26**, 3089 (1988).
10. R.F. Jordan, C.S. Bajgur, R. Willet, and B. Scott, *J. Am. Chem. Soc.*, **108**, 7410 (1986).
11. G.G. Hlatky, H.W. Turner, and R.R. Eckman, *J. Am. Chem. Soc.*, **111**, 2728 (1989).
12. A. Zambelli, L. Pasquale, and A. Grassi, *Macromol.*, **22**, 2186 (1989).
13. P. Pino, M. Cioni, J. Wei, and N. Piccolrovazzi, "Transition Metal and Organometallics for Olefin Polymerization", W. Kaminsky and H. Sinn, Eds., Springer Verlag, Berlin, 269, (1988).
14. S. Collins, B.A. Kuntz, N.J. Taylor, and D.A. Ward, *J. Organomet. Chem.*, **342**, 21 (1988).
15. A. Schafer, L. Zsolnai, G. Huttner, and H.H. Brintzinger, *J. Organometal. Chem.*, **328**, 87 (1987).



16. (a) J.B. Kinsinger and R.E. Hughes, *J. Phys. Chem.*, **63**, 2002 (1959); (b) J.B. Kinsinger and L.E. Ballard, *J. Polymer Sci. A3*, 3963 (1965).
17. G. Odian, **"Principles of Polymerization"**, John Wiley and Sons, New York, 365-368 (1981).
18. B. Rieger, X. Mu, D.T. Mallin, M.D. Rausch, and J.C.W. Chien, *Macromol.*, **23**, 3559 (1990).
19. J.C.W. Chien and R. Sugimoto, *J. Polym. Sci., Polymer Chem. Ed.*, **29**, 459 (1991).
20. D.T. Mallin, M.D. Rausch, Y.G. Lin, S.-H. Dong, J.C.W. Chien, *J. Am. Chem. Soc.*, **112**, 2030 (1990).
21. Y.V. Kissin and L.A. Rishina, *Eur. Polym. J.*, **12**, 757 (1976).
22. G. Natta, I. Pasquon, A. Zambelli, and G. Gatti, *Makromol. Chem.*, **70**, 191 (1964).
23. J. Vizzini, F. Ciardelli, and J.C.W. Chien, Submitted to *J. Am. Chem. Soc.*
24. J.C.W. Chien and B.P. Wang, *J. Polym. Sci., Polym. Chem. Ed.*, **28**, 15 (1990).
25. V. Venditto, G. Guerra, P. Corradini, and R. Fusco, *Polymer*, **31**, 530 (1990).
26. J. Hine, *J. Org. Chem.*, **31**, 1236 (1966).
27. P. Cossee, *J. Catalysis*, **3**, 80 (1964).
28. A.J. Hart-Davis and R. Mawby, *J. Chem. Sci. A.*, 2403 (1969).
29. P. Caddy, M. Green, E. O'Brian, L.E. Smart, and P.J. Woodward, *J. Chem. Soc., Dalton Trans.*, 962 (1980).
30. M.E. Rerek and F. Basolo, *J. Am. Chem. Soc.*, **106**, 5908 (1984).
31. R.D. Barr, M. Green, T.B. Marder, F.G.A. Stone, *J. Chem. Soc., Dalton Trans.*, 1261 (1984).
32. F.H. Kohler, *Chem. Ber.*, **107**, 570 (1974).
33. M. Mlekuz, P. Bougeard, B.G. Sayer, M.J. McGlinchy, C.A. Rodger, M.R. Churchill, J.W. Zeller, S.W. Kanz, and T.A. Albright, *Organomet.*, **5**, 1656 (1986).



34. R.T. Baker and T.H. Tulip, *Organomet.*, **5**, 539 (1986).
35. T.B. Marder, J.C. Calabrese, D.C. Roe, and T.H. Tulip, *Organomet.*, **6**, 2012 (1987).

## CHAPTER VII

### CONCLUSIONS AND FUTURE WORK

In the presented work the stereochemistry, as studied by propylene polymerization and stereoelective polymerization of racemic monomer, of the superactive CH heterogeneous catalyst has been contrasted with earlier systems. The organic components of the system drastically affected the catalyst activity and stereospecificity. And the distribution of active sites was different for the different heterogeneous systems.

It was seen from the MAS-CP NMR of the heterogeneous system that the ester internal Lewis bases are rigidly bound to the  $\text{MgCl}_2$  surface. The nature of the binding on the CH catalyst appears to be different from that for the CW catalyst because of the multiplicity of the carbonyl peak in the CH case. This is most likely due to the greater structural disorder present in the CH support (i.e. a greater number of active sites of a particular nature). There also may be a difference in the coordination of the di(2-ethylhexyl)phthalate and the diisobutylphthalate. This may arise from the difference in the steric size of the alkyl groups in the esters as previously discussed. Indeed, it was seen in chapter III

that those esters which had the larger alkyl groups produced catalysts of relatively poorer performance as far as activity and stereoselectivity. Apparently, for a CH type system, a smaller steric size of the ester is desirable.

Through the stereoelective polymerizations of racemic monomer with a modified CH catalyst, it was shown that the distribution of chiral sites was not the same as that for a modified CW system, even though the two systems have quite similar behavior toward propylene. It was postulated that those sites which have similar behavior toward propylene behave differently toward the branched olefins. In other words, sites that polymerize propylene isospecifically do not polymerize branched  $\alpha$ -olefins (as was previously cited, linear  $\alpha$ -olefins have been shown to polymerize with the same number of active sites as propylene). Even though the CH catalyst has more active sites than the CW catalyst, apparently, these can not accommodate the bulkier olefins. It has been demonstrated through active site counting in 4-methylpentene polymerization that few of the propylene active sites are available for this monomer.

By contrasting the properties of CH catalyst modified with racemic and optically active base, it was seen that the racemic catalyst had a lower activity than the optically active catalyst despite possessing the same isospecificity toward propylene. It was concluded that the

complexation of the ester was enantiospecific. Resulting stereoelectivity of the system would then be dependent upon the relative stability of the different diastereomeric complexes. In those Ti sites that are least Lewis acidic, it was postulated that only the base free sites can polymerize monomer. Therefore, the small stereoelectivities can be explained by a small difference in the complexation equilibria as discussed in chapter IV. Stereoirregular but stereoelective polymerizations may be explained by a fluctuation of the relatively more Lewis acidic active sites with the base dissociating and reassociating in a different manner.

This type of study can be further employed in the CH system through the use of optically active silane external base to determine the role of that component. Little is known about this base. It may deactivate sites by complexation or it may convert the aspecific sites to isospecific sites as discussed in chapter I. The external ester in the CW system (see chapter IV) has been shown to be relatively ineffective in stereoelective induction. But the silane has been shown to behave differently as far as smaller activity depression when used. So a study such as this may be rewarding.

It is also assumed that the actual external base is the product of the base and the aluminum alkyl cocatalyst. An interesting study would be to change the steric size of



aluminum alkyl and observe any changes in the rate profile, stereoselectivity, and, in the manner of the work presented, the stereoelectivity.

It may also be of interest to observe the effect of using a more efficient stereochemical poison. It is known that Ziegler-Natta polymerizations are hindered by internal olefins. An optically active internal olefin may be an efficient poison because of more intimate interaction with the active center than an ester. The olefin should be small so as to be able to interact with most of the active centers. The simplest olefin would be 4-methyl-2-hexene. Since optically pure olefin would not be commercially available, this would have to be synthesized.

The studies of the homogeneous ethylenebis(indenyl)-zirconiumdichloride (EHIZC)/MAO and (S)-ethylenebis(tetrahydroindenyl)zirconiumbis(O-acetyl-(R)-mandalate) ((S)-ETHIZ)/MAO systems gave several interesting findings. It was seen that the statistical distribution of the polymer could be changed by the use of solvents of various polarities. Polymer termination reactions and monomer misinsertions increase in frequency with increase in the dielectric constant of the solvent. Therefore, the solvent either plays a direct role in the processes or provides stability to some ionic intermediate.

Additional evidence for noncorrected misinsertion was provided in the polymerization of racemic 4-methylhexene



using the optically pure (S)-ETHIZ diastereomer. The existence of a low molecular weight fraction of opposite enantiomeric excess than the total polymer showed that at least two states existed for the catalyst during the polymerization with opposite enantiomeric preference. And the results suggest that the one state is more prone to elimination reactions.

It is seen that the environment of the homogeneous active site is dynamic. There is certainly a bias toward one type of chirality as evidenced by the stereoselectivity. But the environment is not as rigid as proposed by Corradini (see chapter VI). Production of "anisotactic" polypropylene with low melting point and  $\gamma$ -crystalline modification is additional evidence of this.

To produce a catalyst of better stereochemical control one may take two routes: increase the asymmetry of the environment so to increase the enantiomeric bias toward monomer and the introduction of bulky groups to the bridge to inhibit fluctuation of the ligand during the polymerization. Concerning the first type of modification, one could use a fluorenyl group on one side of the bridge and an indenyl on the other. The two groups must be of a large steric size to give sufficient stereochemical constraints. It has been shown by our laboratories that use of tetramethylcyclopentadienyl and indenyl bridg-

ed ligands produces a two state catalyst which can polymerize elastomeric polypropylene.

Pursuing the other avenue of modification, one may replace the hydrogens of the ethylene bridge with bulky groups such as phenyl or t-butyl and observe any change in the resulting polymer distribution. If any changes would be observed, it may provide evidence supporting the supposition that the misinsertions are due to the slippage of the ligands.

It may not be prudent to change the length of the ligand bridge. A smaller bridge would force the rings further back from the reactive frontal portion of the catalyst, thus reducing the steric size seen by the monomer. A larger bridge may make the ligand too strained when attached to the metal rendering the resulting complex impossible to synthesize or unstable.

Possibly, the best models to look to for homogeneous catalysts are those of enzymes in biological systems. The enzymes are very stereoselective in their interactions with and modifications of biochemical molecules. If one were to mimic such an environment and make the reactive center a transition metal, perhaps the same type of stereoselectivity can be achieved with Ziegler-Natta systems.

Ziegler and Natta were awarded the Nobel prize for breaking "the monopoly of nature" in the production of

stereoregular polymers. Though we have knowledge of systems which are capable of producing stereoregular polymers, we do not have sufficient knowledge to produce single site heterogeneous systems. We are also incapable of creating enantiomerically pure catalytic systems for the polymerization of only one enantiomer from a racemic mixture. And as has just been previously shown, the "one site" homogeneous systems do not have sufficient steric constraints to achieve error free chiral polymerizations. In this age where it is desirable to tailor make polymers for specific uses, much work must be done to obtain this essential information and capability.

## BIBLIOGRAPHY

- Abis, L. E. Albizzati, U. Giannini, E. Santoro, and L. Noristi, **Makromol. Chem.**, **189**, 1595 (1988).
- Arlman, E.J., and P. Cossee, **J. Catal.**, **3**, 80 (1964).
- Baker, R.T., and T.H. Tulip, **Organomet.**, **5**, 539 (1986).
- Barbe, P.C., G. Cecchin, and L. Noristi, **Adv. in Polym. Sci.**, **81**, 3 (1987).
- Barr, R.D., M. Green, T.B. Marder, and F.G.A. Stone, **J. Chem. Soc., Dalton Trans.**, 1261 (1984).
- Bohm, L.L., **Polymer**, **19**, 545 (1978).
- Boor, J., **"Ziegler-Natta Catalysts and Polymerizations"**, New York: Academic Press (1979).
- Breslow, D.S., and N.R. Newburgh, **J. Am. Chem. Soc.**, **79**, 5072 (1957).
- Bukatov, G.D., S.H. Shepelev, V.A. Zakharov, S.A. Sergeev, and Y.I. Yerkamov, **Makromol. Chem.**, **182**, 2657 (1982).
- Burfield, D.R., **Polymer**, **25**, 1645 (1984).
- Busico, V., P. Corradini, L. DeMartino, A. Protom, V. Savino, and E. Albizzati, **Makromol. Chem.**, **186**, 1279 (1985).
- Caddy, P., M. Green, E. O'Brien, L.E. Smart, and P.J. Woodward, **J. Chem. Soc., Dalton Trans.**, 962 (1980).
- Carlini, C., and F. Ciardelli, **Chim. Ind.**, **63**, 486 (1981).
- Carlini, C., R. Noristi, and F. Ciardelli, **J. Polym. Sci., Polym. Chem. Ed.**, **15**, 767 (1977).
- Caunt, A.D., **J. Polym. Sci., Part C.**, **4**, 49 (1963).
- Cavallo, L., G. Guerra, L. Oliva, M. Vaccatello, and P. Corradini, **Polym. Comm.**, **30**, 16 (1989).
- Chien, J.C.W., and T. Ang, **J. Polym. Sci., Polym. Chem. Ed.**, **25**, 1011 (1987).



- Chien, J.C.W., T. Ang, and C.I. Kuo, *J. Polym. Sci., Polym. Chem. Ed.*, **23**, 723 (1985).
- Chien, J.C.W., L.C. Dickinson, and J. Vizzini, *J. Polym. Sci., Polym. Chem. Ed.*, **28**, 2321 (1990).
- Chien, J.C.W., and Y. Hu, *J. Polym. Sci., Polym. Chem. Ed.*, **25**, 2847 (1987).
- Chien, J.C.W., and Y. Hu, *J. Polym. Sci., Polym. Chem. Ed.*, **26**, 2003 (1988).
- Chien, J.C.W., and Y. Hu, *J. Polym. Sci., Polym. Chem. Ed.*, **26**, 2973 (1988).
- Chien, J.C.W., and Y. Hu, *J. Polym. Sci., Polym. Chem. Ed.*, **27**, 897 (1989).
- Chien, J.C.W., and C.I. Kuo, *J. Polym. Sci., Polym. Chem. Ed.*, **23**, 731 (1985).
- Chien, J.C.W., and C.I. Kuo, *J. Polym. Sci., Polym. Chem. Ed.*, **24**, 1779 (1986).
- Chien, J.C.W., and R. Sugimoto, *J. Polym. Sci., Polym. Chem. Ed.*, **29**, 459 (1991).
- Chien, J.C.W., and B.P. Wang, *J. Polym. Sci., Polym. Chem. Ed.*, **26**, 3089 (1988).
- Chien, J.C.W., and B.P. Wang, *J. Polym. Sci., Polym. Chem. Ed.*, **28**, 15 (1990).
- Chien, J.C.W., S. Weber, and Y. Hu, *J. Polym. Sci., Polym. Chem. Ed.*, **27**, 1514 (1989).
- Chien, J.C.W., J.C. Wu, and C.I. Kuo, *J. Polym. Sci., Polym. Chem. Ed.*, **20**, 2019 (1982).
- Chien, J.C.W., J.C. Wu, and C.I. Kuo, *J. Polym. Sci., Polym. Chem. Ed.*, **21**, 725 (1983).
- Ciardelli, F., G. Montagnoli, D. Pini, O. Pieroni, C. Carlini, and E. Benedette, *Makromol. Chem.*, **147**, 53 (1971).
- Collins, S., B.A. Kuntz, N.J. Taylor, and D.A. Ward, *J. Organometal. Chem.*, **342**, 21 (1988).
- Corradini, P., V. Baroni, and G. Guerra, *Macromol.*, **15**, 1242 (1982).



- Corradini, P., G. Guerra, M. Vacatello, and V. Villani, **Gazz. Chim. Ital.**, **118**, 173 (1988).
- Cossee, P., **J. Catal.**, **3**, 80 (1964).
- Ewen, J.A., **J. Am. Chem. Soc.**, **106**, 6355 (1984).
- Ewen, J.A., R.L. Jones, A. Razavi, and J.D. Ferrara, **J. Am. Chem. Soc.**, **110**, 6256 (1988).
- Fellman, J.D., G.A. Rupprecht, and R.R. Schrock, **J. Am. Chem. Soc.**, **101**, 5099 (1979).
- Gerbasi, R., A. Marigo, A. Martorana, R. Zannetti, G. Guidetti, and G. Baruzzi, **Eur. Polym. J.**, **20**, 967 (1984).
- Hart-Davis, A.J., and Mawby, R., **J. Chem. Soc. A.**, 2403 (1969).
- Hine, J., **J. Org. Chem.**, **31**, 1236 (1966).
- Hlatky, G.G., H.W. Turner, and R.R. Eckman, **J. Am. Chem. Soc.**, **111**, 2728 (1989).
- Hu, Y., and J.C.W. Chien, **J. Polym. Sci., Polym. Chem. Ed.**, **26**, 2003 (1988).
- Ishihara, N., T. Seimiya, M. Kuramoto, and M. Uoi, **Macromol.**, **19**, 2465 (1986).
- IUPAC, "Nomenclature of Inorganic Chemistry", **Pure and Appl. Chem.**, **28**, 1 (1971).
- Ivin, K.J., J.J. Rooney, and C.D. Stewert, **J. Chem. Soc. Comm.**, 603 (1978).
- Jordan, R.F., C.S. Bajgur, R. Willet, and B. Scott, **J. Am. Chem. Soc.**, **108**, 7410 (1986).
- Kaminsky, W., K. Kulper, H.H. Brintzinger, and F.R.W.P. Wild, **Ang. Chem.**, **97**, 507 (1985).
- Kaminsky, W., and H. Sinn (eds.), "Transition Metals and Organometallics for Olefin Polymerization", Berlin: Springer-Verlag (1988).
- Kashiwa, N., and Y. Yoshitake, **Polym. Bull.**, **11**, 479 (1984).
- Kashiwa, N., Y. Yoshitake, and A. Toyota, **Polym. Bull.**, **19**, 333 (1988).

- Keii, T., "Kinetics of Ziegler-Natta Polymerization", Tokyo: Kondansha Ltd. (1972).
- Keii, T., and K. Soga (eds.), "Catalytic Polymerization of Olefins", Tokyo: Kodanashi, Ltd. (1986).
- Keii, T., E. Susuki, M. Tamura, M. Murata, and Y. Doi, *Makromol. Chem.*, **183**, 2285 (1982).
- Kezler, B., G. Bodor, and A. Simon, *Polymer*, **21**, 1037 (1984).
- Kezler, B., and A. Simon, *Polymer*, **23**, 916 (1982).
- Kinsinger, J.B., and L.E. Ballard, *J. Polym. Sci.*, **A3**, 3963 (1965).
- Kinsinger, J.B. and R.E. Hughes, *J. Phys. Chem.*, **63**, 2002 (1959).
- Kissin, Y.V., and L.A. Rishina, *Eur. Polym. J.*, **12**, 757 (1976).
- Kohler, F.H., *Chem. Ber.*, **107**, 570 (1974).
- Lezzaroni, R., P. Salvadori, and P. Pino, *Tetrahedron Lett.*, 2507 (1986).
- Mallin, D.T., M.D. Rausch, Y.G. Lin, S.-H. Dong, and J.C.W. Chien, *J. Am. Chem. Soc.*, **112**, 3030 (1990).
- Marder, T.B., J.C. Calabrese, D.C. Roe, and T.H. Tulip, *Organomet.*, **6**, 2012 (1987).
- Mlekuz, M., P. Bougeard, B.G. Sayer, M.J. McGlinchy, C.A. Rodger, M.R. Churchill, J.W. Zeller, S.W. Kanz, and T.A. Albright, *Organomet.*, **5**, 1656 (1986).
- Montedison S.p.A., British Patent 1,286,867 (1971).
- Montedison S.p.A., British Patent 1,387,890 (1975).
- Montedison S.p.A., U.S. Patent 4,107,413 (1978).
- Montedison S.p.A. and Mitsui Petrochemical Ltd., German Offen. 2,643,143 (1977).
- Natta, G., *J. Polym. Sci.*, **34**, 531 (1959).

- Natta, G., P. Pino, P. Corradini, F. Danusso, E. Mantica, G. Mazzanti, and G. Moragio, *J. Am. Chem. Soc.*, **77**, 1708 (1955).
- Natta, G., and I. Pasquon, *Advances in Catalysis*, **11**, 1 (1959).
- Natta, G., I. Pasquon, A. Zambelli, and G. Gatti, *Makromol. Chem.*, **70**, 191 (1964).
- Odian, G., *"Principles of Polymerization"*, New York: John Wiley and Sons (1981).
- Pino, P., *Adv. Polym. Sci.*, **4**, 393 (1965).
- Pino, P., F. Ciardelli, G.P. Lorenzi, and G. Natta, *J. Am. Chem. Soc.*, **84**, 1487 (1962).
- Pino, P., G. Focchi, O. Piccolo, and U. Giannini, *J. Am. Chem. Soc.*, **104**, 7381 (1982).
- Pino, P., and R. Mulhaupt, *Angew. Chem. Int. Ed. Engl.*, **19**, 857 (1980).
- Pino, P., R. Ratzinger, and E. von Achenbach, *Makromol. Chem. Suppl.*, **13**, 105 (1985).
- Quirk, R.P. (ed.), *"Transition Metal Catalyzed Polymerizations"*, New York: Harwood Acad. Press (1983).
- Quirk, R.P. (ed.), *"Transition Metal Catalyzed Polymerizations"*, Cambridge: Cambridge Univ. Press (1988).
- Rerek, M.E., and F. Basolo, *J. Am. Chem. Soc.*, **106**, 5908 (1984).
- Rieger, B., X. Mu, D.T. Mallom, M.D. Rausch, and J.C.W. Chien, *Macromol.*, **23**, 3559 (1990).
- Rivet, E., R. Aublin, and R. Rivest, *Can. J. Chem.*, **39**, 2343 (1961).
- Rodriguez, L.A.M., and H.M. Looney, *J. Polym. Sci.*, (A-1), **4**, 1951 (1966).
- Schafer, A., L. Zsolnai, G. Huttner, and H.H. Brintzinger, *J. Organometal. Chem.*, **328**, 87 (1987).
- Seppala, J., M. Harkonen, and L. Luciani, *Makromol. Chem.*, **190**, 2535 (1989).

- Sinn, H., and W. Kaminsky, *Adv. Organomet. Chem.*, **18**, 99 (1980).
- Soga, K., J.R. Park, T. Shiono, and N. Kashiwa, *Makromol. Chem., Rapid Commun.*, **11**, 117 (1990).
- Soga, K., T. Sano, K. Yamamoto, and T. Shiono, *Chem. Lett.*, 425 (1982).
- Spitz, R., J.L. Lacombe, and A. Guyot, *J. Polym. Sci., Polym. Chem. Ed.*, **22**, 2641 (1984).
- Terano, M., T. Kataoka, and T. Keii, *J. Polym. Sci., Polym. Chem. Ed.*, **28**, 2035 (1990).
- Venditto, V., G. Guerra, P. Corradini, and R. Fusco, *Polymer*, **31**, 530 (1990).
- Wilchinsky, Z.W., R.W. Looney, and E.G.M. Tornquist, *J. Catal.*, **28**, 399 (1961).
- Wild, F.R.W.P., L. Zsolnai, F. Huttner, and H.H. Brintzinger, *J. Organomet. Chem.*, **232**, 233 (1982).
- Yano, T., T. Inoue, S. Ikai, M. Shimasu, Y. Kai, and M. Tamura, *J. Polym. Sci., Polym. Chem. Ed.*, **26**, 477 (1988).
- Zakharov, V.A., G.D. Bukatov, and Y.I. Yerkamov, *Polymer Sci. and Tech.*, **19** (1983).
- Zambelli, A., L. Pasquale, and A. Grassi, *Macromol.*, **22**, 2186 (1989).
- Zambelli, A., M. Sacchi, P. Locatelli, and G. Zannoni, *Macromol.*, **15**, 211 (1982).



